Effectiveness of Alpha linolenic acid (ALA) and Gamma linolenic Acid (GLA) on ER positive mammary gland carcinoma and redefining its mechanism of action through mitochondria mediated death apoptosis pathway

THESIS

Submitted to
Babasaheb Bhimrao Ambedkar University
(A Central University)
Lucknow

BABASAHEB
BHIMRAO
AMBEDKAR
UNIVERSITY
LUCKNOW
प्रज्ञा शील करुणा
ESTABLISHED 1996

For the Degree of

Doctor of Philosophy

In

PHARMACEUTICAL SCIENCES

By:

Subhadeep Roy

Enrollment No. – 1469/15

Supervisor:

Dr. Gaurav Kaithwas

Associate Professor

DEPARTMENT OF PHARMACEUTICAL SCIENCES
SCHOOL OF BIOMEDICAL AND PHARMACEUTICAL SCIENCES
BABASAHEB BHIMRAO AMBEDKAR UNIVERSITY
(A CENTRAL UNIVERSITY)
VIDYA VIHAR, RAE BARELI ROAD, LUCKNOW-226 025 (U.P.), INDIA

2018

DEDICATED TO MY BELOVED PARENTS, FRIENDS AND TEACHERS

DECLARATION

I hereby declare that the thesis entitled **"Effectiveness of Alpha linolenic acid (ALA) and Gamma linolenic Acid (GLA) on ER positive mammary gland carcinoma and redefining its mechanism of action through mitochondria mediated death apoptosis pathway"** has been prepared by me under the supervision of **Dr. Gaurav Kaithwas** at Department of Pharmaceutical Sciences, School of Biomedical and Pharmaceutical Sciences, Babasaheb Bhimrao Ambedkar University, Lucknow (U.P.).

This work has not been submitted in a part or full to any other University/Institute for any degree/diploma or any other academic award anywhere before. I further declare that the material embodied in the present work is based on original research work and indebtedness to others has been duly acknowledged at relevant places. I hereby also declare that the thesis is essentially free from all kind of plagiarism.

Subhadeep Roy.

Subhadeep Roy
Candidate

16/04/2018

Dr. Gaurav Kaithwas
Supervisor

CERTIFICATE

This is to certify that the thesis titled **"Effectiveness of Alpha linolenic acid (ALA) and Gamma linolenic Acid (GLA) on ER positive mammary gland carcinoma and redefining its mechanism of action through mitochondria mediated death apoptosis pathway"** submitted by **Mr. Subhadeep Roy (Enrollment no. 1469/15)** is an original work and has not been previously submitted in part or full for the award of any other degree or diploma to this or any other university.

The thesis submitted to Babasaheb Bhimrao Ambedkar University Lucknow satisfies all the requirements as stipulated in the Doctor of Philosophy (Ph.D.) regulations -1999 as amended in 2008/2010/2013 and it is fit for submission and evaluation for the award of the degree of Doctor of Philosophy of the University.

Date: 16/4/18

16/04/2018.

Supervisor

Head of the Department

TABLE OF CONTENTS

ACKNOWLEDGEMENT

Foremost I would like to "Thank God", who gave me this opportunity to extend my gratitude to all those people who have helped me and guided me throughout my life. I bow my head in complete submission before him for the blessing poured on me.

I wish to express my gratitude to my supervisor ***Dr. Gaurav Kaithwas,Associate Professor, Department of Pharmaceutical Sciences, Babasaheb Bhimrao Ambedkar University, Lucknow****, for his continuous encouragement and invaluable suggestions during my entire study. I wish to thank him for unflattering trust and constant inspiration, which have been essential to this success.*

I would like to express my sincere gratitude to ***Prof. Shubhini A. Saraf****, Head of Dept. of Pharmaceutical Sciences for her extraordinary support, encouragement and motivation.*

I am grateful to ***Prof. R.C.Sobti, Honourable Vice Chancellor, Babasaheb Bhimrao Ambedkar University, Lucknow*** *for providing the excellent infrastructure and facilities in the University campus.*

I would also like to thanks to the DRC committee members: ***Dr. V.Elongovan, Dr. N.K.S.More*** *and* ***Dr. Sudipta Saha*** *for their valuable and meaningful suggestions.*

I would like to give my heartly thanks to my friends ***Ms. Manjari Singh, Ms. Swetlana, Mr. Rajnish Kumar Yadav, Mr. Lakhveer Singh*** *and* ***Mr. Jitendra Kumar Rawat****. They helped me immensely by giving me encouragement and moral support.*

I wish to thanks to the staff members of the department, ***Mr. Ramesh, Mr. Amar, Mr, Bhandari*** *and* ***Mr. Anand Pandey*** *for smoothing the necessary official works.*

I shall be failing in my duty if I miss to appreciate the help of my dear parents and friends who left no stone unturned in supporting, helping and providing me each facility during

the period of doctoral study. Most importantly, I would like to pay my best regards to my parents, ***Mrs. Dipali Roy*** *and* ***Mr. Subhas Roy*** *for their never ending support.*

Finally, my greatest regards to the Almighty for bestowing upon me the courage to face the complexities of life and complete this work successfully.

Subhadeep Roy

SUBHADEEP ROY

LIST OF TABLES

LIST OF FIGURES

ABBREVIATIONS

- ALA- α-Linolenic acid
- AA-arachidonic acid
- AO-acridinie orange
- AB-alveolar bud
- BSA-bovine serum albumin
- BMRB- biological magnetic resonance data bank
- CPMG- carr–purcell–meiboom–gill
- CEC-cuboidal epithelial cell
- DHA- docosahexaenoic acid
- DMSO-dimethyl sulphoxide
- DMBA-7,12-dimethylbenz(a)anthracene
- DTT-dithiothriol
- DCT- dense connective tissue
- EPA-eiconapentanoic acid
- EBSS- eagle balanced salt solution
- EtBr- ethidium bromide
- ECG-electrocardiogram
- FBS- fetal bovine serum
- FACS- florescence activated cell sorter
- FID- free induction decay
- FT- fourier transformation
- FASN-fatty acid synthase
- GLA-gamma linolenic acid
- GSH-glutathione
- GPC-glycerophosphocholine
- HBSS- hank's balanced salt solution
- H&E- hematoxylin & eosin
- HRV- heart rate variability
- HR- heart rate
- HMBD- the human metabolome database
- HF- high frequency

- HIF-1α- hypoxia inducible factor-1α
- LA-linolenic acid
- LF- low frequency
- LCT- loose connective tissue
- LDL- low density lipoprotein
- MNU-n-methyl-n-nitrosourea
- MTT- 3-(4,5-Dimethyl-2-thiazolyl)-2,5-diphenyl-2H-tetrazolium bromide
- MPTP- mitochondria permeability transition pore
- MEC- mypepithelial cell
- NAG- N-acetyl glycoprotein
- OAG- O-acetyl glycoprotein
- OPLS-DA- Orthogonal projection to latent structure with discriminant analysis
- PUFA- polyunsaturated fatty acid
- PI- propidium iodide
- PS- phosphatidylserine
- PC- phosphocholine
- PCA- principal component analysis
- PLS-DA- partial least squares discriminant analysis
- PHD2- prolyl hydroxylase-2
- RD- recycle delay
- ROS- reactive oxygen species
- SEM- scanning electron microscope
- SOD- superoxide dismutase
- TMX- tamoxifen citrate
- TRU- turbidity reduction unit
- TBARs- thiobarbituric acid reactive substances
- TSP- trimethylsilylpropionic acid
- VLF- very low frequency
- VLDL- very low density lipoprotein

CHAPTER 1
INTRODUCTION

1. Introduction

Fatty acids are aliphatic carboxylic hydrocarbon with a methyl group at one end and carboxylic acid at other end [1]. They may be saturated, containing no double bonds or unsaturated, containing one or more double bonds. The properties of fatty acids are determined by the length and degree of unsaturation of the hydrocarbon chain [2]. The unsaturated fatty acids are further subdivided as monounsaturated (containing one double bond) and polyunsaturated (containing two or more double bonds) in which polyunsaturated fatty acids (PUFA) are of major biological significance [3].

The most important families of PUFAs in human metabolism are ω-6(n-6) and ω-3(n-3) PUFA [4]. PUFAs are the precursors of a broad range of bioactive lipid mediators like eicosanoids and also include the components of membrane phospholipids that play a key role in metabolism, cell signalling and inflammation [5]. The large body of evidences suggests the role of PUFAs metabolites in carcinogenesis and tumour progression as well. PUFA are the precursors for various essential signalling molecules like eicosanoids including the prostanoids, leukotrienes (LTs), and lipoxins (LXs). Prostanoids include prostaglandins (PGs), prostacyclins (PGIs), and thromboxanes (TXs) along with LTs and LXs are key mediators of inflammatory cascade [6]. The majority of physiological disorder considering the inflammatory background of above mentioned diseases and formation of essential signalling molecules (eicosanoids), leads to the assumption that ω-3 and ω-6 PUFAs plays a significant role in their pathophysiology and might be acting through down-regulation/up-regulation of the inflammatory cascade respectively [7]. The ω-3 family of PUFAs mainly comprises of alpha linolenic acid (ALA), eicosapentaenoic acid (EPA) and docosahexaenoic acid (DHA) [8]. They are referred as ω-3 due to

presence of double bond (C=C) at the third carbon atom from the end of carbon chain. ALA cannot be synthesized by the human body and needs to be obtained from dietary sources [9]. ALA is the major plant-based PUFA and is found in walnuts, flaxseeds, hemp seeds and their oils. ALA is also found in rapeseed (canola) oil; and to smaller amounts in soya oil and green-leafy vegetables [10]. ALA is metabolized by series of desaturation and elongation reactions of long chain fatty acids, among which EPA and DHA are of prime biological importance [11]. EPA and DHA are vital in regulating membrane fluidity, protein and cellular functions, eicosanoid metabolism, gene expression and cell signalling [12]. EPA and DHA are obtained from fish oil or derived from plant lipids rich in ALA. EPA and DHA integrate a cascade that runs alongside and emulates with the inflammatory cascade governed by the arachidonic acid (AA) metabolism [13]. A previous report has taken account that the EPA cascade softens the inflammatory effects of AA cascade, suggesting it as an anti-inflammatory agent [14].

Report has also elaborated that ω-3 fatty acids reduce prostate tumor growth, curtail histopathological progression and increase survival [15]. A previous study has also indicated that ALA actively suppresses the overexpression of HER2+ in mammary carcinomas [16]. It was also reported that overiectomized mice produce a significant reduction in tumor growth, when compared with a diet containing no flaxseed oil (rich source of ALA) [17]. Moreover, PUFAs are the integral component of cell membranes and are susceptible to peroxidation and degeneration causing genetic mutations, a critical mechanism for tumor growth. Therefore, ALA seems to be a promising chemotherapeutic agent with desirable characteristics [18]. Although studies have reported anti-

carcinogenic potential of ALA and ALA being a PUFA can moderate the cell membrane integrity in multiple ways, the mechanistic pathway behind the same is unanswered.

The ω-6 fatty acids are majorly composed of gamma linolenic acid (GLA) and AA. Due to presence of final C=C double bond at sixth position from methyl end, they are nominated as ω-6 [22]. The biological metabolism of ω-6 PUFAs leads to formation of ω-6 eicosanoids, which are designated as pro-inflammatory in nature and thereby presumed to promote inflammation [23].

GLA is a member of the ω-6 family of PUFAs and is transfigured into AA by series of desaturation and elongation reactions [24]. AA is further metabolized by cyclooxygenase (COX) enzyme into 2-series prostaglandins or through the 5-lipoxygenase (LOX) enzymes into LTs and 5-hydroxy-eicosatetranoic acid, which are the major determinants for cellular inflammation [25]. GLA is found in animals and plants, oils like sunflower, soy bean and grape seed and is very much found in daily diet. The abundance of GLA is in human milk and it's found in common foods like meat in lesser amounts. The high share of GLA is found in plant oils. The content of GLA in herbaceous plant, blackcurrant, borage and fungal oil is 7–10 g/100 g, 15–20 g/100 g, 18–26 g/100 g, 23–26 g/100 g respectively [26]. All in all, AA sits at the highest of the inflammatory cascade with over twenty completely different signalling pathways. Chronic consumption/production of LA/GLA/AA has been correlated with arthritis, inflammation, and cancer [22]. Infact, high consumption of ω-6 fatty acid has been reported to increase the likelihood, that postmenopausal women will develop breast cancer [23]. The action of both ω-3 and ω-6 fatty acid are different. Previous literature declared that ω-3 has the property to reduce the tumour growth whereas ω-6 has opposite action on tumour growth

[27]. Infact, ω-6 fatty acid intake in humans and animals has been correlates with a high risk of breast, prostate and colon cancer and therefore the quantitative relation of ω-6 to ω-3 fatty acids is usually recommended to be a predictor for cancer progression [28]. The pro-carcinogenic effects of ω-6 fatty acids may be due to AA.

The anti-inflammatory action of GLA is regulated through nuclear factor kappa B (NFκB) factor [29]. GLA also regulates the anti-inflammatory activity by promoting the pervasive peroxisome proliferators activated receptor (PPAR) system [30]. Increasing proof prompt that not like the AA and its downstream metabolites that are related to cancer development, the upstream GLA might possess antitumor effects and so might be a promising dietary supply for cancer interference and medical aid [24]. Evidence shows that GLA is additionally related to anti-cancer activity each *in vitro* and *in vivo*. More interestingly, GLA induced cytotoxicity was shown to exhibit high selectivity toward cancer cells with no significant effect on normal cell growth. Several corroborations including *in vitro* and *in vivo* studies recommend the anticancer activity of GLA. It was previously reported that GLA hinders cell growth of several human neuroblastoma and several rat carcinosarcoma cell lines [31]. GLA also diminished the tumour growth in the implanted WBC256 rat model. It was previously reported that supplementation with GLA rich diets suppressed the mammary gland carcinogenesis and transplanted tumour growth. GLA also inhibits the growth of various cultured human cancer cell lines like ZR-75-1, A549 and PC-3 cells [24].

In summary, the results from pre-clinical studies provide compelling evidence that PUFAs (ALA and GLA) can mediate cancer progression *in vitro* and *in vivo* in several types of cancers models. Mediation may occur through several mechanisms including

regulation of gene expression, angiogenesis, cell migration, and apoptosis. . Additionally, DHA may have chemo-sensitizing effects in humans, but this needs to be confirmed in larger studies. Based on the current literature, the pro-inflammatory and anti-inflammatory characteristics of PUFAs are the key underlying mechanisms mediating their biological effects. Individual PUFAs produce PGs and LTs with distinct biological functions that elicit pro- and anti-inflammatory responses through several signalling pathways that regulate cell proliferation, apoptosis, and angiogenesis. The metabolism of PUFAs is complex and controlled by enzymes that are highly polymorphic and map to a genomic region frequently associated with cancer. Thus, to better delineate the associations between PUFAs and cancer in humans, future studies should consider dietary intake of PUFAs and variation in genes encoding the enzymes in PUFA metabolism. In addition, because the expression of genes encoding the enzymes in the PUFA pathway is frequently lost in the target-tissue, metabolism of PUFAs in tumor tissues may be altered and this needs to be considered. The findings from such studies could allow for the identification of individuals with altered PUFA metabolism that may benefit from personalized diets.

1.2 Literature Review

- ✓ **Nguyen NM et al (2017)** stated that maternal and paternal high fat diet intake before and/or during pregnancy increases mammary cancer risk in several preclinical models. They studied if maternal consumption of a HF diet that began at a time when the fetal primordial germ cells travel to the genital ridge and start differentiating into germ cells would result in a transgenerational inheritance of increased mammary cancer risk. They conclude that maternal HF diet intake during pregnancy induces a transgenerational increase in offspring mammary cancer risk in mice. The mechanisms of inheritance in the F3 generation may be different from the F1 generation because significantly more changes were seen in the transcriptome [32].
- ✓ **Ouldamer L et al (2016)** stated that the microenvironment of breast epithelial tissue may contribute to the clinical expression of breast cancer. Breast epithelial tissue, whether healthy or tumoral, is directly in contact with fat cells, which in turn could influence tumor multifocality. In this pilot study they investigated whether the fatty acid composition of breast adipose tissue differed according to breast cancer focality. These differences in lipid content may contribute to mechanisms through which peritumoral adipose tissue fuels breast cancer multifocality [33].
- ✓ **Wiggins AK et al (2015)** stated that eterogeneity of breast cancer subtypes makes breast cancer treatment difficult. ALA, rich in flaxseed oil, has been shown to reduce growth and increase apoptosis in several breast cancer cell lines, but the mechanism of action needs further understanding.ALA reduces growth of breast

cancer cell lines, by modifying signalling pathways, which differ between breast cancer molecular subtypes. The ALA effect on gene expression is dynamic and changes over time, indicating the significance of incubation period in detecting gene changes [34].

- ✓ **Zou Z et al (2014)** stated that overexpression of the tyrosine kinase receptor ErbB2/HER2/Neu, occurs in 25%–30% of invasive breast cancer with poor patient prognosis. Even if numerous studies have shown prevention of breast cancer by n-3 fatty acid intake, the experimental conditions under which n-3 fatty acids exert their protective effect have been variable from study to study, preventing unifying conclusions. Due to confounding factors, inconsistencies still remain regarding protective effects of n-3 PUFA on breast cancer. When animals are fed with dietary supplementation in n-3 fatty acids (the traditional approach to modify tissue content and decrease the n-6/n-3 ratio) complex dietary interactions can occur among dietary lipids (antioxidants, vitamins…) that can modulate the activity of n-3 fatty acids [35].
- ✓ **Wiggins AKA et al (2013)** stated that breast cancer differs in cell receptors which then determine effective treatments. ALA-rich flaxseed oil reduced ER+ cell growth at low and high estrogen (E2) but its effect is unclear in cells with varying ER, progesterone receptor (PR) and human epidermal growth factor receptor 2 (HER2) [36].
- ✓ **Azrad M et al (2013)** stated that there are so many evidences which claim that PUFAs play a role in cancer risk and progression. The n-3 family of PUFAs includes ALA, EPA and DHA while the n-6 family includes LA and AA. EPA

and DHA are precursors for anti-inflammatory lipid mediators while AA is a precursor for pro-inflammatory lipid mediators. Collectively, PUFAs play crucial roles in maintaining cellular homeostasis, and perturbations in dietary intake or PUFA metabolism could result in cellular dysfunction and contribute to cancer risk and progression. Epidemiologic studies provide an inconsistent picture of the associations between dietary PUFAs and cancer. Clinical trials have shown that supplementation with PUFAs or foods high in PUFAs can affect markers of inflammation, immune function, tumor biology, and prognosis. Pre-clinical investigations have begun to elucidate how PUFAs may mediate cell proliferation, apoptosis and angiogenesis, and the signalling pathways involved in these processes [28].

- ✓ **Zheng JS et al (2013)** investigates the association between intake of fish and n-3 PUFA and the risk of breast cancer and they evaluate the potential dose-response relation. In this study, they conclude that higher consumption of dietary marine n-3 PUFA is associated with a lower risk of breast cancer. The associations of fish and ALA intake with risk warrant further investigation of prospective cohort studies. These findings could have public health implications with regard to prevention of breast cancer through dietary and lifestyle interventions [37].
- ✓ **Murff HJ et al (2011)** stated that breast cancer is the most common cancer in women. Controversy exists regarding the role of dietary fat in breast cancer etiology. They investigated the association of dietary PUFA and the ratio of n-6 PUFAs to marine-derived n-3 PUFAs with breast cancer risk in the Shanghai Women's Health Study, a prospective cohort study including 72,571 cancer-free

participants at baseline. Dietary fatty acid intake was determined using food frequency questionnaires. The relative amounts of n-6 PUFA to marine-derived n-3 PUFAs may be more important for breast cancer risk than individual dietary amounts of these fatty acids [38].

- ✓ **Kim JY et al (2009)** tested the anti-carcinogenic effect of ALA as a single compound. To test the role of ALA in breast cancer cells (MCF-7), they analyzed the anti-proliferative pathway and the pro-apoptotic pathway. ALA exhibited growth inhibition on MCF-7 cells dose-dependently of ALA in 24, 48, and 72 h, without possible cytotoxicity per se. ALA enhanced the cell growth-inhibitory activity in a dose-dependent manner. Second, the pro-apoptotic pathway showed a sub-G(1) accumulation with concomitant upregulation of pro-apoptotic Bax expression, as well as a downregulation of anti-apoptotic Bcl-2 expression dose-dependently, causing the Bcl-2/Bax ratio to decrease by about 50%. Subsequent cytochrome c release and proteolytic activation of caspase-3 followed by proteolytic cleavage of poly (ADP-ribose) polymerase all suggest ensuing progression to apoptosis [39].
- ✓ **Kapoor R et al (2006)** stated that inflammation plays an important role in health and disease. Amongst dietary constituents, fat has gained most recognition in affecting health. Saturated and Trans fatty acids have been implicated in obesity, heart disease, diabetes and cancer while PUFAs generally have a positive effect on health. The PUFAs of omega-3 and omega-6 series play a significant role in health and disease by generating potent modulatory molecules for inflammatory responses, including eicosanoids (PGs and LTs), and cytokines (interleukins) and

affecting the gene expression of various bioactive molecules. GLA is produced in the body from LA, an essential fatty acid of omega-6 series by the enzyme delta-6-desaturase. GLA and its metabolites also affect expression of various genes where by regulating the levels of gene products including matrix proteins. These gene products play a significant role in immune functions and also in cell death (apoptosis) [40].

- ✓ **Menendez JA et al (2006)** stated that data derived from epidemiological and experimental studies suggest that ALA, the main ϖ-3 PUFA present in the Western diet, may have protective effects in breast cancer risk and metastatic progression. A recent pilot clinical trial assessing the effects of ALA-rich dietary flaxseed on tumor biological markers in postmenopausal patients with primary breast cancer demonstrated significant reductions in tumor growth and in HER2 (erbB-2) oncogene expression [41].
- ✓ **Watkins G et al (2005)** investigated the role of n-6 PUFA, GLA on the expression and secretion of secreted protein acidic and rich in cystein (SPARC) from cancer cells. Human breast cancer cell line MCF-7 and MDA-MB-231, human colon cancer cells HT115 and HRT-18 was used in the study. Cancer cells were treated with GLA or other fatty acids over a range of concentrations. Presence of SPARC in the supernatant and in the cell lysate were analysed using Western blotting. Cellular SPARC was also assessed using immunocytochemistry. GLA reduced cell-matrix adhesion in these cancer cells. It is concluded that GLA is a regulator of SPARC secretion and expression in cancer cells. It reduces the secretion of SPARC into surrounding environment,

which may contribute to the reduction of cancer cells adhesion to the extracellular matrix and cell motility [42].

- ✓ **Larsson SC et al (2004)** stated that there are increasing evidence from animal and *in vitro* studies indicates that n−3 fatty acids, especially the long-chain PUFAs, EPA and DHA, present in fatty fish and fish oils inhibit carcinogenesis. Several molecular mechanisms whereby n−3 fatty acids may modify the carcinogenic process have been proposed. These include suppression of AA-derived eicosanoid biosynthesis; influences on transcription factor activity, gene expression, and signal transduction pathways; alteration of estrogen metabolism; increased or decreased production of free radicals and reactive oxygen species; and mechanisms involving insulin sensitivity and membrane fluidity [43].
- ✓ **Kenny FS et al (2000)** stated that GLA has been proposed as a valuable new cancer therapy having selective anti-tumour properties with negligible systemic toxicity. Proposed mechanisms of action include modulation of steroid hormone receptors. They investigated the effects of GLA with primary hormone therapy in an endocrine-sensitive cancer. The effects of GLA on ER function and the apparent enhancement of tamoxifen-induced ER down-regulation by GLA require further investigation [44].

1.3 Aim and Objectives

The aim of the present study was to establish a mechanistic link underlying the role of dietary PUFA supplementation in cancer prevention and chemotherapy. The specific objectives of the project are as described below:

Objective 1: To study the effect of ALA and GLA on proliferation of ER+MCF-7 breast cells.

Objective 2: To study the effect of ALA and GLA on N-methyl-n-nitrosourea (MNU) induced breast carcinogenesis in female albino wistar rats.

Objective 3: To study the effect of ALA and GLA on 7, 12-dimethyl benzanthracene (DMBA) induced breast carcinogenesis in female albino wistar rats.

Objective 4: To identify the role of UCHL-1 in mammary gland carcinoma and trying to establish it as a proteomic marker.

Objective 5: Redefine the role of mitochondria mediated death apoptosis pathway in ER+ mammary gland carcinoma.

1.4 Plan of work

1. Literature survey & procurement of materials

2. *In vitro* cell line study

- ❖ MTT assay
- ❖ Acridine orange/ethidium bromide (AO/EtBr) staining
- ❖ JC-1 staining
- ❖ Cell cycle analysis
- ❖ Annexin V-FITC dot plot assay

3. *In vivo* animal study

- ❖ Hemodynamic study
- ❖ Morphological analysis
- ❖ Antioxidant markers
- ❖ Serum caspase3 and caspase 8 estimation
- ❖ ^{1}H NMR study
- ❖ Western blotting and qRT-PCR studies

4. *C.elegans* study

- ❖ Aldicarb assay
- ❖ Estimation of Ach and AchE activity
- ❖ Mitotracker red staining
- ❖ Nile red staining

5. Statistical Analysis

6. Compilation of Data

CHAPTER 2
DRUG PROFILE

2.1 GLA

GLA is an omega-6 fatty acid produced in the body as the delta 6-desaturase metabolite of LA [45]. It is converted to dihomo-GLA, a biosynthetic precursor of monoenoic prostaglandins such as PGE1 [46]. It's available in many vegetable-based oils, including evening primrose oil, borage seed oil, and black currant seed oil [47]. GLA has been promoted as medication for a variety of ailments including breast pain and eczema. However, more recently, topical application of borage seed oil (an oil with a high concentration of GLA) has been shown to reduce the symptoms of atopic dermatitis in a double-blind, placebo-controlled clinical trial. Another single source suggests that evening primrose oil with adjuvant vitamin E may reduce breast pain [48].

Molecular formula: $C_{18}H_{30}O_2$

Molecular weight: 278.436 g/mol

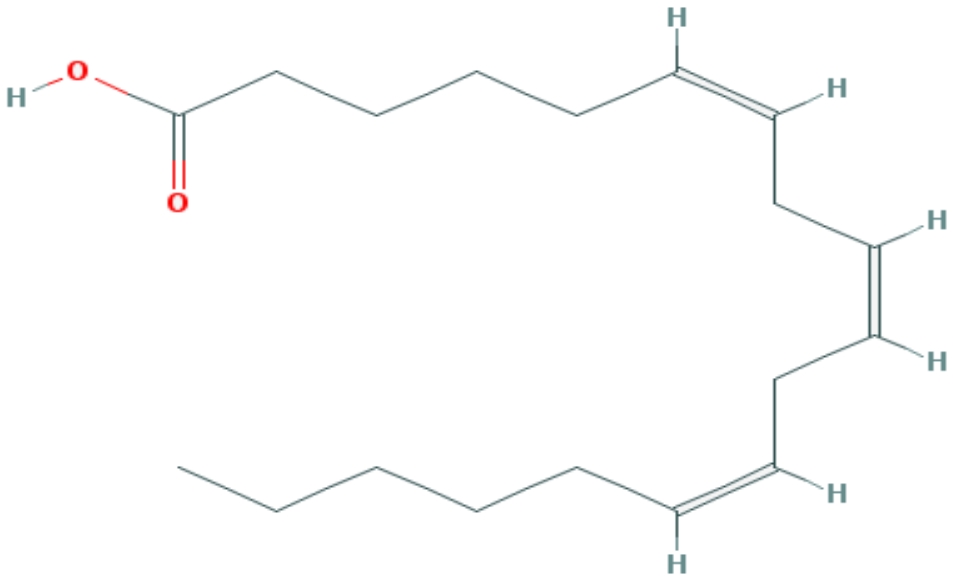

2.2 ALA

ALA is a member of the group of essential fatty acids called omega-3 fatty acids. ALA in particular, is not synthesized by mammals and therefore is an essential dietary requirement for all mammals [49]. Certain nuts and vegetable oils (canola, soybean, flaxseed/linseed, and olive) are particularly rich in ALA. Omega-3 fatty acids get their name based on the location of one of their first double bond [50]. In all omega-3 fatty acids, the first double bond is located between the third and fourth carbon atom counting from the methyl end of the fatty acid (n-3). Although humans and other mammals can synthesize saturated and some monounsaturated fatty acids from carbon groups in carbohydrates and proteins, they lack the enzymes necessary to insert a cis double bond at the n-6 or the n-3 position of a fatty acid [51]. Omega-3 fatty acids like ALA are important structural components of cell membranes. When incorporated into phospholipids, they affect cell membrane properties such as fluidity, flexibility, permeability and the activity of membrane bound enzymes [52]. Omega-3 fatty acids can modulate the expression of a number of genes, including those involved with fatty acid metabolism and inflammation [53].

Molecular formula: $C_{18}H_{30}O_2$

Molecular weight: 278.436 g/mol

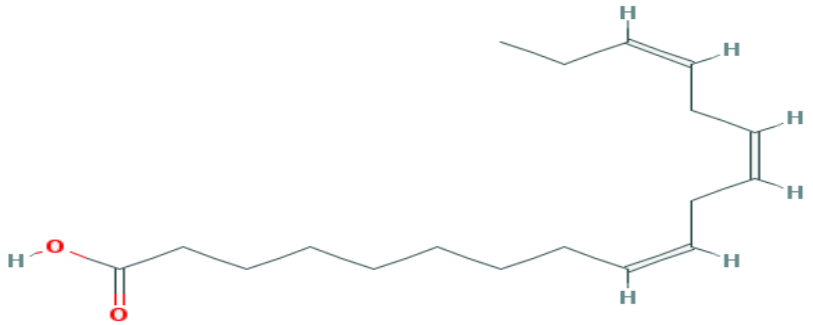

2.3 Toxicants

2.3.1 MNU

MNU is a direct carcinogen and it doesn't require any other intermediate to react. MNU induced mammary gland carcinoma is a well-established model for the evaluation of many chemoprotective drugs [54]. The possible site of alkylation in guanine base pair is either in nitrogen or oxygen because of high abundance of electron. This alkylation leads to generation of a fast (N (7)-methyl guanine) as well as a slow (O (6)-methyl guanine) intermediate [55]. The hydrogen bonding properties of guanine was changed due to methylation at the O (6)-position and thereby inducing guanine to adenosine transition followed by DNA damage [56].

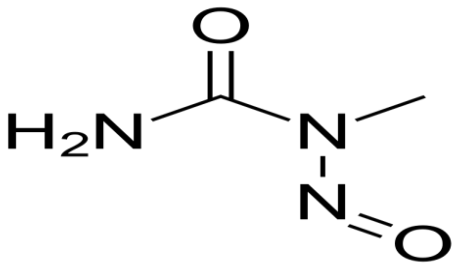

The toxicant was prepared in glacial acetic acid and water with pH 4.5-5. The MNU was given in a dose of 47mg/kg, i.v. once in the whole study.

2.3.2 DMBA

DMBA is a polycyclic aromatic hydrocarbon and is used to induce mammary gland carcinoma in experimental animals [57]. The mammary tumors produced from DMBA are morphologically and histopathologically very similar to human tumors. DMBA is an indirect carcinogen, and requires metabolic activation by cytochrome P450 enzymes to reactive metabolites, i.e. dihydrodiolepoxides and forms mutagenic DNA adduct. Mainly two enzymes viz cytochrome P4501B1 (CYP1B1) and microsomal epoxide hydrolase (EPHX1) are responsible for DMBA bioactivation [58].

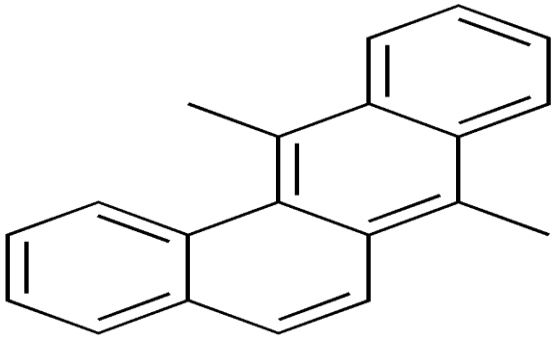

The toxicant was prepared in olive oil as a suspension. The DMBA was given in a dose of 8mg/kg, i.v. once in the whole study.

CHAPTER 3
MATERIALS AND METHODS

3.1 Materials

3.1.1 Drugs and chemicals

ALA (463-40-1) (0.914gm/ml) was purchased from TCI Chemicals (India) Pvt. Ltd. GLA (GLA-120) was purchased from Dr. Reddy's Laboratory (India). RPMI 1640 (Gibco, USA); fetal bovine serum (FBS) (Gibco-10270); trypsin (Gibco, USA); eagle balanced salt solution (EBSS)(Gibco,2018-11); hank's balanced salt solution (HBSS) (Himedia, TL1190); EtBr(Himedia,MB071); AO(Himedia,MB116); JC-1 assay kit (Thermo Scientific, M34152); propidium iodide (PI) (SC-3541); tamoxifen citrate (TMX) (Tammodex 20,Biochem Pharmaceuticals India); penicillin- streptomycin (Thermo Scientific, 15410-163); gentamycin (Thermo Scientific,15710-049);3-(4,5-Dimethyl-2-thiazolyl)-2,5-diphenyl-2H-tetrazolium bromide (MTT) (Himedia, TC191); RNase (SRL, 58895); dimethyl sulfoxide (DMSO) (Merck,1.16743.0521); DMBA(Sigma Aldrich,57-97-6); MNU (Sigma Aldrich,N1517); ponceau S (Himedia,ML045); sodium cacodylate (Sigma Aldrich, C0250); collagenase type 4 (Himedia,TC-214); hyaluronidase (Himedia, TC331); hematoxylin (Himedia,S058); eosin (Himedia,S007); RIPA lysis buffer (Amresco, N653); protein assay kit (Amresco,M173); bovine serum albumin (BSA) (Genetix,PG-2330); transfer buffer (Genetix, GX-9411AR), trizol reagent (Sigma-T9424), cDNA synthesis kit (Genetix-K1612). Caspase 3 (SC-4263) and caspase 8 (SC-4267) assay kits were procured from Santacruz Biotechnology Inc., California, Delaware. All others chemicals were of molecular biology grade and purchased from Genetix Biotech Asia Pvt. Ltd, New Delhi.

C. elegans strains, Bristol N2 (wild type) were procured from Caenorhabditis Genetics Center, (University of Minnesota, MN, USA) and grown on nematode growth medium (NGM) prepared by adding 50mM sodium chloride (Himedia Laboratories, India), 2.5

mg/l peptone (Himedia Laboratories, India) and 17 mg/l agar (Himedia Laboratories, India) in 975ml double distilled water q.s. and autoclaved (Tomy High Pressure Steam sterilizer ES-215) for 40 min at 15 lb per inch2. 1ml of 5 mg/ml cholesterol (Himedia Laboratories, India) solution, 1mM calcium chloride (Merk, Germany) (autoclaved), 1mM magnesium sulphate (Merk, Germany) (autoclaved) and 25mM potassium dihydrogen phosphate (Merk, Germany) (autoclaved) were added to the medium and cooled to 60ºC. The media was poured in petri dishes. Escherichia coli OP50 were used as a food source. Amplex red acetylcholine/acetylcholineesterase (Ach/AchE) estimation kit was procured from Life Technologies Co. U.S.A. (Cat. no. A12217). Mitotracker red CM-H2XROS was purchased from Invitrogen Pvt. Ltd. (Cat no-M7513). All experiments were conducted at 22ºC**.**

3.1.2Equipment used

Table 1: Lists of equipments used

Serial no.	**Equipment**	**Manufacturer and Model**
1.	Cooling centrifuge	Eppendorf India Limited, Chennai 5418R
2.	Vortex shaker	Remi Mumbai CM101
3.	Refrigerator	Godrej, Lucknow
4.	Homogenizer	Remi, Mumbai RQT-127A
5.	Microvolume Spectrophotometer	Agilent Technologies, Mumbai Carry 500
6.	Weighing balance	Sartorius, Mumbai BSA224S-CW
7.	pH meter	Labman Scientific Instruments, Lucknow LMPH-10
8.	Micropipette	Genetix Biotech Asia Pvt. Ltd. New Delhi

9.	Deep freezer	Celfrost, BFS150,Lucknow
10.	Microplate Reader	Bio-Rad Laboratories Inc. Model 680XR
11.	Inverted fluorescence microscope	Niken Leica M165FC
12.	Fluorescence activated cell sorter (FACS)	BD Influx cell sorter
13.	Bio-amplifier (ML-136) and channel power lab (ML-826)	AD Instruments, Australia
14.	Digital biological microscope	N 120, BR-Biochem Life Sciences, New Delhi
15.	Scanning electron microscope (SEM)	JEOL JSM-6490LV
16.	SDS-PAGE	GX-SCZ2, Genetix Biotech Asia Pvt. Ltd. New Delhi
17.	Semidry transfer unit	GX-ZY3, Genetix Biotech Asia Pvt. Ltd. New Delhi
18.	Light cycler-480 machine	Roche Diagnostics, Germany

3.2Methodology

3.2.1 *In vitro* study

3.2.1.1 Cell Line

The ER+MCF-7cells were cultured and routinely maintained in RPMI 1640 medium supplemented with 10% heat inactivated FBS, penicillin (100 units/ml), streptomycin (100µg/ml), gentamycin (100µg/ml) and were incubated at 37 °C in a humidified atmosphere containing 5% CO_2 inside a CO_2 incubator [59].

3.2.1.2 Cytotoxicity study with MTT

Cytotoxicity was measured by using MTT assay. ER+MCF-7 cell ($1x10^5$) were seeded in 96 well sterile plates and were treated with different concentrations of ALA and GLA (1µM, 5µM, 10µM, 15µM, 20µM, 25µM) for 24h, compared against control and standard (TMX) (27µM). Subsequently media form upper layer was removed and

incubate with 20µl MTT (5mg/ml) and 100µl of fresh media for 2h. Blue colored formazans were released from the cells by adding 100µl DMSO with gentle shaking at 37°C. After 30 min incubation, the absorbance of the color solution was quantified by measuring at a wavelength of 570 nm by micro plate reader (Model 680 XR Bio-Rad laboratories lnc). IC50 value and ½ IC50 values of ALA and GLA against ER+MCF-7 cells were determined after 24 h [60].

3.2.1.3 Detection of apoptosis through AO/EtBr staining

Characteristic apoptotic morphological changes were observed by inverted fluorescence microscopy by using AO/EtBr staining. ER+MCF-7 cells ($1x10^6$) were treated with ½ IC 50 and IC50 dose of ALA, GLA and TMX for 18 h, and were observed under the inverted fluorescence microscope for morphological changes. The untreated control cells and ALA treated cells were harvested separately, washed with PBS and stained with AO (100µg/ml) and EtBr (100µg/ml) (1:1). The cells were immediately mounted on slides and visualized under an inverted fluorescence microscope (Nikon Leica, M165 FC) for the changes in morphological features of apoptosis [61].

3.2.1.4 Identification of mitochondrial morphology through JC-1 dye

Alteration in the ΔΨm was analyzed by inverted fluorescence microscope using the mitochondrial membrane potential sensitive dye JC-1. JC-1 forms J-aggregate in control cells in intact mitochondrial membrane potential. Stock solution of 1mg/ml JC-1 was prepared in 1% DMSO and stored at -20 °C shortly before use. After incubation for 24 h with ½ IC 50 and IC 50 dose of ALA and GLA, cells were washed three times with PBS and 200µl of JC-1(1mg/ml) dye was added into each well. After incubation for 20 min, cells were washed three times with PBS and imaged with an inverted fluorescence microscope (Nikon Leica, M165 FC) [62].

3.2.1.5 Cell cycle analysis using PI

The cells were treated with a fluorescent dye PI that quantitatively stains DNA. The amount of DNA was measured by the fluorescence intensity of the stained cells. For the investigation of cell cycle arrest stage , $1x10^6$ cells were treated with IC 50 and ½ IC 50 of ALA and GLA for 18 h. Cells were washed with PBS, fixed with methanol and kept at -20 °C for 3 min. Subsequently, cells were suspended in cold PBS and kept at 4 °C for 90 min. Cells were pelleted down, dissolved in PBS, treated with RNase for 30 min at 37 °C, stained with PI and kept in dark for 15 min. Cell cycle phase distribution of nuclear DNA was determined on FACS, fluorescence detector equipped with 488 nm argon laser light source and 623 nm band pass filter (linear scale) using BD FACS software 1.2.0.87 (BD Influx cell sorter, USA) [63].

3.2.1.6 Annexin-V FITC dot plot assay

Annexin-V FITC is a 35–36 kDa Ca^{2+}dependent phospholipid-binding protein, which has high affinity for phosphatidyl serine (PS), and it binds to the exposed cell surface of apoptotic cell. The ER+MCF-7 cells ($1X10^6$) were treated with individual IC50 and ½ IC 50 dose of ALA and GLA for 18 h. The cells were pellet down, centrifuged at 2000 rpm for 8 min at 4 °C and washed with annexin-V FITC binding buffer provided in apoptosis kit. After centrifugation at 2000 rpm at 4 °C, the cell pellets were dissolved in annexin-V FITC binding buffer containing annexin-V FITC and PI. The flow cytometric analysis was done after 15 min in dark at room temperature. All the data were acquired with a BD Influx cell sorter, USA. The reading were taken by using 488 nm excitation and band pass filters of 530/30 nm (for FITC detection) and 585/42 nm (for PI detection). For the alignment of X and Y mean values of annexin-V FITC or PI stained quadrant populations, live statistics were used. Data analysis was performed with BD FACS software 1.2.0.87 [64].

3.2.2*In vivo* study

3.2.2.1 Hemodynamic Study

The animals were anesthetized on 111thday of the study by using the combination of ketamine hydrochloride (50 mg/kg, i.m.) and diazepam (2.5 mg/kg, i.m.) and mounted on a wax tray. The platinum hook electrodes were placed on the skin of the dorsal and ventral thorax to record the electrocardiogram (ECG) signal. The electrodes were connected to Bio-amplifier (ML-136) and channel power lab (ML-826) to convert analogue to digital signals (AD Instruments, Australia).The ECG signals were saved on the hard disk and analyzed offline using Lab Chart Pro-8 (AD Instruments, Australia).

Heart rate variability (HRV) analysis was conducted on multiple segments of continuous ECG signals. Firstly, all the raw signals were inspected manually to ensure that all the R-waves were detected correctly. Subsequently, heart rate (HR) was calculated by plotting the number of R waves per unit time. Following the same, time and frequency domain parameters of HRV were also calculated using Lab Chart Pro-8 (AD Instruments, Australia) [65].

3.2.2.2 Morphological analysis of mammary gland tissue

Carmine staining of whole mounts mammary gland

The mammary glands obtained from female albino wistar rats were stretched onto a slide and kept in a fixative solution (60:30:10 ratio of ethanol: chloroform: acetic acid), stained with a carmine solution for 2 days, washed with 90%, 70%, 35% and 15% ethyl alcohol for 1 h respectively and lastly rinsed with distilled water for three times at 5 min interval. The tissue sample was dehydrated in ascending grades of alcohol and dipped in xylene at least for two days. Carmine alum stain was prepared with 1 gm carmine and 2.5 gm aluminum potassium sulfate in 450 ml distilled water and boiled

for 20 min. The final volume was adjusted to 500 ml with distilled water. Whole mounts were examined under the 4X microscope and evaluated for alveolar buds (ABs) [66, 67].

Histopathology of mammary gland tissue

A small piece of mammary gland tissue was fixed in 10% solution of formaldehyde and embedded in the wax. 5µm sections were prepared using microtome followed by staining with hematoxyline and eosin (H&E). The sections were visualized and photographed at 40X using digital biological microscope (N120, BR-Biochem Life Sciences, New Delhi, India) [68].

SEM of mammary gland tissue

The HCl-collagenase and enzymatic digestion methods were used for the purpose of SEM. Small sections of mammary gland tissues treated with HBSS containing 100µg/ml collagenase (type 4) and 2.5 TRU (turbidity reduction unit)/ml of hyaluronidase for 30 min at 37°C. After digestion, the tissue was rinsed in the HBSS and then fixed in 4% glutaraldehyde in 0.1 M cacodylate/HCl buffer (pH 7.2) at room temperature for 3 h. Post fixation was done with 1% osmium tetraoxide. Tissue sample was subsequently placed in 8 N HCl for 30 min at 60°C.After HCI digestion, the tissue was rinsed three times with distilled water to remove the acid. The sample was dried with 70%, 80%, 90% and 100% acetone. All the specimens were dehydrated, dried by the critical point method and examined under SEM(X1000) (JEOL JSM-6490LV) [69].

3.2.2.3 Antioxidant markers

The mammary gland tissue homogenates (10% w/v) were prepared in 0.15M KCl and centrifuged at 10,000 rpm. The supernatants were evaluated for oxidative stress markers, including thiobarbituric acid reactive substances (TBARs), superoxide

dismutase (SOD), catalase, glutathione (GSH) and protein carbonyl (PC) using the methods established in our laboratory [70].

3.2.2.4 ^{1}H-NMR based serum metabolomics

Sample preparation for NMR spectroscopy

The stored serum samples were thawed at room temperature, 250µl of serum was taken and mixed with 250µl of sodium-phosphate buffer of strength 20mM, pH 7.4 with 0.9% saline prepared in D_2O (as a co-solvent and to provide a deuterium field/frequency lock). To remove any precipitates or cellular debris, the samples were further centrifuged at 10,000 rpm for 5 min at room temperature. The clear supernatant fluid of 400µl was finally used in 5 mm NMR tubes (Wilmad Glass, USA) for data acquisition with a co-axial insert containing the 0.1mM concentration of trimethylsilylpropionic acid-d4 (TSP) (used here as external standard reference to aid spectral calibration). D_2O and sodium salt of TSP used for NMR experiments were purchased from Sigma-Aldrich (Rhode Island, USA) [71].

NMR data acquisition

The ^{1}H NMR spectra of all the samples were acquired on 800 MHz NMR spectrometer (BrukerAvance-III) equipped with the cryoprobe at 300 Kelvin (K). On each serum sample, the 1D ^{1}H transverse relaxation-edited CPMG (Carr–Purcell–Meiboom–Gill) NMR spectra were recorded using the standard Bruker's pulse program library sequence (cpmgpr1d) with pre-saturation of the water peak through irradiating it continuously during the recycle delay (RD) of 5 sec. Each spectrum consisted of the accumulation of 128 scans and lasted for approximately 15 min. To remove broad signals from proteins and fats, a total spin–spin relaxation time of 60 ms (n=300 and 2τ=200µs) was applied. Each FID (free induction decay) was zero filled and Fourier-transformed to 64 K data points following manual phase and baseline-correction. A

line broadening factor of 0.3 Hz and a sine–bell apodization function was applied to FIDs before Fourier Transformation (FT). The raw NMR data were processed using Bruker software Topspin-v2.1 (BrukerBioSpin GmbH, Silberstreifen 4 76287 Rheinstetten, Germany) [72].

Assignment of the ^{1}H NMR spectra

The metabolite resonances in the 1D ^{1}H CPMG NMR spectra were assigned using the Chenomx NMR suite (Chenomx Inc., Edmonton, AB, Canada). The remaining peaks in the CPMG ^{1}H NMR spectra were assigned as far as possible, by comparing them with the chemical shifts available using previously reported NMR assignments of metabolites, data obtained from BMRB database (Biological Magnetic Resonance Data Bank) and HMDB (The Human Metabolome Database) [73].

Multivariate statistical analysis

The ^{1}H NMR spectra of all the serum samples were manually phase adjusted and baseline corrected after referencing to the alanine resonance at δ(1.46) ppm. The CPMG δ 9.5-0.7 ppm spectra were binned and automatically integrated using AMIX package (Version 3.8.7, Bruker, BioSpin), to reduce the complexity to the NMR data and facilitate pattern recognition. The region distorted due to water suppression δ (5.5-4.5) ppm, were excluded from the CPMG data set. Finally, the selected regions were reduced to spectral bins of δ 0.01 ppm. The resultant CPMG, data sets were eventually used for univariate and multivariate analysis in statistical analysis module of MetaboAnalyst, an open access web-based tool for metabolomics studies.

Using standard procedures for multivariate statistical analysis in MetaboAnalyst, partial component analysis (PCA), partial least square discriminant analysis (PLS-DA), and orthogonal projection to latent structure with discriminant analysis (OPLS-DA) were performed on all the groups to get an overview of the grouping trends and to

separate the effective treatment dose. The PLS-DA model was further used for pairwise analysis to identify the metabolites responsible for discrimination based on their higher values of variable importance on projection scores (i.e. VIPs >1). Furthermore, unpaired t-test was applied to assess the significance of change in the metabolic profile and p-value <0.05 was used as the criterion for statistical significance. Metabolites meeting the above said criteria were considered to be significant. A 10-fold cross-validation algorithm using the top 5 latent variables, was used which helped to evaluate 100% classification accuracy, along with the goodness-of fit parameter (R2) and the goodness of prediction parameter (Q2) values to assess the quality (or predictability) of the models, respectively [74].

3.2.2.5 Assay for caspase 3 and caspase 8

Caspase 3 and caspase 8 fluorometric assays were performed using the methods elaborated in the literature provided with the kits. The assay was carried out in amber colored 96-well plate. Equal volumes of serum sample from both control and experimental animals were diluted with reaction buffer. Dithiothriol (DTT) was added to a final concentration of 10mM. To the reactant mixture 5µl of IETD-AFC/DEVD-AFC substrate was added and incubated for 1 h at 37°C. Free AFC levels formed were measured in a plate reader with a 400 nm excitation and a 505 nm emission. The results were expressed as fluorescence units/mg of protein [75].

3.2.2.6 Western Blotting

Total protein lysates were obtained by lysing the mammary gland tissue in RIPA lysis buffer. The protein content was quantified using the Bradford reagent [76]. According to the principles of Laemmli with slight modifications, proteins were resolved on 12.5% SDS-PAGE gel and transferred to PVDF membrane (IPVH 00010 Millipore, Bedford, MA USA. Subsequently, membrane was blocked with 3 % BSA and 3 % not

fat milk in TBST for 3 h and incubated overnight with primary antibody against, Bcl-xl (MA-5-15142), Bcl-2 (SC-7382), BAX (SC-23959), BAD (SC-8044) VDAC (SC-390996), cytochrome c (SC-13561), Apaf-1 (SC-65891) and procaspase 9 (SC-73548) NFκBp65 (MA5-1616), UCHL-1 (MA1-83428), prolyl hydroxylase-2 (PHD-2) (SC-67030), hypoxia inducible factor-1α (HIF-1α) (SC-13515), fatty acid synthase (FASN) (SC-55580), SREBP-1c (SC-13551), α-7nAChR (SC-5544), TNF-α (SC-1350) and HMGB-1 (SC-56698) at 4°C. β-actin (MA5-15739-HRP) was used as a standard reference. The membrane was washed with TBST thrice and incubated with the corresponding anti-rabbit (SC-2030), anti-goat (SC-2020), anti-mouse (31430, Pierce Thermo Scientific, USA) HRP conjugated secondary antibody (1:5000 dilutions) at room temperature for 3 h. After single TBST wash membrane were developed using an enhanced chemiluminescence substrate (Western Bright ECL HRP substrate, Advansta, Melanopark, California, US) in gel dock system. The quantification of protein was done through densitometry digital analysis of protein bands using Image J software [77].

3.2.2.7 qRT-PCR study

The qRT-PCR primers were designed through primer quest tool from the IDT DNA Technologies website (www.idtdna.com). The amplicon size was kept between 100 to 200 base pairs; GC% was held above 50% and melting temperature was maintained between 58°C to 62°C. The sequence of primers was mentioned in table 2.

Total RNA was extracted using trizol reagent (Invitrogen, Life Technologies) using the provided literature. Mammary gland tissues were washed off using 0.1% DEPC water and crushed in 250µl trizol reagent. The final volume was made upto 1ml, followed by addition of 200µl of chloroform and vortex mixing for 2 to 5 min. The suspension was centrifuged at 14,000 rpm, 4°C for 15 min and upper aqueous phase was collected in

the fresh vials. The RNA was precipitated using isopropanol and quantified through nanodrop (Qua Well Q5000) using the method described previously. RNA thus obtained was used for the cDNA synthesis in a 96 well thermal cycler (BioRad, C1000) using high capacity cDNA synthesis kit (Applied Biosystems). cDNA sample was quantified using nanodrop and was stored at -80°C until use. 125ng of cDNA was used as a template for each reaction of qRT-PCR with β-actin as housekeeping control using light cycler 480 machine (Roche Diagnostics, Germany). For each primer pair, a melting curve analysis was performed according to the instrument. The program in brief was an initial incubation of 50°C for 2 min hold (UDG incubation) and 95°C for 10 min followed by 40 cycles at 95°C for 15 s (denaturation), 58°C for 30 s (annealing) and final extension at 72°C for 20 s. Differential expression was calculated by the 2-ΔΔCT method. β-actin was used as internal control and used to normalize ratios between samples [78].

3.2.3 *C.elegans* study

3.2.3.1 ALA treatment

Different concentration of ALA i.e. 5%, 10%, 20%, 40% were mixed with Escherichia coli OP50 and 100µl of the food was seeded on to NGP plates and incubated overnight at 37ºC. Age synchronized embryos were added onto the treatment plates and the experiments were conducted using adult worms.

3.2.3.2 Effect on synaptic Ach levels as deduced through aldicarb assay

Aldicarb assay is an indirect assay to check the relative effect on neurotransmission and Ach levels within the synapse. The age-synchronized embryos were added to treatment plates and incubated at 22°C for 48 h. Adult worms were washed thrice from treatment plates using M9 buffer. A fixed number of worms say 30 to 40 were transferred to 0.5mM aldicarb NGM plates. The worms were scored for paralysis every

30 min and were prodded using eye lash. As a convention, the worms that lacked movement even after prodding thrice were considered as paralyzed. Any worms lost or damaged were disregarded from the study. The experiment was done in duplicate sets and percentage of worms paralyzed was calculated [79].

3.2.3.3 Relative quantification of Ach levels and AchE activity

Ach levels and AchE activity were determined using Amplex Red Ach/AchE estimation kit according to the manufacturer's protocol. The age-synchronized embryos were added to treatment plates and incubated at 22°C for 48 h. Adult worms were washed thrice using M9 buffer and sonicated in 1X reaction buffer (supplied in the kit) for 3 min. Worm suspension was then centrifuged at 7000 rpm for 7 min.

For estimation of Ach levels 100µl of supernatant was added to 100µl of reaction mixture which was prepared by adding 200µl of 20mM amplex red solution (prepared by dissolving 1mg of amplex red in 200µl of DMSO), 100µl of 200U/ml HRP solution (prepared by adding 1ml of 1X reaction buffer to 1 vial of HRP), 100µl of 100U/ml AchE solution (prepared by dissolving contents of one vial of AchE in 600µl of 1X reaction buffer) and 100µl of 20U/ml choline oxidase solution (prepared by dissolving contents of 1 vial of choline oxidase in 600µl of 1X reaction buffer) in 10ml q.s. of 1X reaction buffer in black well plates.

For estimation of AchE activity, 100µl of supernatant was added to 100 µl of reaction mixture which was prepared by adding 200 µl of 20mM amplex red solution, 100 µl of 200 U/ml HRP solution, 10 µl of 100 mM Ach solution and 100 ml of 20 U/ml choline oxidase solution in 10 ml q.s. of 1X reaction buffer in black well plates.

The plates for both Ach and AchE activity were incubated at room temperature for 30 min and fluorescence was read using 96 well plate fluorimeter (BMG Polarstar Galaxy) at excitation 544 nm and emission at 590 nm. The relative fluorescence was

normalized with protein content of sample calculated using Bradford method and RFU per µg of protein was calculated to estimate the relative Ach levels [80].

3.2.3.4 Staining of active mitochondria using Mitotracker red

Mitotracker Red is a mitochondria specific dye which stains active mitochondria on the basis of membrane potential. Briefly, mitotracker red CM-H2XRos was mixed with E. coli OP50 before seeding it to the NGM plates to check the healthy mitochondrial staining. Mitotracker red stock solution was prepared by dissolving 50µg mitotracker red CM-H2XRos in 1ml of 10% DMSO. A working concentration of 10µM mitotracker red was fed to the worms by mixing it with E. coli OP50. The synchronous embryos were transferred onto the mitotracker red with 1% BSA containing plates and grown for 48 h at 22ºC. Worms were washed off using M9 buffer and kept in OP50 solution for 30 min and again washed thrice with M9 buffer. Backdrop background suppressor has been used for respective red channel to reduce the background noise and enhance signal to noise ratio. The worms has been fixed using BD Cytofix/Cytoperm kit and mounted with gold-antifade reagent in coverslip. The staining of mitochondria was measured using fluorescence microscope in TRITC channel [81].

3.2.3.5 Estimation of lipid content using Nile red staining

The effect on lipid content of *C. elegans* was studied by staining worms with a lipid specific dye, Nile Red. A stock solution of nile red was prepared by dissolving 0.5mg nile red dye in 1 ml of acetone. The stock solution was further diluted in bacteria E. coli at a dilution of 1:250 and was seeded onto treatment plates. Age synchronized embryos, isolated through sodium hypochlorite treatment were transferred onto the Nile red-containing treatment plates and incubated for 48 h at 22°C and 48 h at 15°C. The worms were washed thrice with M9 Buffer and were anesthetized by adding 10 µl

of 100mM sodium azide in 100µl of worm suspension. The coverslip was mounted with gold-antifade reagent and sealed using transparent nail paint. The worms were observed in fluorescence microscope (Leica) for visualization lipid droplets using TRITC filter [82].

3.2.3.6 qRT-PCR study

The qRT-PCR primers were designed through primer quest tool from the IDT DNA Technologies website (www.idtdna.com). The amplicon size was kept between 100 to 200 base pairs; GC% was held above 50% and melting temperature was maintained between 58°C to 62°C. The sequence of primers was mentioned in table 2.

Total RNA was extracted using trizol reagent (Invitrogen, Life Technologies) using the provided literature. Worms were washed off using 0.1% DEPC water and crushed in 250µl trizol reagent. The final volume was made upto 1ml, followed by addition of 200µl of chloroform and vortex mixing for 2 to 5 min. The suspension was centrifuged at 14,000 rpm, 4°C for 15 min and upper aqueous phase was collected in the fresh vials. The RNA was precipitated using isopropanol and quantified through nanodrop (Qua Well Q5000) using the method described previously. RNA thus obtained was used for the cDNA synthesis in a 96 well thermal cycler (BioRad, C1000) using high capacity cDNA synthesis kit (Applied Biosystems). cDNA sample was quantified using nanodrop and was stored at -80°C until use. 125ng of cDNA was used as a template for each reaction of qRT-PCR with β-actin as housekeeping control using light cycler 480 machine (Roche Diagnostics, Germany). For each primer pair, a melting curve analysis was performed according to the instrument. The program in brief was an initial incubation of 50°C for 2 min hold (UDG incubation) and 95°C for 10 min followed by 40 cycles at 95°C for 15 s (denaturation), 58°C for 30 s (annealing) and final extension at 72°C for 20 s. Differential expression was calculated

by the 2-ΔΔCT method. β-actin was used as internal control and used to normalize ratios between samples [83].

Table 2: Reverse and forward sequence of primers

Primer	Sequence
Bcl2 F	GTGGATGACTGAGTACCTGAAC
Bcl2 R	GAGACAGCCAGGAGAAATCAA
Bcl-xl F	CCCTCGTATCTGGAAGCCAC
Bcl-xl R	CAGCGGAGACCTCGTTTTCT
BAD F	CTCCGAAGAATGAGCGATGAA
BAD R	ATCCCACCAGGACTGGATAA
BAX F	CTCCGAAGAATGAGCGATGAA
BAX R	ATCCCACCAGGACTGGATAA
VDAC F	GGAGTTTGGTGGCTCCATTTA
VDAC R	GACCTGATACTTGGCTGCTATTC
Cytochrome-c F	TCCATTTCCCTTCCTTGGGC
Cytochrome-c R	ATCGGGGCTGTCCAACAAAA
Apaf-1F	GAACATAGACTCCCGGGTAAAG
Apaf-1R	CTTGTCTCCCAGACCCTTATTG
Procaspase9 F	GGCTCTCTGGCTTCATTCTT
Procaspase9 R	GGGTCCAGCTTCACTACTTTC
PHD2 F	ACGCAGTTCATACCCAGTTAG
PHD2 R	CCTGTCCACTCTCAGCTTTAC
HIF1-α F	GATGGGTTATGAGCCAGAAGAA
HIF1-α R	CTGTGGTGACTTGTCCTTTAGT
FASN F	GGCGAGTCTATGCCACTATTC
FASN R	GCTGATACAGAGAACGGATGAG
SREBP-1c F	TCCGAGTTCCAGGTAGGGTT
SREBP-1c R	CTTGGCGCACACCAAATACC
UCHL-1 F	CGCCTCTGCCCTGAGTTATT
UCHL-1 R	CCGTCTGGGTCAATCCTCTG
NFκBp65 F	GGGCTACGAAGTCAAACCCA
NFκBp65 R	TTCTCCTCAATCCGGTGACG
α-7nachr F	AGACCTGGTATGGAGACCCC
α-7nachr R	ATCTTGCTGGGCTGAGCATT
HMGB-1 F	AAGACGACGAGGAGGATGAA
HMGB-1 R	ACTGCGCTAGAACCAACTTATT
TNF-α F	GCAGGTCTACTTTGGAGTCATT
TNF-α R	GGCTCTGAGGAGTAGACGATAA
β-actin F	TGCAGGATCGTGAGGAACAC
β-actin R	AGCGTGATTGTAACGCCTGA
ace-1 F	CTG CTA CCA CGT CAG ATA C
ace-1 R	TGA GCC AGA GCC ATT TC
ace-2 F	CTG TAG CTC ACC GGA TAT G
ace-2 R	GTC GCC CTG GAA GAA AT
cho-1 F	GTC GCC CTG GAA GAA AT
cho-1 R	CCA CCG GTG AAT GTG TAG
cha-1 F	GGG AAA GGG AAG AAA CGA
cha-1 R	GGA CCA CTG CAC CAT AC
unc-17 F	ACC ATC ACA ACC TGG ATG TCC GAA
unc-17 R	TCC ATA GCC AAC CCA ACC ATA GCA
unc-29 F	CGA GGA CCA AGA ACT CAT C
unc-29 R	ACT GTC CAA CTC CTG GTA
unc-38 F	CGC TGA CAG CAA CTA CA
unc-38 R	CAG GAG CCG AAC TTC AA
unc-50 F	CAT CCC AGT CAC CGA TTT
unc-50 R	TGA GAG CTT GGC GAA TG

CHAPTER 4
RESULTS AND DISCUSSION

4. Results

4.1 *In vitro* study

4.1.1 MTT assay

ALA and GLA (1µM, 5µM, 10µM, 15µM, 20µM, and 25µM) significantly inhibited the growth of ER+MCF-7 cells compared with control and tamoxifen (TMX) treated cells. The IC50 value of ALA and GLA was found to be 17.55µM and 16.77µM against ER+MCF-7 cells respectively (Figure1 and 2) after 24 hr treatment. MTT assay confirmed significant cytotoxic and apoptotic potential of ALA and GLA against ER+ MCF-7 cells.

Figure 1: Cytotoxicity assessment of ALA

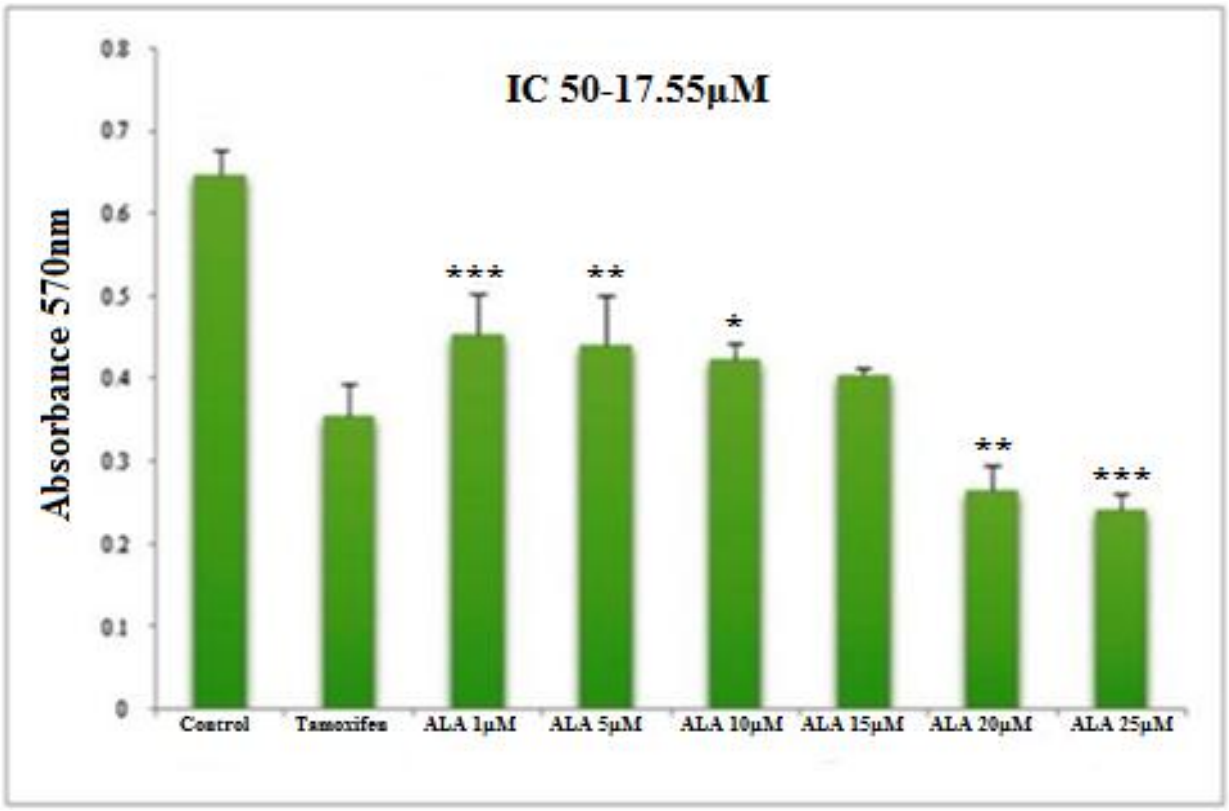

Histogram reveals the effect of ALA (1µM, 5µM, 10µM, 15µM, 20µM and 25µM) on cell cytotoxicity by MTT assay on ER+MCF-7 cells after 24 h incubation. The O.D. at 570 nm was compared with the untreated cell and TMX (27µM) treated cells. Reduction

in the O.D. at 570 nm was observed in a dose dependent manner. Values are presented as mean ± SD and denote significant decreased in O.D. at 570 nm from control values. The comparisons were made by one-way ANOVA followed by Bonferroni multiple test.

Figure 2: Cytotoxicity assessment of GLA

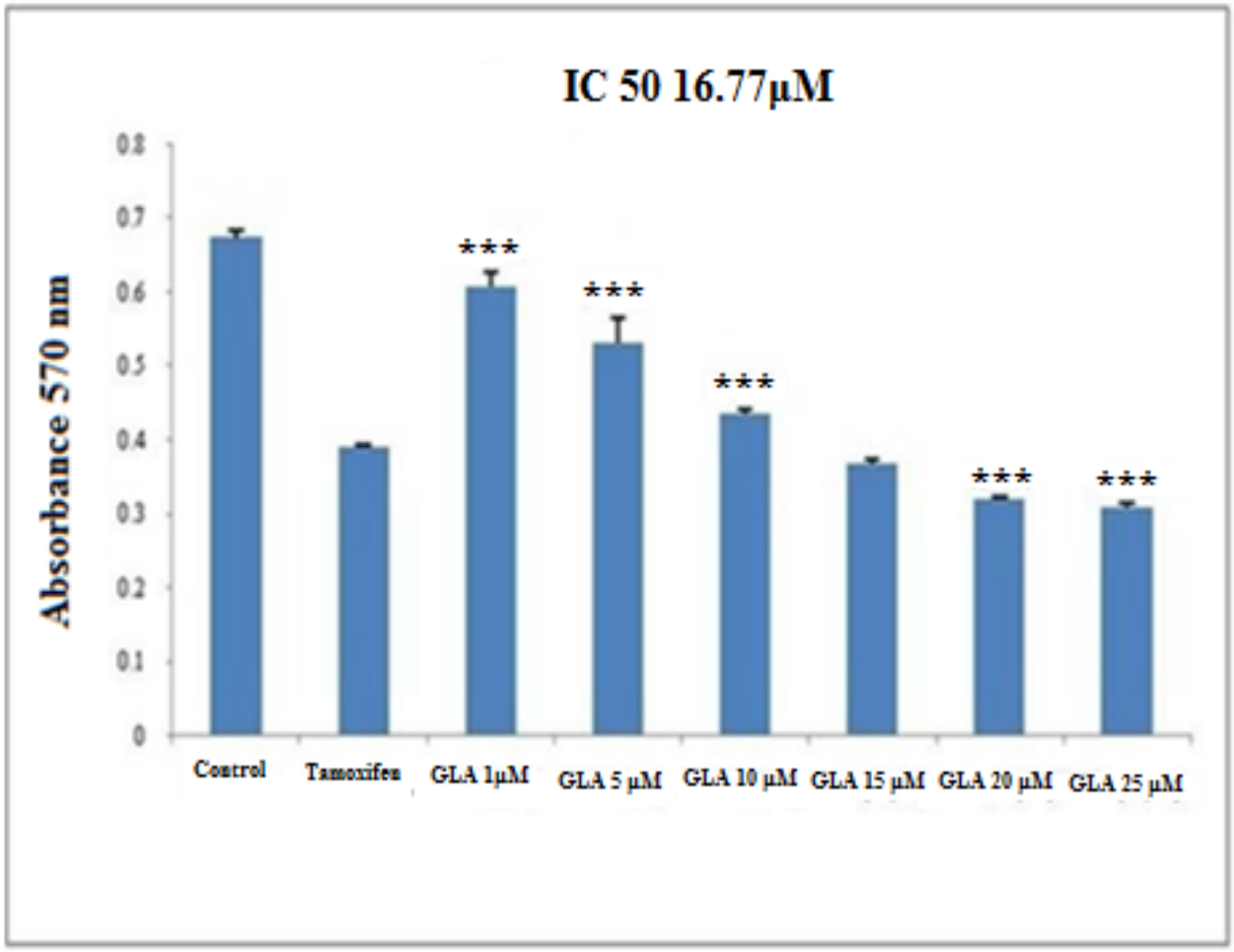

Histogram reveals the effect of GLA (1µM, 5µM, 10µM, 15µM, 20µM and 25µM) on cell cytotoxicity by MTT assay on ER+MCF-7 cells after 24 h incubation. The O.D. at 570 nm was compared with the untreated cell and TMX (27µM) treated cells. Reduction in the O.D. at 570 nm was observed in a dose dependent manner. Values are presented as mean± SD and denote significant decreased in O.D. at 570 nm from control values. The comparisons were made by one-way ANOVA followed by Bonferroni multiple test.

4.1.2 Morphological studies for detection of apoptosis

Fluorescence microscopic observations of the ER+MCF-7cells stained with AO/EtBr (color-red or orange), revealed the presence of early and late apoptotic signals including membrane blebbing and fragmented nuclei. AO/EtBr staining affirmed late and early apoptotic changes in the ER+ MCF-7 cells induced by ALA and GLA treatment. The images were captured with 40X resolution (Figure 3 and 4).

Figure 3: Effect of ALA on early apoptotic changes studied through AO/EtBr staining

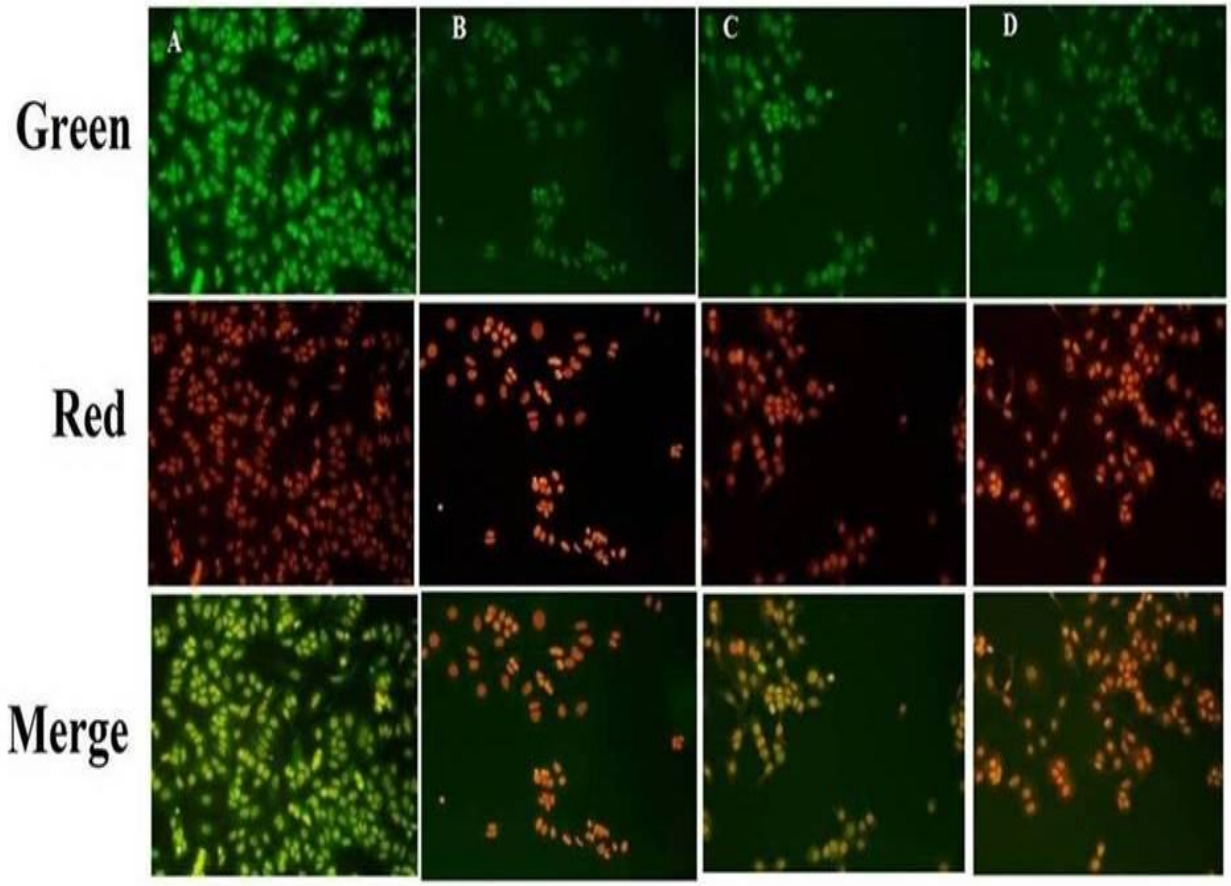

In fluorescence microscopic study of control (A); standard: TMX (B); ALA (1/2 IC50) (C); ALA (IC50) (D) with dual staining [AO (100µg/ml): EtBr (100µg/ml) in 1:1 ratio]. The fluorescence was measured in three respective channels (green, red and merged) with 20X magnification, which reveals the morphological changes of apoptosis in experimental procedure after 18h drug treatment.

Figure 4: Effect of GLA on early apoptotic changes studied through AO/EtBr staining

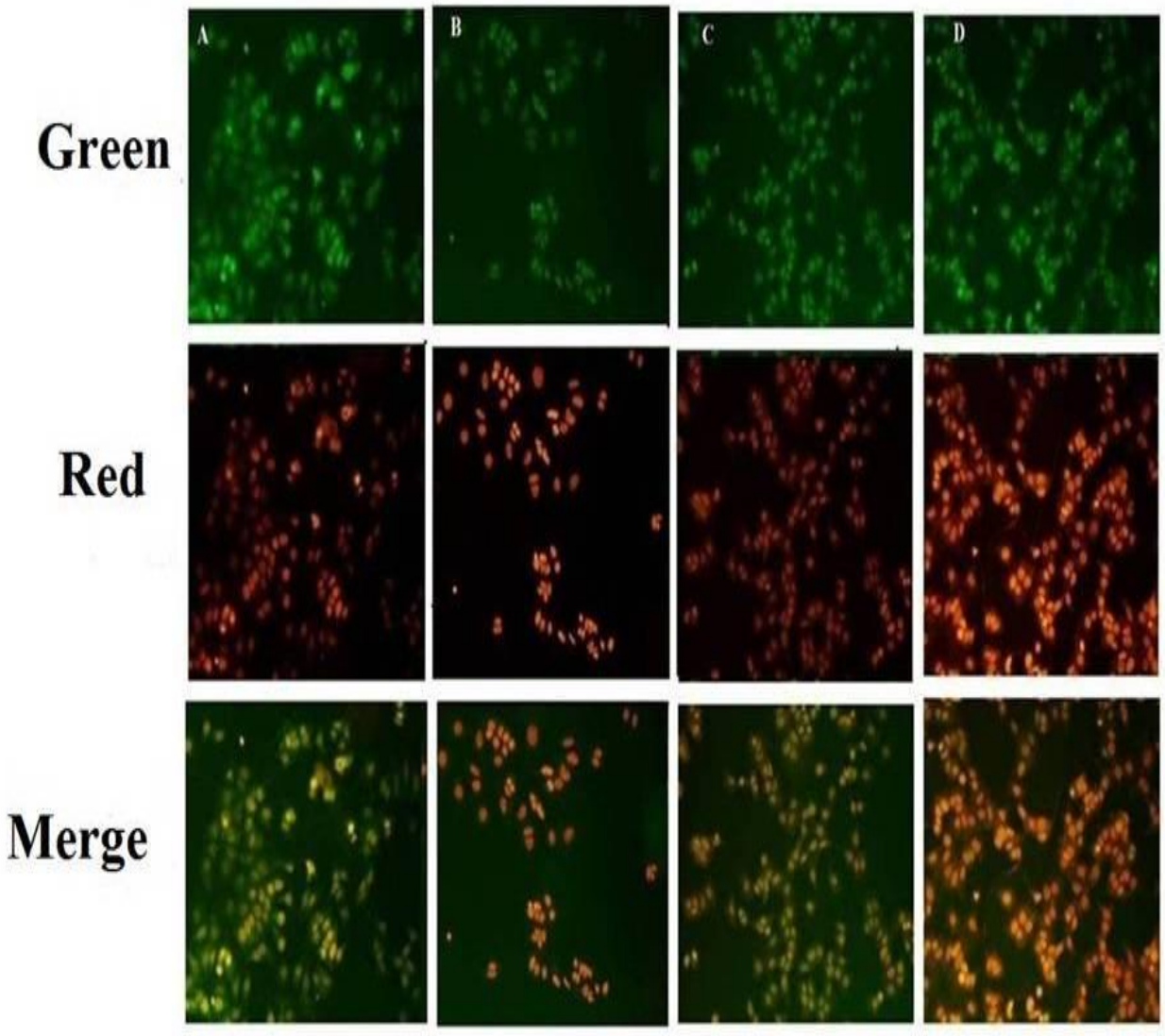

Control (A); TMX (B); GLA (1/2 IC 50) (C) and GLA (IC 50) (D) were dual stained with AO/EtBr (100µg/ml) dye in 1:1 ratio. Green, red and merged channels were used for the measurement of fluorescence with 40X magnification. The conversion in fluorescence spectra from complete green (control) to red (treated) is a clear indication of AO accumulation in apoptotic cell, which is more clearly reflected in the presence of fragmented nuclei and membrane blebbing.

4.1.3 Measurement of mitochondrial membrane potential

JC-1 is a cationic dye, used to study mitochondrial depolarization. Mitochondrial depolarization is indicated by an increase in green fluorescence intensity and decrease in orange intensity due to failure in intracellular accumulation of J-aggregates. The monomeric forms representing disruption of active mitochondrial membrane and loss of conformation in mitochondria permeability transition pore (MPTP). ALA and GLA treated ER+ MCF-7 apoptotic cells failed to accumulate the J-aggregrate due to loss of membrane potential. Inhibition of J-aggregrate formation was clearly noticeable through an increase in intensity of green fluorescence. The images were captured with 40X resolution (Figure 5 and 6).

Figure 5: Effect of ALA on mitochondrial membrane potential (Δψ)

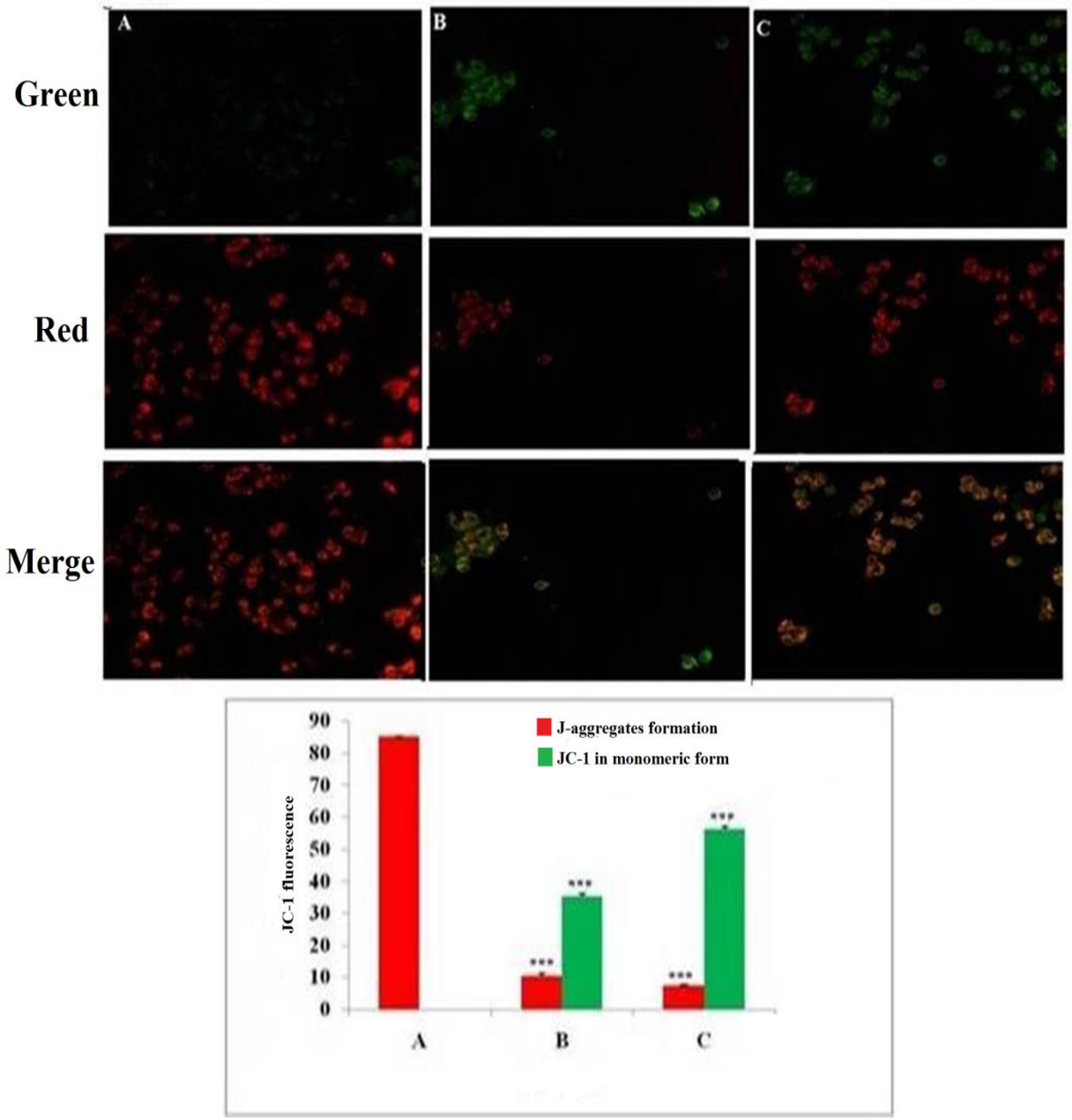

ER+MCF-7 cells treated with control (A); ALA (1/2 IC50)(B); ALA (IC50) (C) for 18h and proceeded with JC-1 dye (5 mg/ml) for 1h. The cells were examined under inverted fluorescence microscope in three respective channels (green, red and merged). Internal accumulations of JC-1 aggregate in apoptotic cells are represented through change in ratio of orange to green fluorescence intensity in merged channel. Values are presented as mean ± SD and the comparisons were made on the basis of one-way ANOVA followed by Bonferroni multiple test.

Figure 6: Effect of GLA on mitochondrial membrane potential (Δψ)

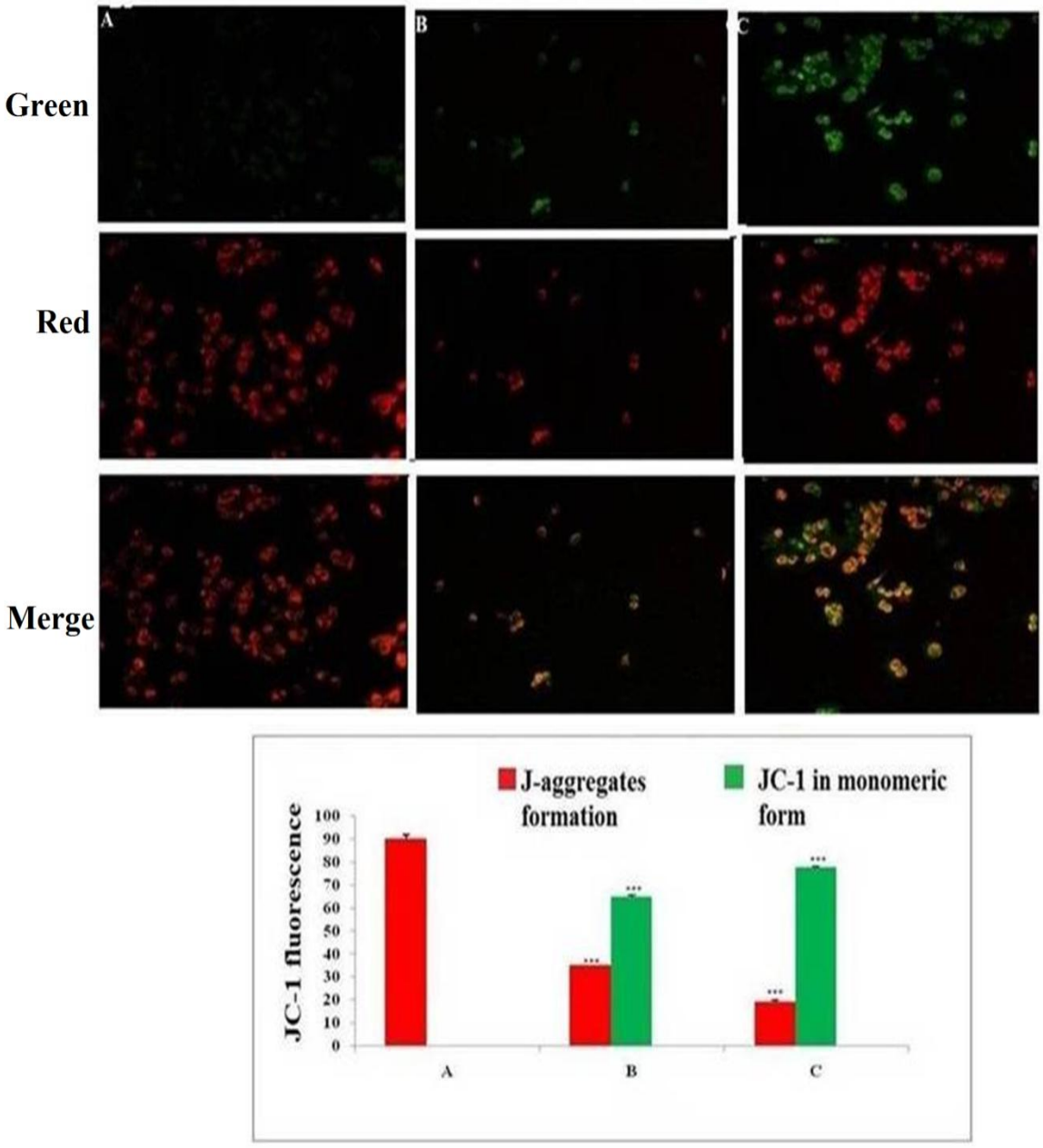

Control (A); GLA (1/2 IC 50) (B) and GLA (IC 50) (C) were proceeded with JC-1 dye (1mg/ml) for 1h. Green, red and merged channels were used under inverted fluorescence microscope with 40X magnification. GLA treated ER+ MCF-7 cells are failed to accumulate the JC-1 due to loss of membrane potential (Δψ), which clearly vivid through increase in green fluorescence from JC-1 monomeric form. The observed results are expressed as mean ± SD and the comparisons are made on the basis of one-way ANOVA followed by Bonferroni multiple test.

4.1.4 Cell cycle analysis using PI

Flow cytometric analysis showed that treatment with ½ IC50 dose of ALA increased the DNA content by 1.20 fold than that of control in G0/G1 phase (P3). ALA also increased apoptotic cell burden by 2.07 fold in apoptotic phase (P6). ALA treatment was evident for the cell death in S (P4) and G2M (P5), along with increase in the apoptotic cell burden by 7.86 fold. The results indicated that ALA treatment arrested the cell cycle in G2/M phase (Figure 7).

GLA treated ER+ MCF-7 cells when compared with control cell population ($1X10^6$) after PI staining; a drop in G0/G1 cell population (10%) was noted after flow cytomertic analysis which clearly correlate the decreased number of dividing cells in G0/G1 phase of cell cycle with an increase in apoptotic cell burden (P6) (Figure 8).

Figure 7: Role of ALA on cell cycle arrest of ER+MCF-7 cells

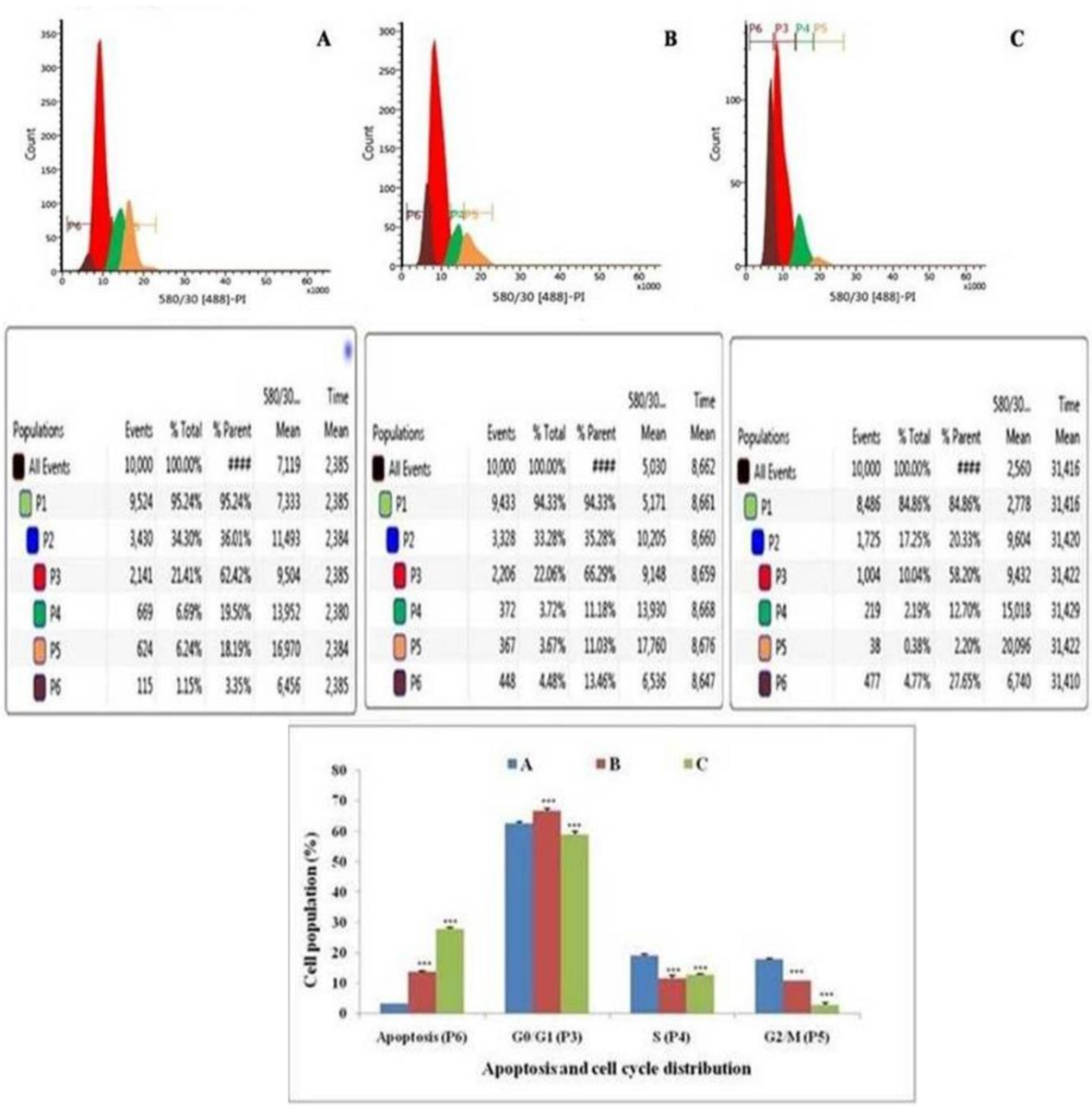

Flow cytometric analysis of cell cycle phase distribution was performed in control (A); ALA (1/2 IC50) (B); ALA (IC50) (C) after 18 h of treatment using PI staining. The histogram represents various content of DNA with actual number of cell present in three stages G0/G1 (P3), S (P4) and G2/M (P5). (X axis denotes fluorescence intensity of PE Texas red and Y axis denotes count). Values are presented as mean ± SD and the comparisons were made on the basis of one-way ANOVA followed by Bonferroni multiple test.

Figure 8: Role of GLA on cell cycle arrest of ER+MCF-7 cells

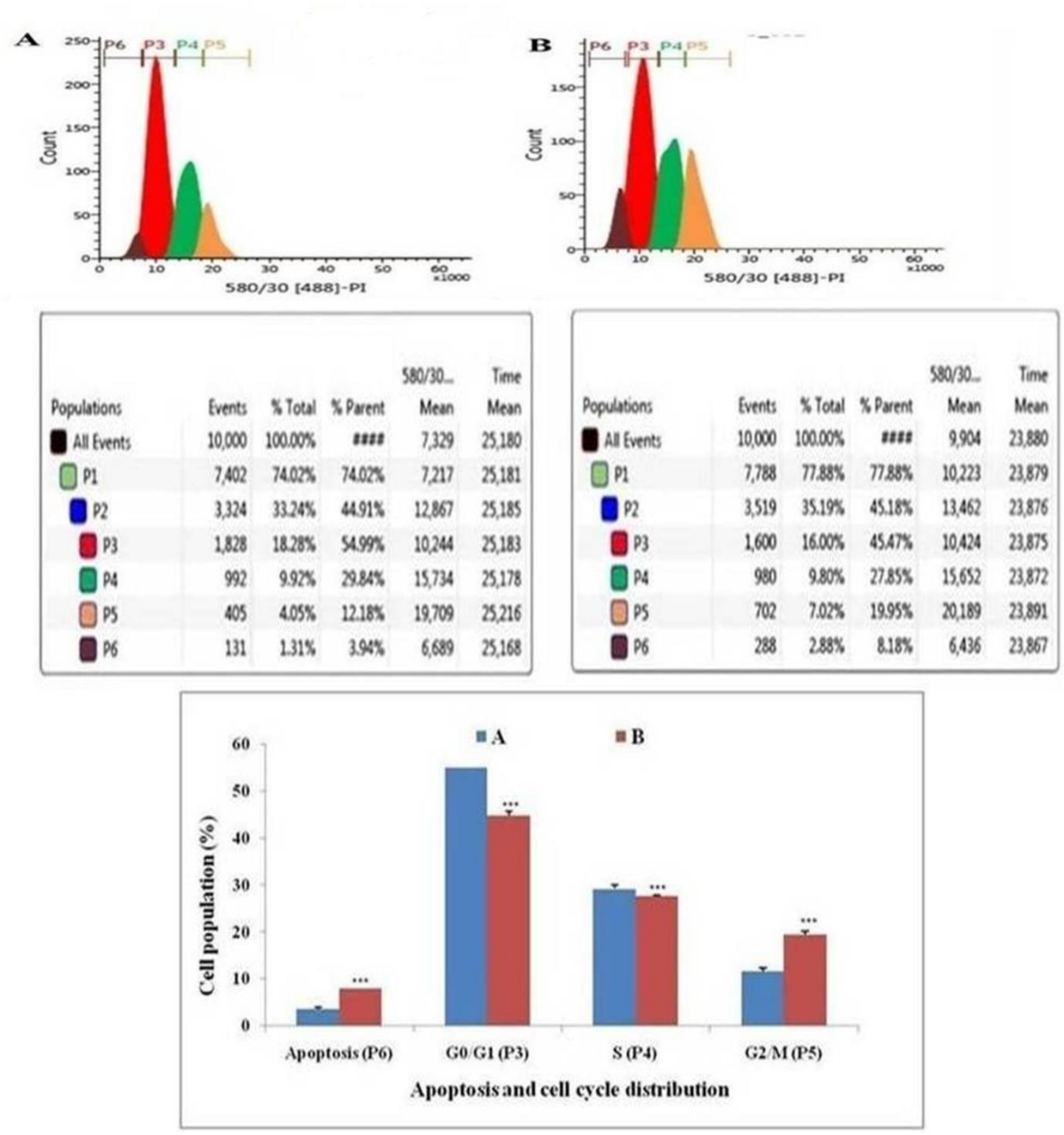

Populations	Events	% Total	% Parent	580/30... Mean	Time Mean
All Events	10,000	100.00%	####	7,329	25,180
P1	7,402	74.02%	74.02%	7,217	25,181
P2	3,324	33.24%	44.91%	12,867	25,185
P3	1,828	18.28%	54.99%	10,244	25,183
P4	992	9.92%	29.84%	15,734	25,178
P5	405	4.05%	12.18%	19,709	25,216
P6	131	1.31%	3.94%	6,689	25,168

Populations	Events	% Total	% Parent	580/30... Mean	Time Mean
All Events	10,000	100.00%	####	9,904	23,880
P1	7,788	77.88%	77.88%	10,223	23,879
P2	3,519	35.19%	45.18%	13,462	23,876
P3	1,600	16.00%	45.47%	10,424	23,875
P4	980	9.80%	27.85%	15,652	23,872
P5	702	7.02%	19.95%	20,189	23,891
P6	288	2.88%	8.18%	6,436	23,867

Control (A) and GLA IC50 (B) treated cells were stained with PI. The content of DNA along with actual number of cells are represented in histogram as P6 (apoptosis), P4 (S) and P5 (G2/M). Experiments were performed in triplicate. The data is represented as mean ± SD and the comparisons are made on the basis of one-way ANOVA followed by Bonferroni multiple test.

4.1.5 Annexin-V FITC dot assay

Translocation of PS to the outer leaflet of the cellular membrane form inner leaflet is a key hall mark of apoptosis and could be validated through Annexin-V, (calcium-dependent phospholipid binding protein) labeled with FITC and PI [84]. Lower left quadrant (Q1) is regarded as the population of live cells, lower right quadrant (Q2) is considered as the cell population at early apoptotic stage, upper right (Q3) quadrant represents the cell population at late apoptotic stage and upper left (Q4) quadrant is considered as necrotic cell population. Flow cytometric data analysis revealed that after 18 h of treatment with ½ IC50 and IC50 dose of ALA, ER+MCF-7 cells were in LR quadrant (Q2) in a dose dependent manner(4.58% against 2.42%)(Figure 9).

GLA treated control cells exhibited a very low population of cells (0.01%) in the apoptotic region (P2-Q2) whereas GLA ½ IC 50 (P2-Q2) (3.34%) and GLA IC 50 (P2-Q2) (6.75%) dose dependently increased the apoptotic cell burden in P2-Q2 region in the dot plot assay (Figure 10).

Figure 9: Effect of ALA on cell cycle arrest studied through Annexin-V FITC binding

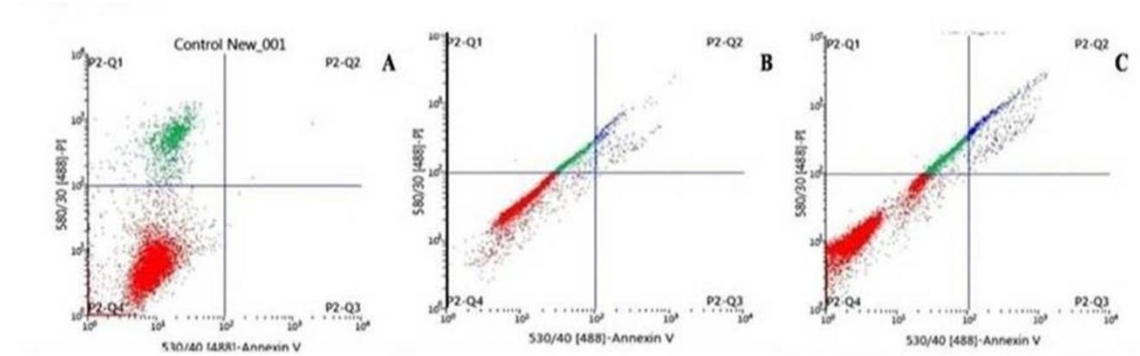

Populations	Events	% Total	% Parent	530/40... Mean	580/30... Mean
All Events	10,000	100.00%	####	9	70
P1	8,376	83.76%	83.76%	10	80
P2-Q1	1,168	11.68%	13.94%	18	531
P2-Q2	1	0.01%	0.01%	258	128
P2-Q3	2	0.02%	0.02%	115	24
P2-Q4	7,205	72.05%	86.02%	9	7

Populations	Events	% Total	% Parent	530/40... Mean	580/30... Mean
All Events	10,000	100.00%	####	14	36
P1	4,039	40.39%	40.39%	30	73
P2-Q1	595	5.95%	14.73%	51	147
P2-Q2	242	2.42%	5.99%	202	372
P2-Q3	4	0.04%	0.10%	107	79
P2-Q4	3,198	31.98%	79.18%	13	37

Populations	Events	% Total	% Parent	530/40... Mean	580/30... Mean
All Events	10,000	100.00%	####	27	74
P1	9,869	98.69%	98.69%	24	72
P2-Q1	1,444	14.44%	14.63%	46	159
P2-Q2	458	4.58%	4.64%	266	699
P2-Q3	0	0.00%	0.00%	####	####
P2-Q4	7,967	79.67%	80.73%	6	20

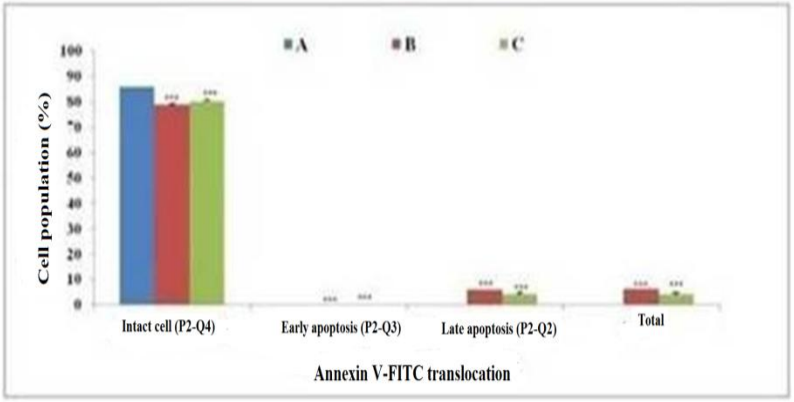

Study represent detection of cycle arrest in the ER+MCF-7 cells treated with control (A); ALA (1/2 IC50) (B); ALA (IC50) (C). Cells were treated with Annexin V FITC and PI. Dual parameter dot plot of FITC-fluorescence (x-axis) vs. PI-fluorescence (y-axis) shows logarithmic intensity. Values are presented as mean ± SD and the comparisons were made on the basis of one-way ANOVA followed by Bonferroni multiple test.

Figure 10: Effect of GLA on cell cycle arrest studied through Annexin-V FITC binding

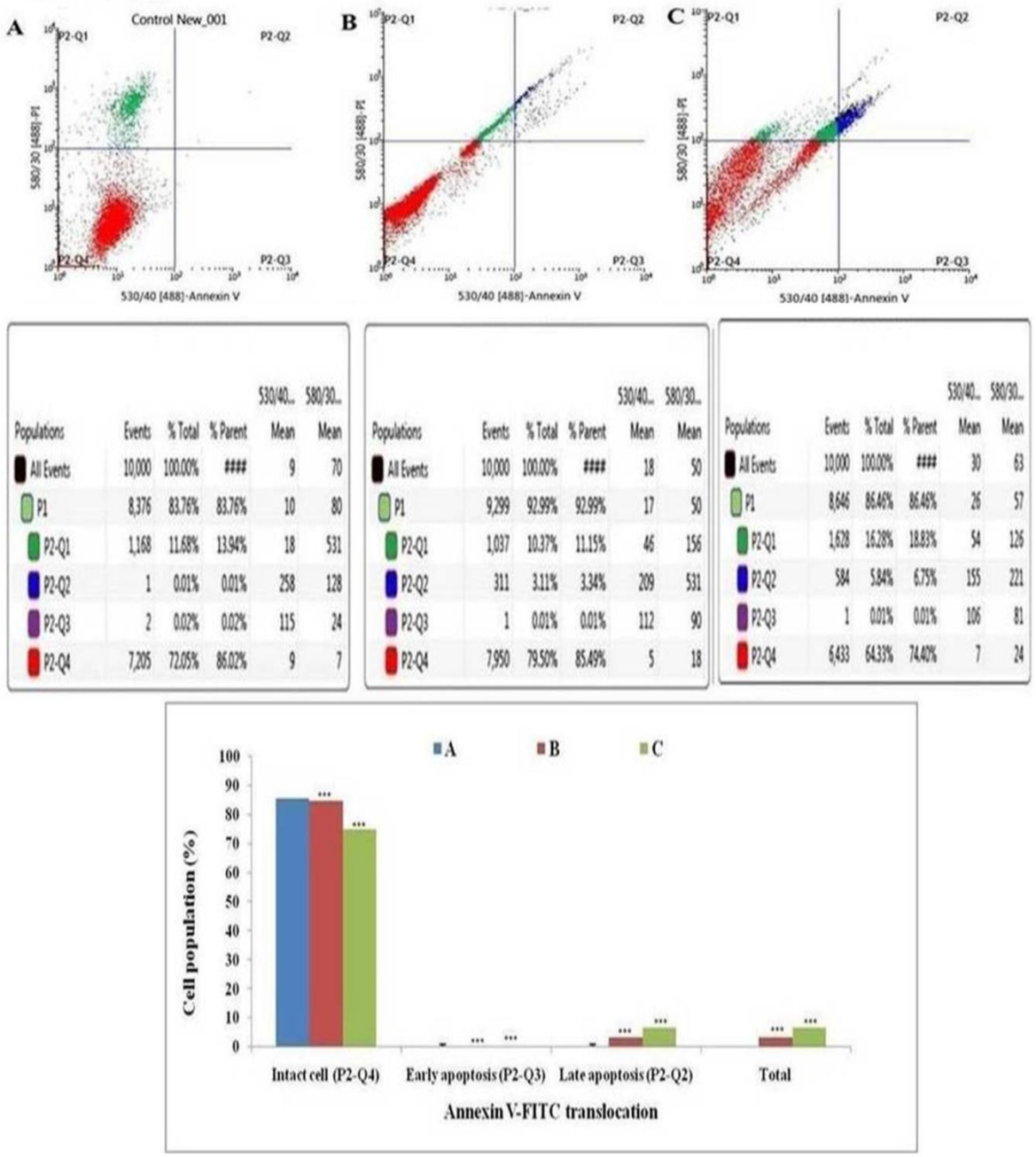

Populations	Events	% Total	% Parent	530/40... Mean	580/30... Mean
All Events	10,000	100.00%	####	9	70
P1	8,376	83.76%	83.76%	10	80
P2-Q1	1,168	11.68%	13.94%	18	531
P2-Q2	1	0.01%	0.01%	258	128
P2-Q3	2	0.02%	0.02%	115	24
P2-Q4	7,205	72.05%	86.02%	9	7

Populations	Events	% Total	% Parent	530/40... Mean	580/30... Mean
All Events	10,000	100.00%	####	18	50
P1	9,299	92.99%	92.99%	17	50
P2-Q1	1,037	10.37%	11.15%	46	156
P2-Q2	311	3.11%	3.34%	209	531
P2-Q3	1	0.01%	0.01%	112	90
P2-Q4	7,950	79.50%	85.49%	5	18

Populations	Events	% Total	% Parent	530/40... Mean	580/30... Mean
All Events	10,000	100.00%	####	30	63
P1	8,646	86.46%	86.46%	26	57
P2-Q1	1,628	16.28%	18.83%	54	126
P2-Q2	584	5.84%	6.75%	155	221
P2-Q3	1	0.01%	0.01%	106	81
P2-Q4	6,433	64.33%	74.40%	7	24

Control (A); GLA (1/2 IC 50) (B) and GLA (IC 50) (C) were dual stained with Annexin-V FITC and PI for cell cycle arrest analysis. Data are presented as mean ± SD and the comparisons are made on the basis of one-way ANOVA followed by Bonferroni multiple test.

4.2 *In vivo* study

4.2.1 Hemodynamic study: Autonomic dysfunction associated with cardiovascular complications, poor quality of life and premature mortality are well reported phenomenon in the breast cancer survivors. Infact, autonomic dysfunction is now a day is considered as a non-invasive prognostic marker for chemotherapeutic regime [85]. Treatment with ALA and GLA helped to restore the autonomic control and therefore, could be designated to have good prognostic value in chemoprevention regime as proposed through ALA and GLA.

i) ALA (DMBA)

ECG analysis revealed an increase in HR after DMBA treatment (353.2±0.42beats/min). Treatment with ALA helped to restore the HR significantly close to normal (297.8±0.79 beats/min). No significant variability was recorded in the P wave duration after either of the treatments (Table 3). The HRV analysis of the ECG complex revealed the sharp decrease in the low frequency (LF) (9.24± 0.01ms^2), high frequency (HF) (37.77± 0.05ms2) and very low frequency (VLF) (41.41±0.08 ms^2) after the DMBA treatment. Treatment with ALA perceived dose-dependent restoration of the HRV parameters (Table 4).

Table 3: Effect of ALA on electrocardiographic changes in DMBA induced mammary gland carcinoma

ECG Parameters	Control (0.9% normal saline, p.o)	Toxic control (DMBA 8mg/kg, i.v.)	DMBA +ALA (8mg/kg i.v. +0.25 ml/kg, p.o.)	DMBA +ALA (8mg/kg i.v. +0.5 ml/kg, p.o.)
RR Interval (s)	0.17±0.01	0.18±0.01	0.20±0.009**	0.17±0.01
Heart Rate (BPM)	331.3±0.17**	353.2±0.42	306.6±0.09***	297.8±0.79***
PR Interval (s)	0.04±0.002	0.04±0.002	0.04±0.003	0.05±0.004***
P Duration (s)	0.01±0.004	0.01±0.001	0.01±0.001	0.01±0.002
QRS Interval (s)	0.01±0.004	0.01±0.004	0.01±0.003	0.02±0.006***
QT Interval (s)	0.04±0.01	0.05±0.08	0.06±0.09	0.05±0.01
QTc (s)	0.1±0.02	0.1±0.01	0.1±0.02	0.1±0.02
JT Interval (s)	0.02±0.01	0.04±0.01	0.04±0.01	0.03±0.01
T peak Tend Interval (s)	0.01±0.007	0.02±0.009	0.02±0.007	0.01±0.005
P Amplitude (mV)	0.05±0.01	0.09±0.03	0.02±0.2	0.05±0.07
Q Amplitude (mV)	0.03±0.03	0.02±0.01	0.007±0.03	0.005±0.07
R Amplitude (mV)	1.4±0.48***	2.0±0.2	0.7±0.2***	0.9±0.4***
S Amplitude (mV)	-0.2±0.1	-0.1±0.06	-0.1±0.005*	-0.09±0.2
ST Segment (mV)	-0.08±0.1	0.07±0.06	0.04±0.05	-0.04±0.08
T Amplitude (mV)	0.35±0.06	0.34±0.1	0.15±0.1**	0.12±0.1***

(Values are presented as Mean ± SD). Each group contains eight animals. Comparisons are made on the basis of the one-way ANOVA followed by Bonferroni multiple test. All groups are compared to the toxic control group (*p<0.05, **p<0.01, ***p<0.001).

Table 4: Effect of ALA on HRV changes in DMBA induced mammary gland carcinogenesis

	Control (0.9% normal saline, p.o)	Toxic control (DMBA 8 mg/kg i.v)	DMBA+ ALA (8mg/kg i.v. + 0.25ml/kg, p.o.)	DMBA+ ALA (8mg/kg i.v. + 0.5ml/kg, p.o.)
Time Domain				
Average RR (ms)	166.2±0.02 ***	172.1±0.02	181.3±0.05***	165.5±0.01***
Median RR (ms)	166.6±0.06***	172.8±0.05	182.3±0.09***	165.5±0.09***
SDRR (ms)	6.25±0.01***	3.66±0.7	6.79±0.01***	5.63±0.01***
CVRR	0.12±0.01	0.02±0.01	0.12±0.02 ***	0.18±0.02***
Frequency Domain				
LF (ms^2)	11.32±0.06***	9.24±0.01	14.02±0.04***	12.22±0.06***
HF (ms^2)	39.70±0.09***	37.77±0.05	46.24±0.09***	43.30±0.07***
LF/HF	0.34±0.02	0.32±0.04	0.24±0.08	0.21±0.1
VLF (ms^2)	42.13±0.07***	41.41±0.08	38.47±0.04***	42.87±0.09***

(Values are presented as Mean ± SD). Each group contains eight animals. Comparisons are made on the basis of the one-way ANOVA followed by Bonferroni multiple test. All groups are compared to the toxic control group (*p<0.05, **p<0.01, ***p<0.001).

ii) ALA (MNU)

ECG analysis revealed that HR was increased after MNU treatment (353.2±0.41beats/min) which was restored to normal after ALA treatment (310.2±0.31 beats/min) (Table 5). The HRV analysis of the ECG complex revealed the sharp decrease in the low frequency (LF) (9.24±0.37ms^2), high frequency (HF) (37.77±0.6ms^2) and LF/HF ratio (0.32±0.28) after the MNU treatment. ALA treatment successfully restores the HRV parameters (Table 6).

Table 5: Effect of ALA on ECG changes in MNU induced mammary gland carcinogenesis

ECG Parameters	Control (Normal saline p.o.)	Toxic control (MNU, 47 mg/kg, i.v.)	MNU +ALA (47 mg/kg i.v.) + (0.25ml/kg, p.o.)
RR Interval (s)	0.17±0.01	0.18±0.01	0.19±0.02
Heart Rate (BPM)	331.3±0.53***	353.2±0.41	310.2±0.31 ***
PR Interval (s)	0.04±0.02	0.04±0.07	0.04±0.04
P Duration (s)	0.01±0.04	0.01±0.04	0.01±0.01
QRS Interval (s)	0.01±0.04	0.01±0.05	0.01±0.01
QT Interval (s)	0.04±0.01	0.05±0.01	0.05±0.01
QTc (s)	0.1±0.02	0.1±0.03	0.1±0.04
JT Interval (s)	0.02±0.01*	0.04±0.01	0.03±0.02
T peak Tend Interval (s)	0.01±0.07	0.02±0.01	0.02±0.01
P Amplitude (mV)	0.05±0.01	0.09±0.05	0.1±0.08
Q Amplitude (mV)	0.03±0.03	0.02±0.01	0.01±0.02
R Amplitude (mV)	1.4±0.48	2.0±0.41	1.4±0.54
S Amplitude (mV)	-0.2±0.1	-0.1±0.2	-0.1±0.1
ST Segment (mV)	-0.08±0.1**	0.07±0.08	0.09±0.07
T Amplitude (mV)	0.3±0.06	0.3±0.06	0.14±0.08 ***

(Values are presented as mean ± SD), each group contains eight animals. Comparisons are made on the basis of the one-way ANOVA followed by Bonferroni multiple test. All groups are compared to the toxic control group (*p<0.05, **p<0.01, ***p<0.001).

Table 6: Effect of ALA 0.25 ml/kg on HRV changes in MNU induced mammary gland carcinogenesis

HRV	**Control** (normal saline)	**Toxic control** (MNU 47 mg/kg i.v)	**ALA+ MNU** (0.25 ml/kg, p.o. + 47 mg/kg i.v.)
Time Domain			
Average RR (ms)	166.2±0.21***	172.11±0.26	186.2±0.88***
Median RR (ms)	166.66±0.3***	172.83±0.42	187±0.8***
SDRR (ms)	6.25±0.2***	3.66±0.2	2.79±0.04***
CVRR	0.02± 0.01	0.02± 0.01	0.01± 0.007
Frequency Domain			
LF (ms^2)	11.32± 0.42***	9.24± 0.37	12.54± 0.65***
HF (ms^2)	39.70± 0.2***	37.77± 0.6	53.52± 0.4***
LF/HF	0.34± 0.22	0.32± 0.28	0.54± 0.12
VLF (ms^2)	42.13± 0.5 ***	44.74± 0.2	24.363± 0.3 ***

(Values are presented as Mean ± SD), each group contains eight animals. Comparisons are made on the basis of the one-way ANOVA followed by Bonferroni multiple test. All groups are compared to the toxic control group (*p<0.05, **p<0.01, ***p<0.001).

iii) GLA (DMBA)

ECG analysis divulged an increase in HR after DMBA treatment (355.2±0.42 beats/min). Treatment with GLA helped to restore the HR significantly close to normal (299.8±0.79beats/min). No significant variability could perceive in the P wave duration after either of the treatments (Table 7). The HRV analysis of the ECG complex revealed the sharp decrease in the LF (9.84± 0.01ms^2), HF (37.97± 0.05ms^2) and VLF (41.81± 0.08ms^2) after the DMBA treatment. Treatment with GLA perceived dose-dependent restoration of the HRV parameters (Table 8).

Table 7: Effect of GLA on electrocardiographic changes in DMBA induced mammary gland carcinoma

ECG Parameters	Control (0.9% normal saline, p.o)	Toxic control (DMBA 8mg/kg, i.v.)	DMBA +GLA (8mg/kg i.v. +0.25 ml/kg, p.o.)	DMBA +GLA (8mg/kg i.v. +0.5 ml/kg, p.o.)
RR Interval (s)	0.18±0.01	0.19±0.01	0.21±0.009**	0.18±0.01
Heart Rate (BPM)	332.3±0.17**	355.2±0.42	308.6±0.09***	299.8±0.79***
PR Interval (s)	0.05±0.002	0.05±0.002	0.05±0.003	0.06±0.004***
P Duration (s)	0.01±0.004	0.01±0.001	0.01±0.001	0.01±0.002
QRS Interval (s)	0.01±0.004	0.01±0.004	0.01±0.003	0.03±0.006***
QT Interval (s)	0.05±0.01	0.06±0.08	0.07±0.09	0.06±0.01
QTc (s)	0.1±0.02	0.1±0.01	0.1±0.02	0.1±0.02
JT Interval (s)	0.03±0.01	0.05±0.01	0.05±0.01	0.04±0.01
T peak Tend Interval (s)	0.02±0.007	0.03±0.009	0.03±0.007	0.02±0.005
P Amplitude (mV)	0.06±0.01	0.08±0.03	0.03±0.2	0.06±0.07
Q Amplitude (mV)	0.04±0.03	0.03±0.01	0.008±0.03	0.006±0.07
R Amplitude (mV)	1.5±0.48***	2.5±0.2	0.8±0.2***	0.10±0.4***
S Amplitude (mV)	-0.3±0.1	-0.2±0.06	-0.2±0.005*	-0.08±0.2
ST Segment (mV)	-0.09±0.1	0.08±0.06	0.05±0.05	-0.03±0.08
T Amplitude (mV)	0.36±0.06	0.35±0.1	0.16±0.1**	0.13±0.1***

(Values are presented as Mean ± SD). Each group contains eight animals. Comparisons are made on the basis of the one-way ANOVA followed by Bonferroni multiple test. All groups are compared to the toxic control group (*p<0.05, **p<0.01, ***p<0.001).

Table 8: Effect of GLA on HRV changes in DMBA induced mammary gland carcinogenesis

	Control (0.9% normal saline, p.o)	**Toxic control** (DMBA 8 mg/kg i.v)	**GLA+ DMBA** (0.25 ml/kg, p.o.+ 8 mg/kg i.v.)	**GLA + DMBA** (0.5 ml/kg, p.o.+ 8 mg/kg i.v.)
Time Domain				
Average RR (ms)	167.2±0. 02 ***	174.11±0.02	183.3±0.05***	167.5±0.01***
Median RR (ms)	168.6±0.06***	175.83±0.05	188.3±0.09***	169.5±0.09***
SDRR (ms)	6.35±0.01***	3.76±0.7	6.89±0.01***	5.93±0.01***
CVRR	0.04±0.01	0.05±0.01	0.18±0.02 ***	0.21± 0.02***
Frequency Domain				
LF (ms^2)	11.72±0.06***	9.84±0.01	14.92±0.04***	12.72±0.06***
HF (ms^2)	39.80±0.09***	37.97±0.05	46.94±0.09***	43.80±0.07***
LF/HF	0.44±0.02	0.42±0.04	0.44±0.08	0.41± 0.1*
VLF (ms^2)	42.93±0.07***	41.81±0.08	38.67±0.04 ***	42.77±0.09***

(Values are presented as Mean ± SD). Each group contains eight animals. Comparisons are made on the basis of the one-way ANOVA followed by Bonferroni multiple test. All groups are compared to the toxic control group (*p<0.05, **p<0.01, ***p<0.001).

4.2.2 Morphological evaluation in DMBA and MNU induced mouse model

Carmine staining of whole mounts mammary gland

Cellular proliferation and angiogenesis are well-defined hallmarks for cancer progression [67] and the same was estimated against DMBA and MNU induced mammary gland carcinoma models. The carmine staining was evident for the development of proliferative lesions as represented by increase in AB after DMBA and MNU treatment. The AB represents the largest bulbous structure located at the distal end of the mammary epithelial tree and is the site for the malignant transformation [86].There was a marked increase in the lobules (1) and ABs (2). ALA and GLA afforded a marked protection against the same (Figure 11 A-C, 12, 13, 14 A-D).

H&E staining of mammary gland tissue

The histopathological examination of the control tissue elaborated presence of duct (3); adipocytes (4); loose connective tissue (LCT) (5); dense connective tissue (DCT) (6) myoepithelial cells (MEC) (7); lymphocytes (8) and cuboidal epithelial cells (CEC) (9) (Figure 11D, 12, 13, 14E). Treatment with DMBA and MNU recorded loss of duct, adipocytes, LCT, DCT and lymphocytes along with scattered CEC (Figure 11E, 12, 13, 14F). Infact, DMBA and MNU treatment distorted the histological architecture of the mammary gland tissue. Concomitant treatment with ALA and GLA imparted dose dependent restoration of the cellular architecture close to control (Figure 11F, 12, 13, 14 G, H).

SEM analysis of mammary gland tissue

Marked cellular proliferation after the DMBA and MNU treatment was also evident for increase in micro vessel formation, loss of intra-arterial cushion and vascular

conglomeration when perceived through SEM analysis. The control tissue was evident for the features like intra-arterial cushion/collagenous covering, collagen layer (10) and duct (11) (Figure 11G, 12, 13, 14 I). DMBA and MNU treatment evidenced loss of intra-arterial cushion (Figure 11H, 12, 13, 14 J); development of small tumor micro-vessels (12) and development of nodules (13) (Figure 11H, 12, 13, 14 J). Subsequent ALA and GLA administration perceived decrease in tumor micro-vessel formation representing the deep impression of ALA and GLA on the branching sites along with restoration of intra-arterial cushion (Figure 1I1, 12, 13, 14 K, L).

Figure11: Microscopic evaluation of mammary gland tissue treated with ALA and MNU

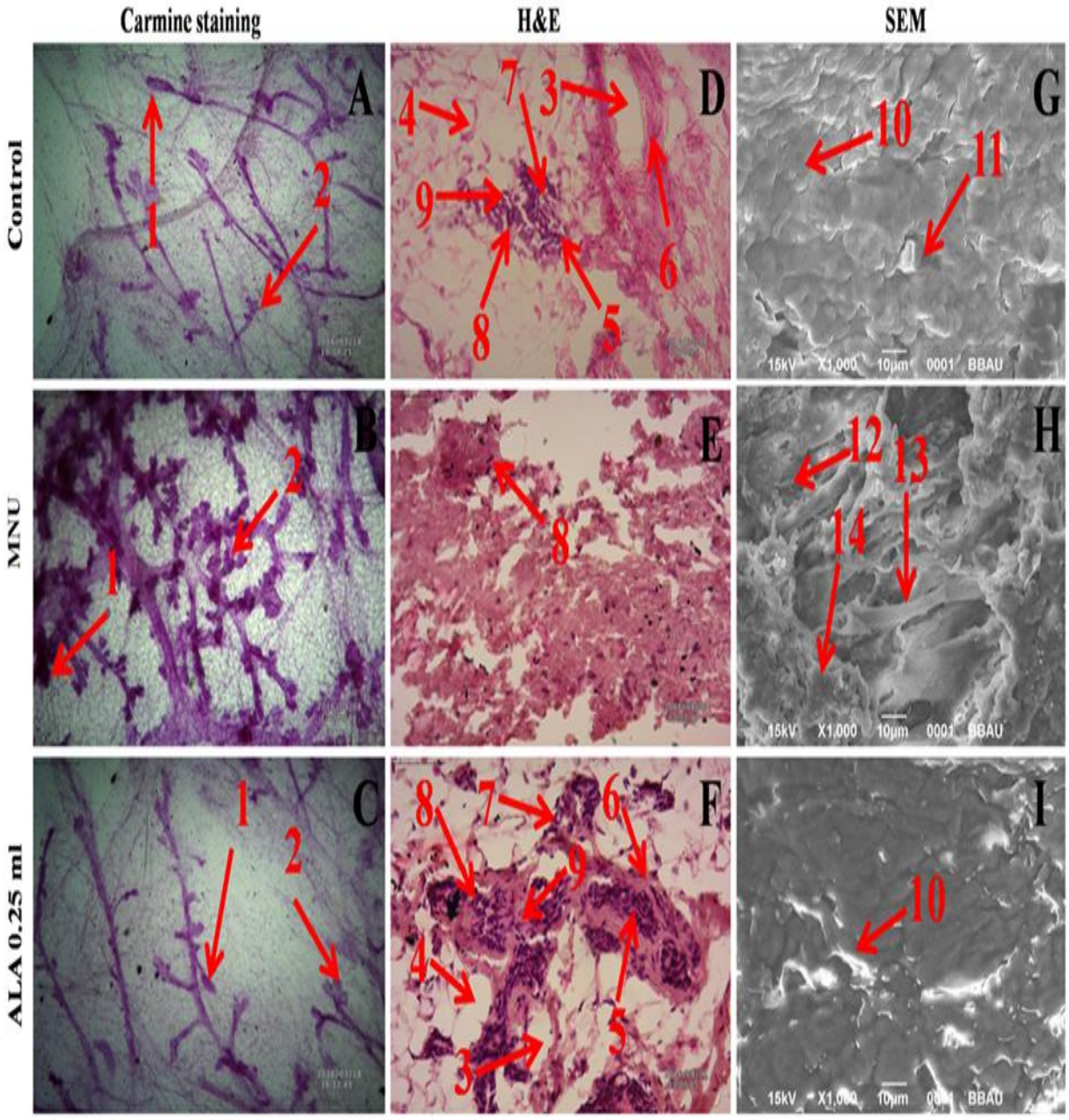

Carmine staining of mammary gland tissue revealed the presence of lobules (1) and AB (2) (A, B and C). In MNU treated group (B) the number of ABs are more which was subsided after ALA treatment(C). H&E staining of control and ALA treated group (D and F) revealed the presence of duct (3), adipocytes (4), LCT (5), DCT (6), MEC (7), lymphocytes (8) and CEC (9).In MNU treated group (E), the cell morphology was distorted and cell organelles were absent. SEM analysis of control (G), MNU treated (H) and ALA treated (I) revealed the difference in collagen layer (10), duct (11), small capillary network (12), large capillary network (13) and nodules (14) in respective groups.

Figure12: Microscopic evaluation of mammary gland tissue treated with ALA and DMBA

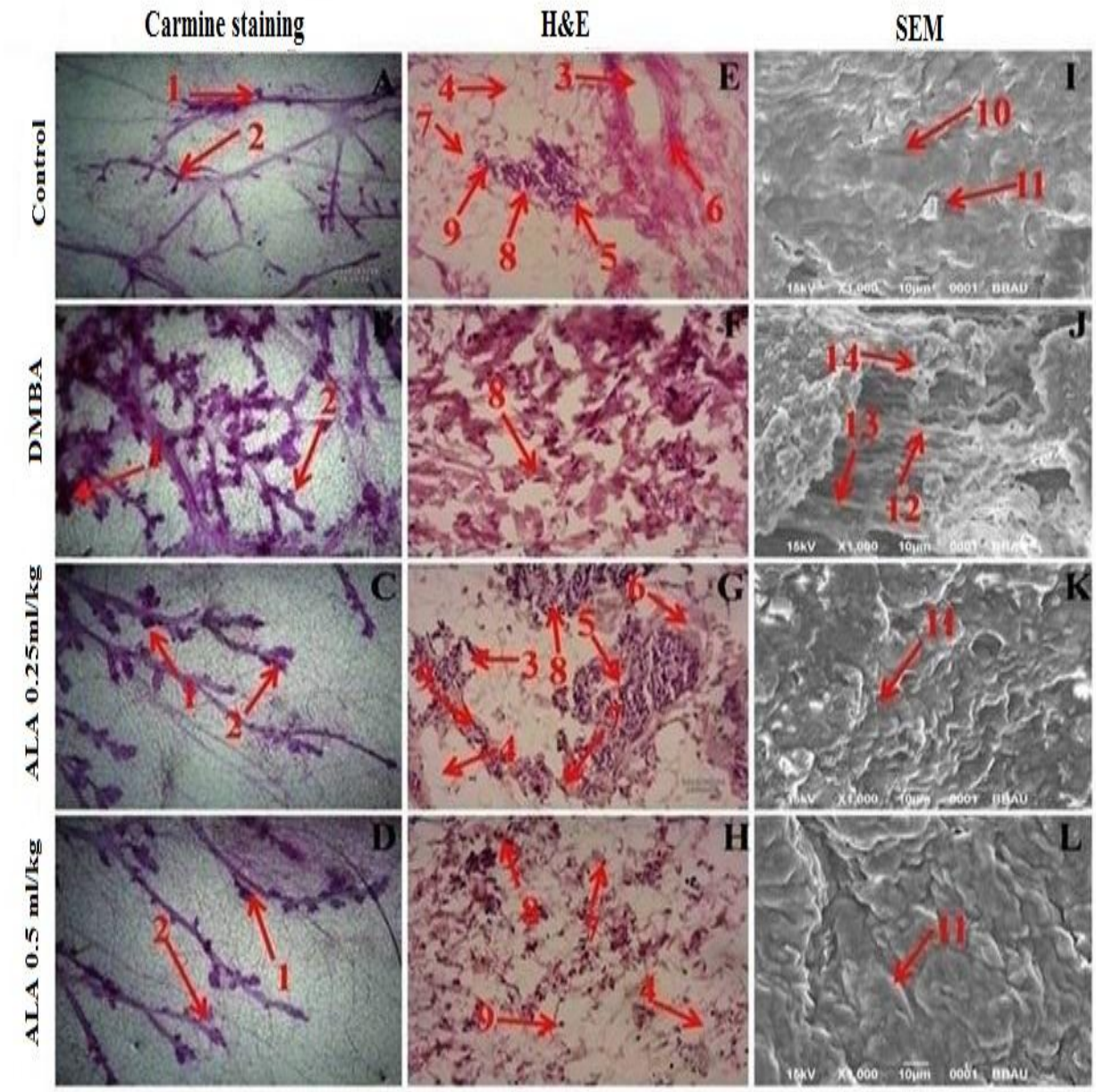

Whole mount carmine alum staining of ductal epithelium reveals the presence of lobules (1) and AB (2) (A, B, C and D). The extent of AB and lobules formation was excessive in the DMBA treated group (B) which was subsided through respective treatment (C and D). H&E staining of three respective groups (E, G and H) revealed duct (3), adipocytes (4), LCT (5), DCT (6), MEC (7), lymphocytes (8) and CEC (9) in control as well as ALA treated groups (E, G and H). In DMBA treated group (F), the cell morphology was distorted and cell organelles were absent. SEM analysis of control (I), DMBA treated (J) and treatment group (K and L) revealed the differences in collagen layer (10), duct (11), small capillary network (12) and nodules (13) in respective groups.

Figure13: Microscopic evaluation of mammary gland tissue treated with GLA and MNU

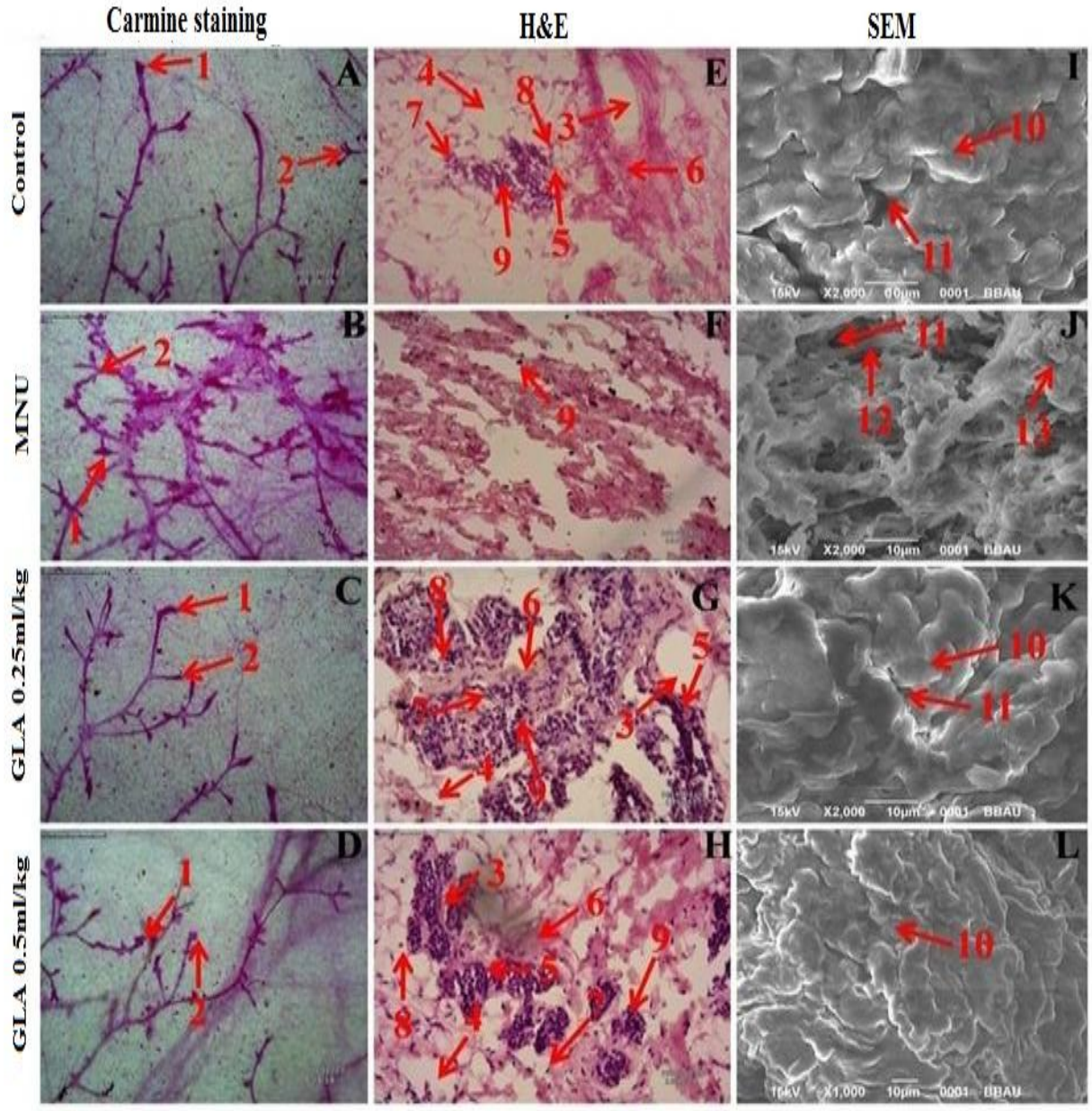

The mammary gland tissues revealed the presence of lobules (1) and AB (2) (A, B, C and D). MNU treated group (B) represents the excessive formation of AB and lobules. GLA treatment (C and D) curtailed the formation of AB and lobules in dose dependent manner. H&E staining of control and GLA treated groups (E, G and H) revealed the presence of duct (3), adipocytes (4), LCT (5), DCT (6), MEC (7), lymphocytes (8) and CEC (9) in control as well as GLA treated groups (E, G and H). The cell morphology and cell organelles were distorted after MNU treatment (J). SEM analysis revealed difference in collagen layer (10), duct (11), small capillary network (12) and nodules (13) in control (I), MNU treated (J) and GLA treated (K and L) groups respectively.

Figure14: Microscopic evaluation of mammary gland tissue treated with GLA and DMBA

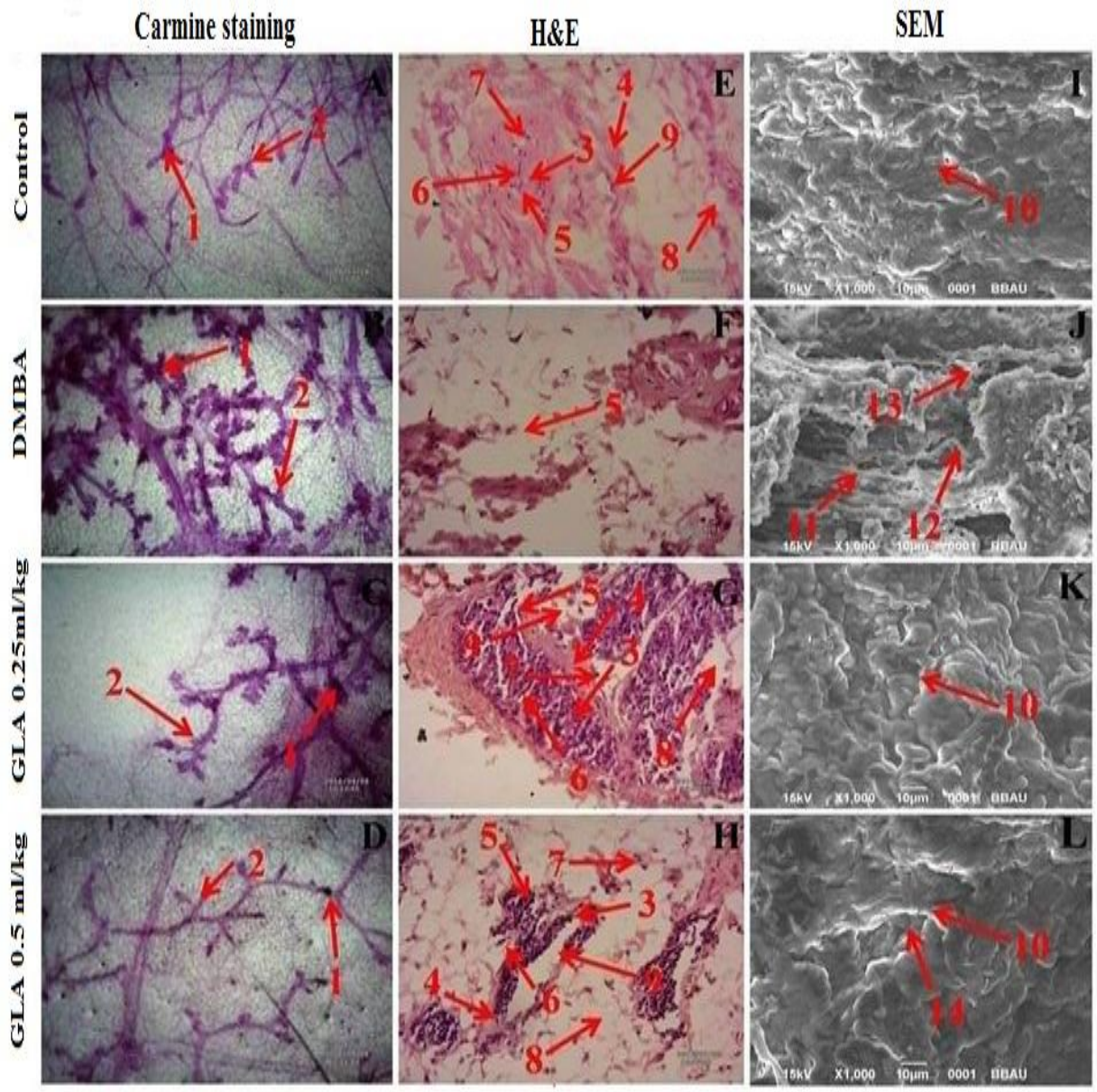

Carmine staining of mammary gland tissue reveals the presence of lobules (1) and AB (2) (A–D). DMBA treated group (B) revealed the presence of presence of lobules and AB which was subsided after GLA treatment in dose dependent manner (C and D). H&E staining of control and GLA treated group (E, G and H) revealed the presence of duct (3), adipocytes (4), LCT (5), DCT (6), MEC (7), lymphocytes (8) and CEC (9). In DMBA treated group (F), the cell morphology was distorted and cell organelles were absent. SEM analysis of control (I), DMBA treated (J) and treatment group (K and L) revealed the difference in collagen layer (10), duct (11), small capillary network (12), large capillary network (13) and nodules (14) in respective groups.

4.2.3 Antioxidant markers: The biochemical markers could be majorly categorized as the ones associated with antioxidant defense or to the physiological mechanisms and in the present study, both parameters were validated. Reactive oxygen species (ROS) are constantly produced in all aerobic cells and are counter balanced by the antioxidant enzymatic defense [87]. However, during anaerobic/hypoxic conditions like cancer (due to increased cellular proliferation), the counter balance effects of antioxidant enzymes are subsided [88]. The damage to the cellular lipids and proteins can be validated through increased production of TBARs and PC respectively; which was very well evident after the DMBA and MNU treatment. The increased ROS production also inhibits the enzymatic antioxidant defense of GSH, SOD and catalase, as they all work in tandem to curtail ROS through series of peroxidation, dismutation and oxidation reactions. The decrease in the enzymatic defense of SOD, catalase and GSH suggest their increased utilization, which was profoundly evident after the DMBA and MNU treatment. It would be appropriate to remark that ALA and GLA administration curtailed the levels of TBARs and PC with restoration of enzymatic antioxidant defense of SOD, catalase and GSH.

i) ALA (DMBA)

Treatment with ALA validated the restoration of the antioxidant defense system in comparison to DMBA treated group. The protein and lipid peroxidation was very well evident after DMBA treatment. The ALA successfully decreased the level of PC (32.95±0.9 nM/ml unit). Significant changes in the TBARs (0.21±0.02 nM of MDA/µg of protein) were also observed after ALA treatment. The level of GSH in DMBA treated group (1.03±0.09 mg %) was significantly restored after ALA treatment (1.19±0.01mg

%). Corresponding to the levels of SOD (0.037±0.01units of SOD/mg of protein) and catalase (13.91±0.97nM of H_2O_2/ min/mg of protein) in DMBA treated group; ALA significantly accompanied to restore the same (i.e. 0.044±0.01units of SOD/mg of protein and 22.00±0.90 nM of H_2O_2/mg of protein) comparable to normal control (Table 9).

ii) ALA (MNU)

Treatment with ALA validated the restoration of antioxidant defense system in comparison to MNU treated group. The lipid peroxidation was very well evident after MNU treatment. The ALA successfully curtailed down the level of TBARs (1.41±0.nM of MDA/µg of protein). The level of GSH in normal control (0.56±0.03mg %) was significantly decreased in toxic control (0.46±0.01mg %). The GSH level was upregulated after the treatment with ALA (0.53±0.02mg %). Corresponding to the levels of SOD (0.86±0.06units of SOD/mg of protein) and catalase (7.84±0.60of H_2O_2/ min/mg of protein) in MNU treated group; ALA significantly downregulate the level of SOD and catalase (i.e. 0.74±0.04units of SOD/mg of protein and 6.06±0.65nM of H_2O_2/mg of protein) to normal control (Table 10).

iii) GLA (DMBA)

GLA treatment validated the restoration of antioxidant defense system in comparison to DMBA treated group. The lipid peroxidation was very well evident after DMBA treatment. The GLA successfully curtailed down the level of TBARs (0.19±0.07nM of MDA/µg of protein) and PC (25.98±1.57 nM/ml unit). The level of GSH in normal control (1.21±0.06mg %) was significantly decreased in toxic control (1.09±0.09mg %). The GSH level was upregulated after the treatment with GLA (1.24±0.02mg %). Corresponding to the levels of SOD (0.059±0.008 units of SOD/mg of protein) and

catalase (32.19±0.07of H_2O_2/ min/mg of protein) in DMBA treated group, GLA significantly downregulate the level of SOD and catalase (i.e0.045±0.008 units of SOD/mg of protein and 24.2±0.09 nM of H_2O_2/mg of protein) to normal control (Table 11).

Table 9: Effect of ALA on oxidative stress markers against DMBA induced mammary gland carcinoma

Groups	**TBARs** (nM of MDA/µg of protein)	**GSH** (mg %)	**SOD** (Units of SOD/mg of protein)	**Catalase** (nM of H_2O_2/ min/mg of protein)	**Protein carbonyl** (nM/ml unit)
Control (0.9% normal saline, p.o.)	0.15±0.03***	1.10±0.06***	0.042±0.01	18.45±0.3***	40.43±0.11***
Toxic control (DMBA 8mg/kg, i.v.)	0.30±0.02	1.03±0.09	0.037±0.01	13.91±0.97	45.57±0.92
DMBA 8mg/kg, i.v.+ ALA 0.25 ml /kg, p.o.	0.23±0.19***	1.11±0.02***	0.042±0.02	19.60±0.03***	34.42±0.68***
DMBA 8mg/kg,i.v.+ ALA 0.5 ml/kg, p.o.	0.21±0.02***	1.19±0.01***	0.044±0.01	22.00±0.90***	32.95±0.9***

(Values are Mean ± SD), each group contains eight animals. Comparisons are made on the basis of the one-way Anova followed by Bonferroni test. All groups are compared to the DMBA treated group (*p<0.05, **p<0.01, ***p<0.001).

Table 10: Effect of ALA on antioxidant markers against MNU induced mammary gland carcinoma

Groups	**TBARs** (nM of MDA/µg of protein)	**GSH** (mg %)	**SOD** (Units of SOD/mg of protein)	**Catalase** (nM of H_2O_2/ min/mg of protein)
Control (Normal saline 0.9%, p.o.)	1.40±0.01***	0.56±0.03***	0.70±0.12**	5.06±0.55***
Toxic control (MNU 47mg/kg, i.v.)	1.54±0.01	0.46±0.01	0.86±0.06	7.84±0.60
ALA 0.25 ml/kg + MNU 47mg/kg, i.v.)	1.41±0.11***	0.53±0.02***	0.74±0.04*	6.06±0.65***

(Values are Mean ± SD), each group contains eight animals. Comparisons are made on the basis of the one-way Anova followed by Bonferroni test. All groups are compared to the toxic control group (*p<0.05, **p<0.01, ***p<0.001)

Table 11: Effect of GLA on oxidative stress markers against DMBA induced mammary gland carcinoma

Groups	**TBARs** (nM of MDA/µg of protein)	**GSH** (mg %)	**SOD** (Units of SOD/mg of protein)	**Catalase** (nM of H_2O_2/ min/mg of protein)	**Protein Carbonyl** (nM/ml unit)
Control 0.9% normal saline, p.o.)	0.17±0.03***	1.21±0.06*	0.044±0.009**	19.5±0.03***	20.43±5.11***
Toxic control DMBA 8mg/kg, i.v.)	0.35±0.02	1.09±0.09	0.059±0.008	32.19±0.07	41.57±0.92
GLA 0.25 ml/kg, p.o. + DMBA 8mg/kg, i.v.	0.22±0.09***	1.19±0.05*	0.040±0.007	17.6±0.03***	29.70±2.18***
GLA 0.5 ml/kg, p.o. + DMBA 8mg/kg, i.v.)	0.19±0.07***	1.24±0.02**	0.045±0.008**	24.2±0.09***	25.98±1.57***

(Values are Mean ± SD), each group contains eight animals. Comparisons are made on the basis of the one-way Anova followed by Bonferroni test. All groups are compared to the toxic control group (*p<0.05, **p<0.01, ***p<0.001).

4.2.7 Assay for caspase 3 and caspase 8

i) ALA (DMBA)

ALA (0.25 ml/kg) increased the levels of caspase 3 and caspase 8 in the DMBA treated animals significantly (Figure 15).

ii) ALA (MNU)

ALA treatment significantly upregulated the levels of caspase3 and caspase8 in comparison to MNU treated group (Figure 16).

iii) GLA (DMBA)

GLA (0.25 ml/kg) upregulated the levels of caspase 3 and caspase 8 in the DMBA treatedanimals significantly (Figure 17).

iv) GLA (MNU)

GLA dose dependently upregulated the level of caspase 3 and 8 in MNU treated animals Figure 18).

Figure 15: Effect of ALA and DMBA on serum caspase 3 and caspase 8 level

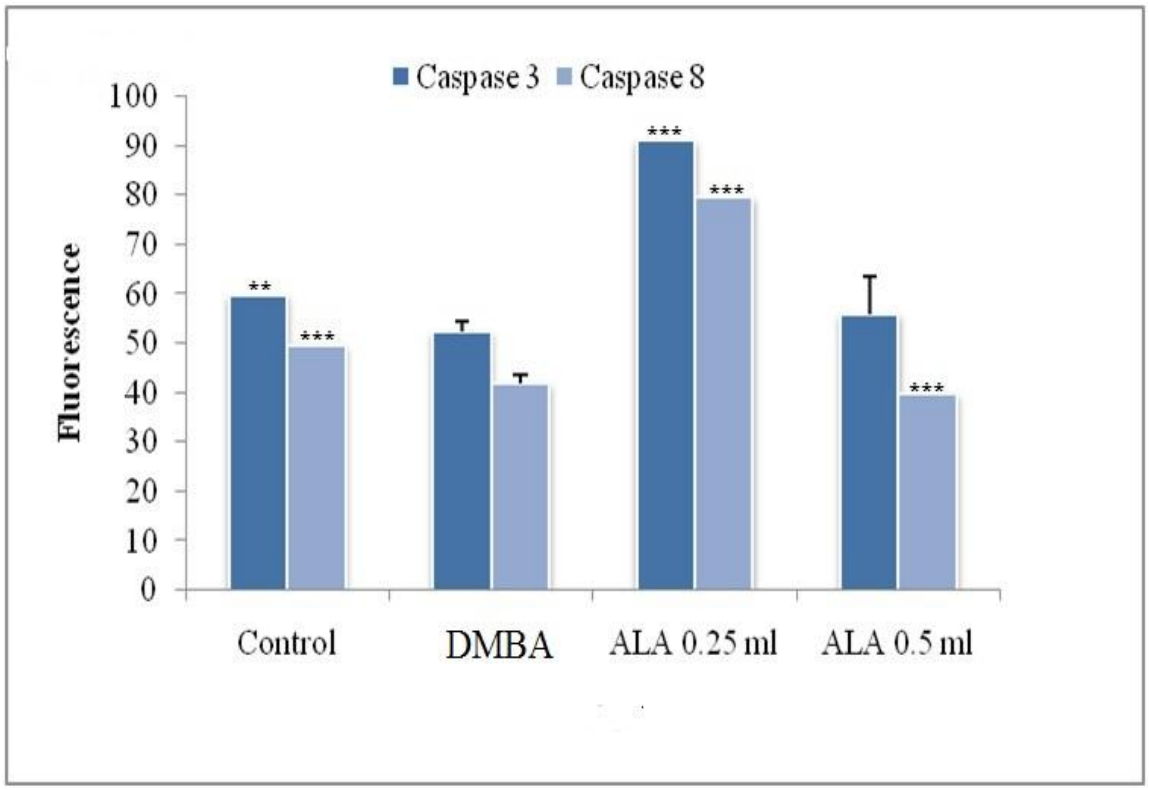

The activity of caspase was detected by commercial fluorescence based assay. Data are expressed as mean+ SD of individual groups. Comparisons were made by the one-way ANOVA followed by Bonferroni multiple test. All groups were compared to the DMBA treated group (*p<0.05, **p<0.01, ***p<0.001).

Figure 16: Effect of ALA and MNU on serum caspase 3 and caspase 8 level

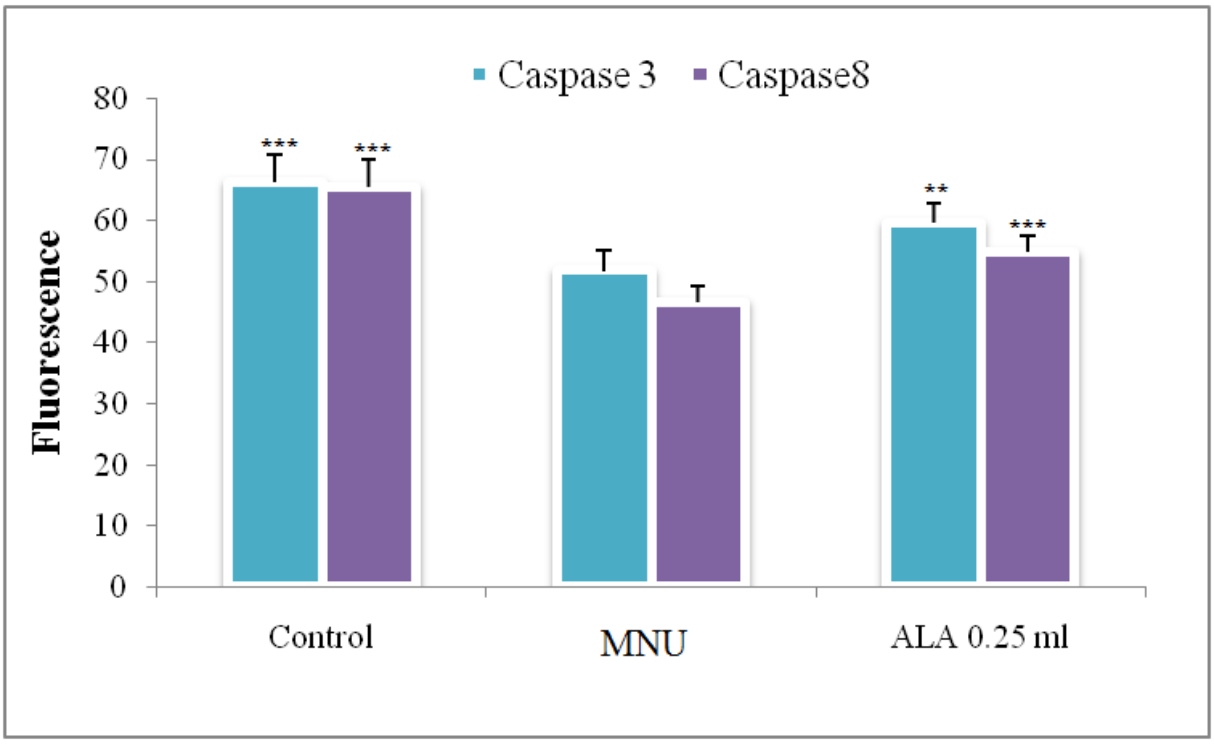

The activity of caspase was detected by commercial fluorescence based assay. Data are expressed as mean + SD of individual groups. Comparisons are made by the one-way ANOVA followed by Bonferroni multiple test. All groups are compared to the MNU treated group (*p<0.05, **p<0.01, ***p<0.001).

Figure 17: Effect of GLA and DMBA on serum caspase 3 and caspase 8 level

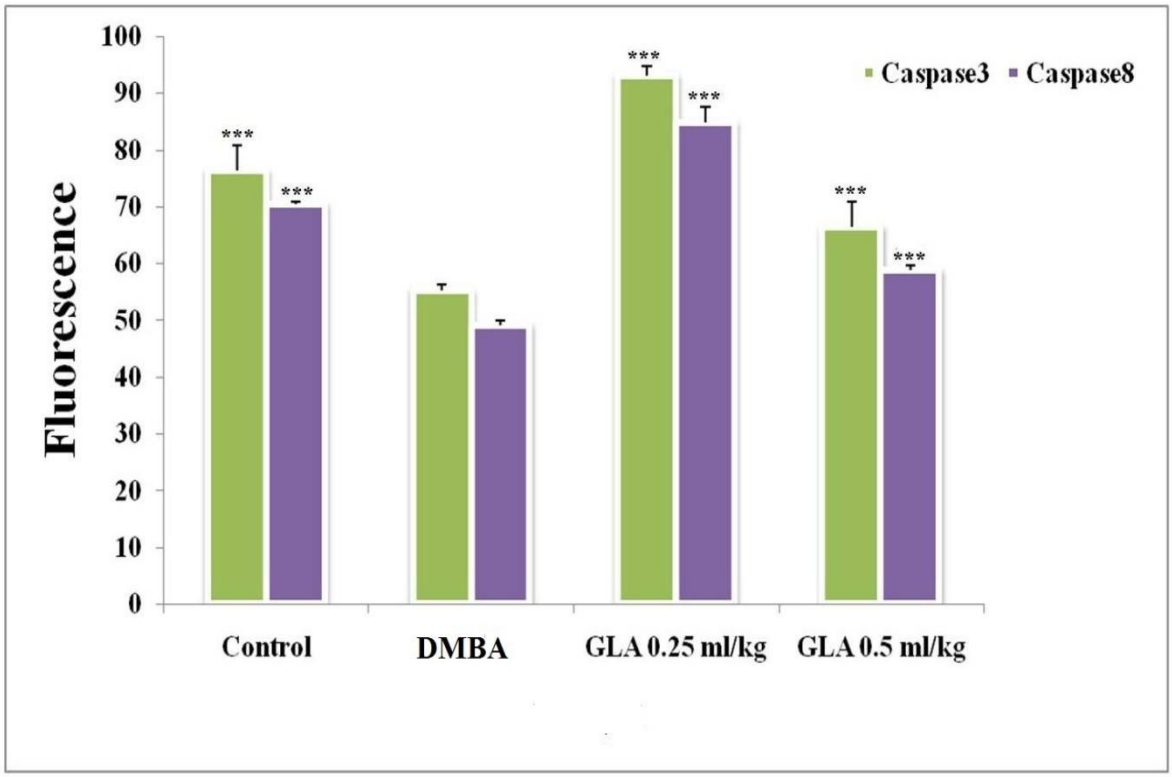

The caspase 3 and caspase 8 activities was detected using commercial fluorescence based assay kits. Data are represented as mean + SD of individual groups. Comparisons are made by the one-way ANOVA followed by Bonferroni multiple test. All groups are compared to the DMBA treated group (*$p < 0.05$, **$p < 0.01$, ***$p < 0.001$).

Figure 18: Effect of GLA and MNU on serum caspase 3 and caspase 8 level

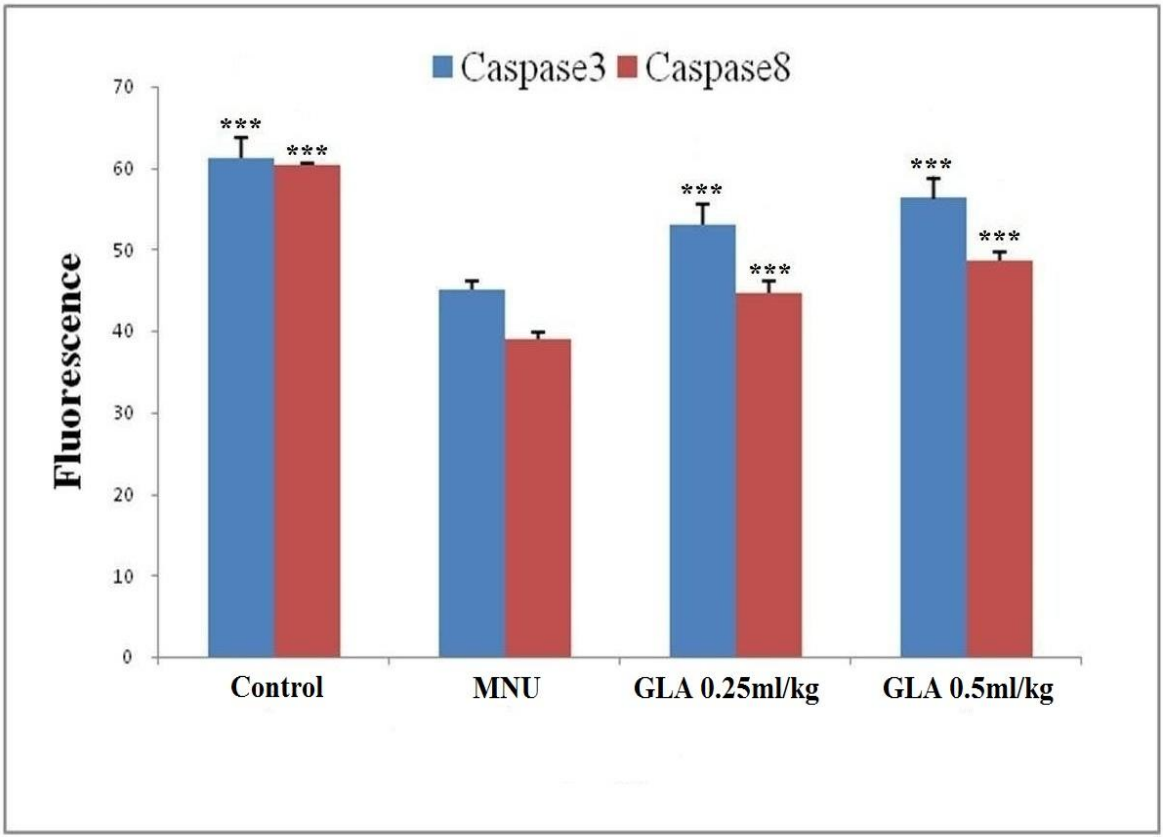

A fluorescence based commercial assay kit was used for the detection of caspase 3 and caspase 8. The observed data are represented as mean ± SD of individual groups. Comparisons are made on the basis of the one-way ANOVA followed by Bonferroni multiple test. All groups are compared to the MNU treated group (*p<0.05, **p<0.01, ***p<0.001).

4.2.4 ^{1}H-NMR study for serum metabolites profiling of ALA (DMBA)

A typical ^{1}H CPMG NMR spectra of serum samples obtained from different groups is shown in Figure 19. The NMR spectra showed signals, mainly from lipids/lipoproteins [(e.g. low density lipoprotein (LDL), very low density lipoprotein (VLDL), PUFAs etc.)], membrane metabolites [(e.g. choline, phosphocholine (PC), and glycerophosphocholine (GPC)], N-acetyl and O-acetyl glycoproteins (NAG, OAG), and amino acids [(e.g. leucine, isoleucine, valine, alanine, lysine, proline, glutamine, glutamate, histidine,

tyrosine, and phenylalanine etc.)]. Other identified metabolites were, glucose, lactate, acetate, citrate, creatine and allantoin.

Figure 19: Stack plot of representative 1D ^{1}H NMR spectra of rat sera obtained from different groups (control, DMBA and ALA)

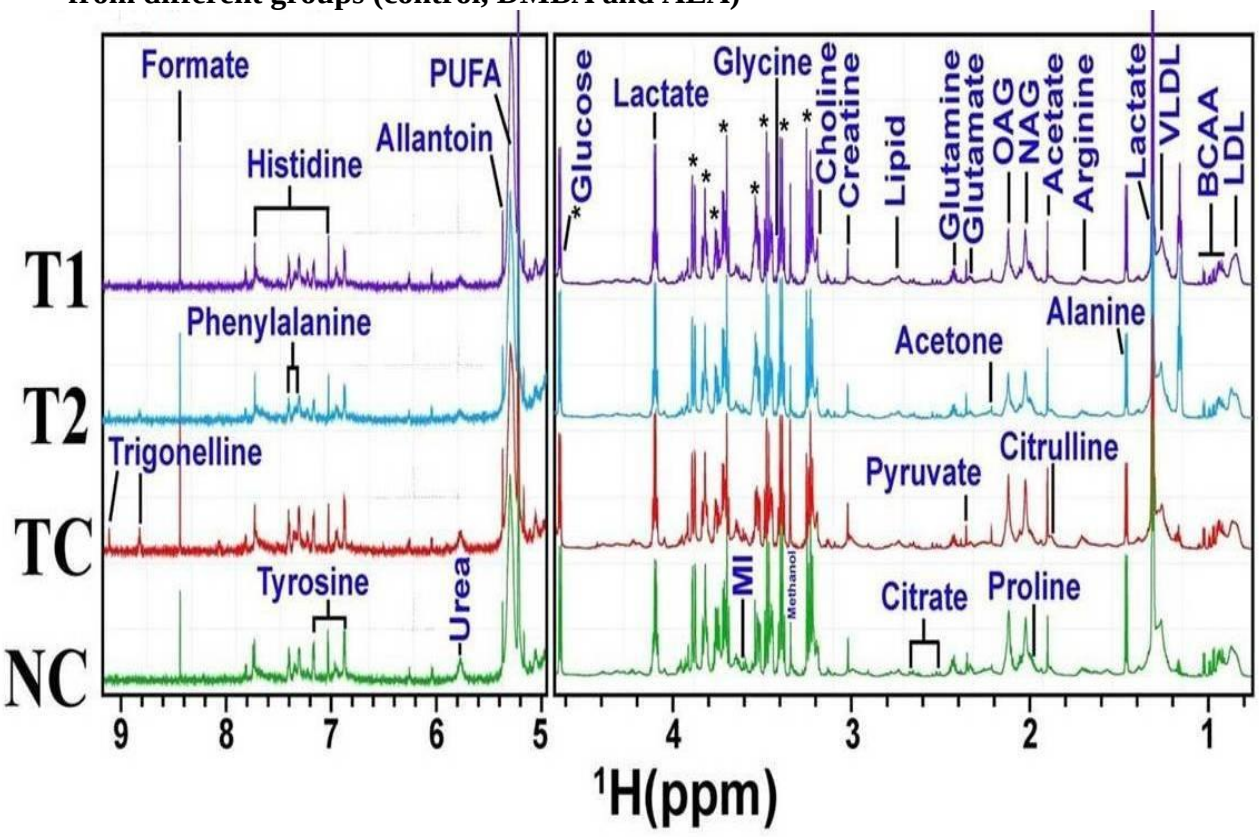

The representative1D^{1}H CPMG NMR spectra of rat serum obtained from different groups. The peaks annotated in the figure shows the assignments of serum metabolites. Groups were differentiated as: normal control (NC), toxic control -DMBA (TC), ALA-0.25 ml/kg (T1) and ALA-0.5 ml/kg (T2). The abbreviations used are LDL/VLDL: low/very-low-density lipoproteins; PUFA: polyunsaturated fatty acids; BCAA: branched chain amino acids: isoleucine, leucine, valine; MI: myo-inositol, OAG: O-acetyl glycoproteins; NAG: N-acetyl glycoproteins.

4.2.4.1 Multivariate statistical analysis

The multivariate data analysis was performed to find out specific metabolic changes induced by DMBA treatment and to further reveal the effect of ALA treatment on these metabolic alterations. The ^{1}H-NMR dataset was analyzed using standard multivariate

analysis methods including PCA, PLS-DA and OPLS-DA to study trends and show clusters among the groups (Figure 20A). First, unsupervised PCA score plots were constructed for an initial overview of the data set and identify the outlier samples (Figure 20a). The majority samples were located in 95 % confidence interval. Therefore, all of the samples were used in the analysis to ensure the maximum information. Supervised PLS-DA score plots were generated to further improve the separation between the four groups. PLS-DA score plots showed that ALA treated groups were well separated from the normal control group, with a significantly higher quality of fit and predictability (i.e. R2, Q2> 0.5, Figure 20b). Next, to minimize the possible contribution of intergroup variability and to improve the group discriminatory features, OPLS-DA was performed. As shown in Figure 20c, the OPLS-DA score plots depicted excellent grouping of samples within each group and improved separation for the different treatments with significantly well explained variation and predictive capability (i.e. R2Y, Q2> 0.5, Figure 20c). The OPLS-DA score plot analysis further revealed that ALA (0.25ml/kg) and ALA (0.5ml/kg) treatments are progressively mitigating the toxic effect of DMBA treatment as evident by the shifting of these groups within the control group.

To further reveal the biochemical effects produced by DMBA treatment and ascertain if ALA treatment could reset back these changes, the pairwise PLS-DA analysis with respect to normal control rats was performed. Figure 20B shows the 2D score plots derived from PLS-DA analysis in each case. The quality and reliability parameters (R2 and Q2) assessed for each paired PLS-DA model (Figure 20B) were found to satisfactorily higher (R2, Q2>0.5) suggesting that PLS-DA can be employed to evaluate the biochemical effects of ALA treatment. Discriminatory (PLS-DA) analysis between

DMBA treated, and normal control groups revealed twenty five metabolite entities significantly perturbed in DMBA treated group with respect to control, using VIP score >1 for discrimination significance.

Figure 20: Multivariate analysis of different groups (control, DMBA and ALA)

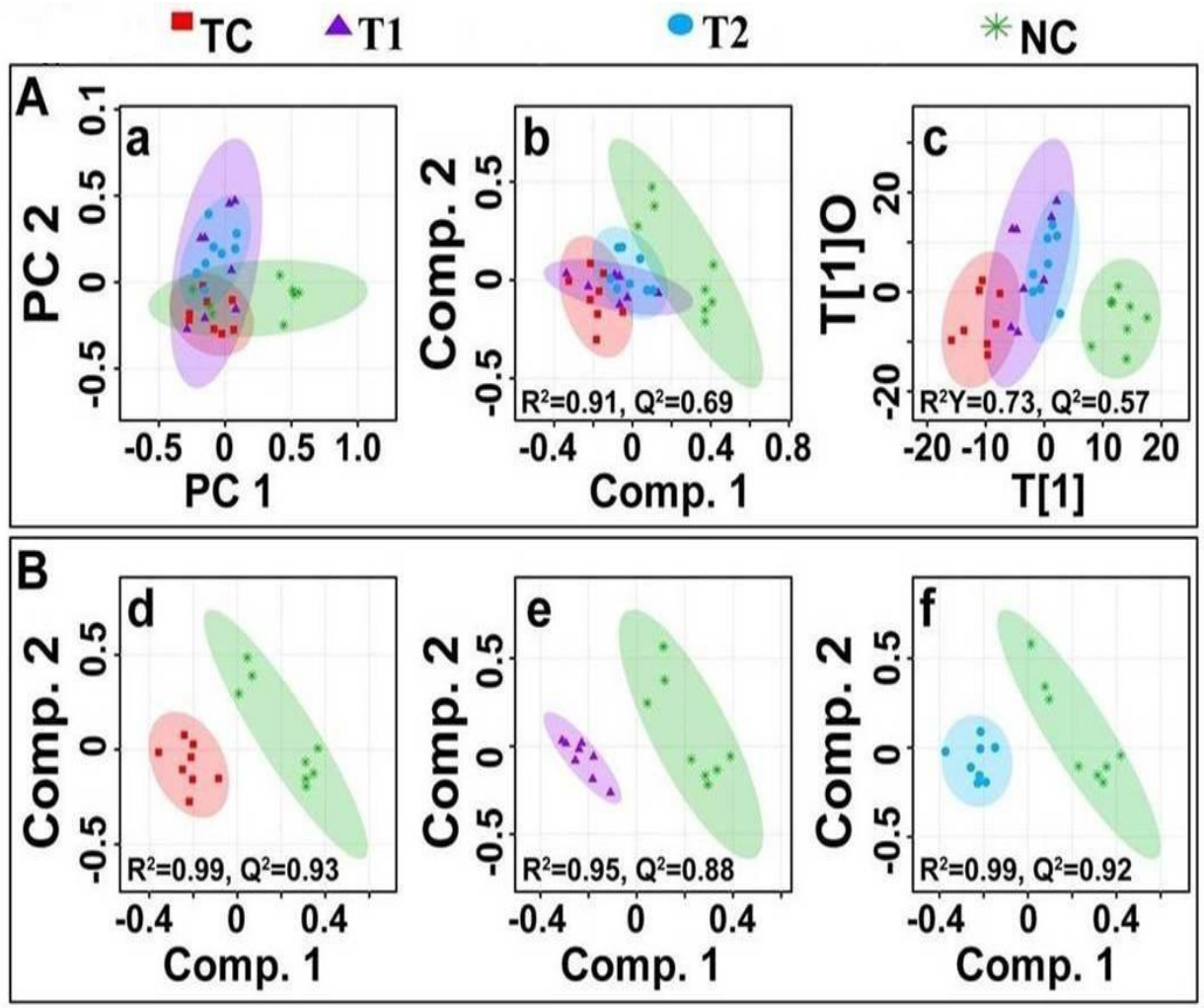

The combined2D PCA (a) and 2D PLS-DA (b) 2D OPLS-DA (c) score plots derived from cumulative analysis of 1D ^{1}H CPMG NMR spectra comprising of all the groups: normal control (NC), toxic control -DMBA (TC), ALA-0.25 ml/kg (T1) and ALA-0.5 ml/kg (T2). Color circles indicate the 95% confidence interval for each class (B). The pairwise PLS-DA score plots (d-f): (d) between normal control (NC) and DMBA treated toxic control (TC) group, (e) between NC and DMBA+0.25ml/kg-AL and (f) between NC vs DMBA+ALA-0.5ml/kg.

As listed in table 12, twenty five metabolites were found to be significantly perturbed in the sera of DMBA treated rats compared with normal control rats. DMBA treated rats had elevated levels of lipids, VLVL/LDL lipoprotein, lactate, NAG, OAG, PUFA, arginine, citrulline, creatine, myo-inositol, glycine, allantoin, tyrosine, histidine, phenylalanine, formate and trigonelline in their sera. Moreover, decreased levels of glucose, choline/GPC, and several amino acids including, alanine, isoleucine, valine, glutamate and glutamine was recorded as well. Further, we found that the metabolic alterations which were observed in DMBA treated group were ameliorated after the ALA treatment as evident from the box plot (Figure 21).

Figure 21: Biochemical effects of ALA treatment upon DMBA toxicity

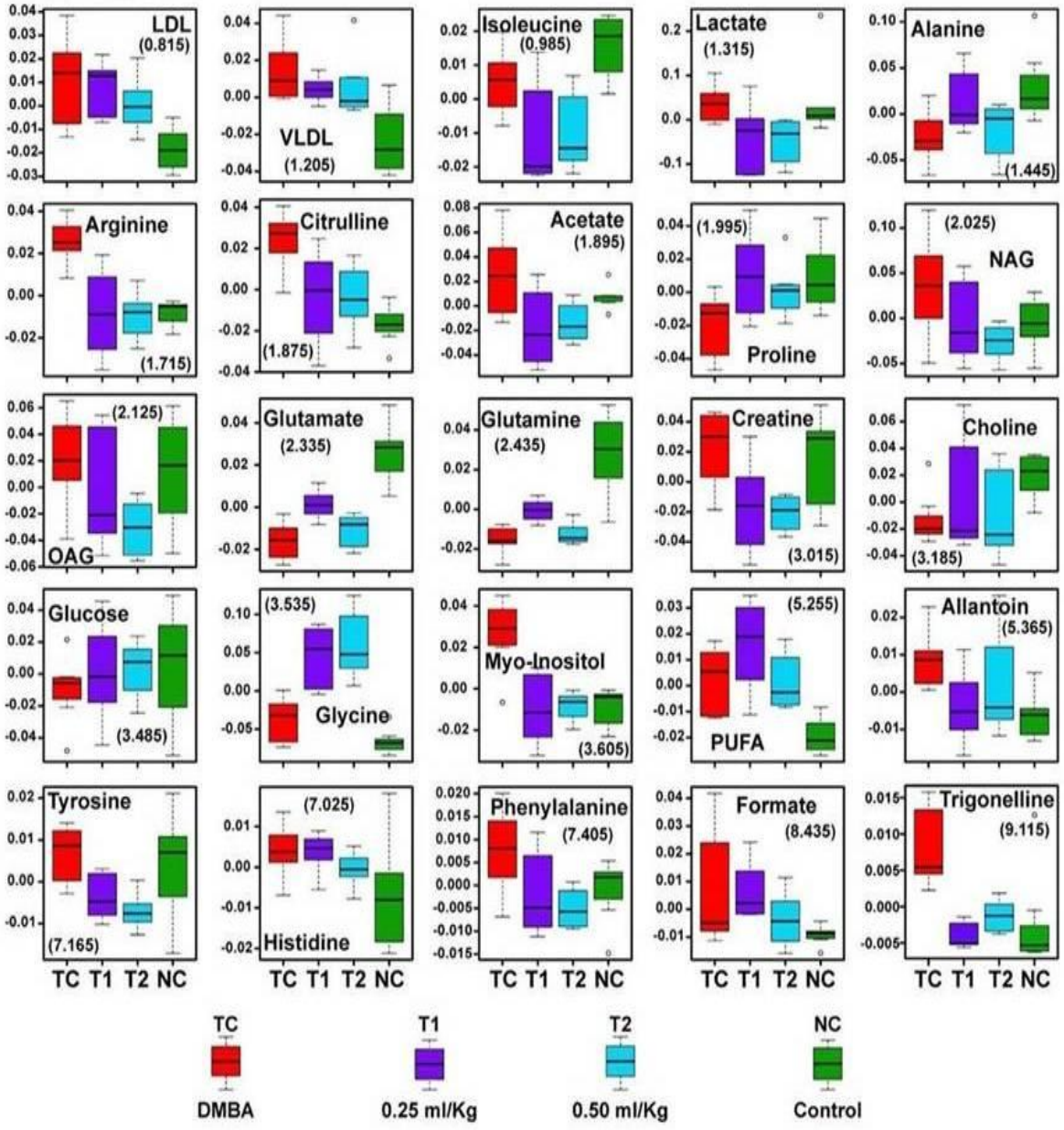

Representative box-cum-whisker plots showing quantitative variations of relative signal integrals for serum metabolites relevant in the context of pathophysiology of mammary gland cancer. For presented metabolite entities, the VIP score >1 and statistical significance is at the level of $p \leq 0.05$. In the box plots, the boxes denote interquartile ranges, horizontal line inside the box denote the median, and bottom and top boundaries of boxes are 25^{th} and 75^{th} percentiles, respectively. Lower and upper whiskers are 5^{th} and 95^{th} percentiles, respectively.

4.2.5 Serum metabolic profiling using 1D ^{1}H NMR of GLA (MNU)

The representative 1D ^{1}H CPMG NMR spectra of rat serum samples obtained from different groups with the assigned resonances of relevant metabolites are shown in Figure 22A. The NMR spectra showed signals mainly from lipids/lipoproteins [e.g. low-density lipoprotein (LDL), very low density lipoprotein (VLDL), PUFAs etc.] and amino acids [e.g. alanine, valine, lysine, leucine, isoleucine, phenylalanine, histidine, tyrosine, glutamine, glutamate and proline etc.]. Other identified metabolites were glucose, choline, creatine, creatinine, pyruvate, aceto-acetate, acetate, citrate, lactate, N-acetyl and O-acetyl glycoproteins (NAG, OAG) (Figure 22B). We performed the multivariate data analysis to find out the MNU induced metabolic alterations and to further reveal the effect of GLA treatment on MNU induced metabolic alterations (Figure 22B).

Figure 22A: Stack plot of representative 1D ^{1}H NMR spectra of rat sera with MNU and GLA

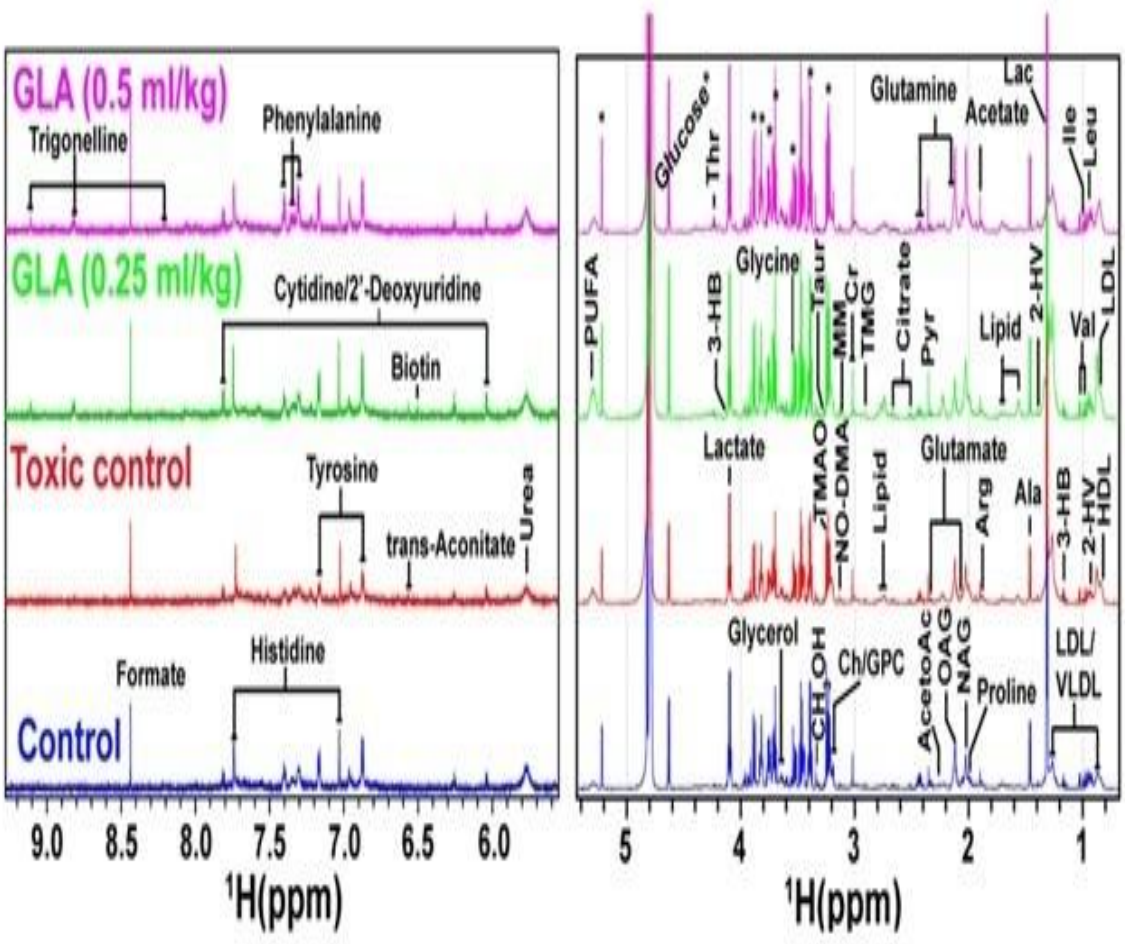

The assignment of serum metabolites was representing through peaks. The abbreviations used are: LDL/VLDL: Low/very-low density lipoproteins; HDL: high density lipoproteins; PUFA: polyunsaturated fatty acids; Ile: isoleucine; Leu: leucine; Val: valine, 3-HB: 3-hydroxy-butyrate; 2-HV: 2-hydroxy-valerate; Lac: lactate; NAG: N-actylglycoproteins; OAG: O-acetylglycoprotein; AcetoAc: acetoacetate; Pyr: pyruvate; Taur: taurine; DMG: dimethylglycine; Cr: creatine/creatinine; NoDMA: N-nitrosodimethyl amine; Ch: choline; GPC: glycerophosphocholine, TMAO: trimenthylamine-N-oxide.

Figure 22B: Box-cum-whisker plot of representative 1D ^{1}H NMR spectra of rat sera with MNU and GLA

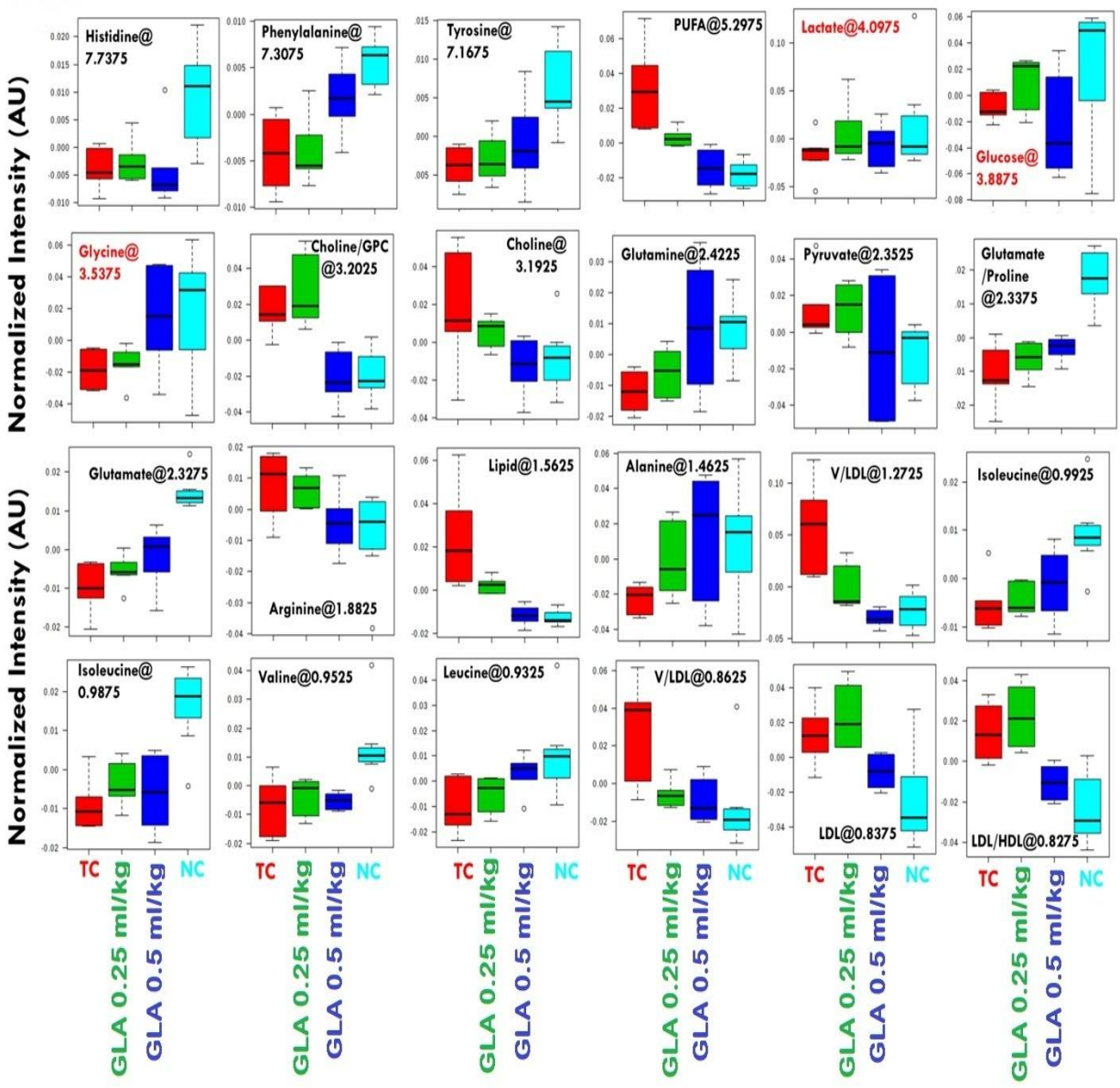

Box-cum-whisker plots are the representation of quantitative variations in serum metabolites. For presented metabolite entities, the VIP score >1 and statistical significance is at the level of $p \leq 0.05$(the metabolites highlighted in red are having p>0.05).In the box plots, the boxes denotes interquartile ranges, horizontal line inside the box denote the median and bottom and top boundaries of boxes are 25th and 75th percentiles respectively. 5th and 95th percentiles show the lower and upper whiskers respectively.

Unsupervised PCA score plots were constructed for an initial overview of the data set and identifying the outlier samples. The outliers were excluded from both the data sets and the resulted data sets were then subjected to PLS-DA to minimize the possible contribution of intergroup variability and to further improve the separation between the four groups (Figure 23). The combined PCA score plot (Figure 23A) showed clear trend of clustering in different groups and no further outlier sample was detected. The combined PLS-DA score plot for all the three groups (Figure 23B) showed that treated groups are well separated from normal control (NC) group with a significantly higher quality of fit and predictability (i.e. R2, Q2> 0.5,Figure 23C).The careful inspection of the combined PLS-DA score plot also revealed that GLA 0.25ml/kg and GLA 0.5ml/kg treatments are mitigating the effects of MNU induced toxicity as inferred by the progressively shifting 2D PLS-DA scores of these groups within the control group. The ameliorative effect of GLA became more evident to the 2D score plot obtained from combined OPLS-DA analysis for all the three groups. OPLS-DA was performed using standard procedures for multivariate statistical analysis using Metabo Analyst. Next, to obtain satisfactory classification and identify the discriminatory metabolic marker, pair-wise PLS-DA analysis was further performed with each of the three treated groups [toxic control (TC), GLA 0.25ml/kg and GLA 0.5ml/kg] with respect to normal control group (Figure 23D-F).The model parameters for the explained variation R2, and the predictive capability, Q2, were significantly high [(R2>0.98, Q2> 0.6), displayed in their respective PLS-DA score-plots] in each case, indicating that the pair-wise PLS-DA models constructed from CPMG spectra possessed satisfactory fit with good discriminatory power.

The visual inspection of pair wise score plots showed a clear differentiation between normal samples and MNU treated samples indicating that significant metabolic changes were induced by MNU treatment (Figure 23D), whereas the separation decreased progressively after treatment with GLA 0.25ml/kg and GLA 0.5ml/kg (Figure 23E, 23F). Next to evaluate the biochemical effects of GLA treatment on MNU induced toxicity, we identified the metabolic markers using variable importance on projection (VIP) score >1 for discrimination significance and further tested for statistical significance at the level of $p<0.05$ derived from Wilcoxon Mann–Whitney test. Overall, we identified twenty two metabolic markers significantly perturbed in the sera of MNU treated rats compared to normal control rats. These marker metabolic entities along with their chemical shifts, VIP score and p-value are listed in table 13. Compared with control group, MNU treated rats had significant elevation of lipids, VLDL/LDL lipoprotein, choline/glycerophosphocholine (GPC), arginine, pyruvate, and N-nitroso-dimethylamine in their sera, whereas, they were having decreased levels of glucose and several amino acids including glycine, alanine, leucine, isoleucine, valine, phenylalanine, histidine, tyrosine, glutamate and glutamine (Figure 22 and table 13). Further, we found that the metabolic alterations which were observed in MNU treated group were ameliorated after the GLA treatment (Figure 22). For example, the significantly increase levels of metabolites in the MNU treated group such as lipids, LDL/VLDL, PUFAs, pyruvate, choline, GPC, arginine and N-nitroso-dimethylamine were decreased in the GLA treated groups (Figure 22). Similarly, the levels of amino acids were increasing towards normal after GLA treatment.

Figure 23: Multivariate PCA and PLS-DA analysis of rat sera with MNU and GLA

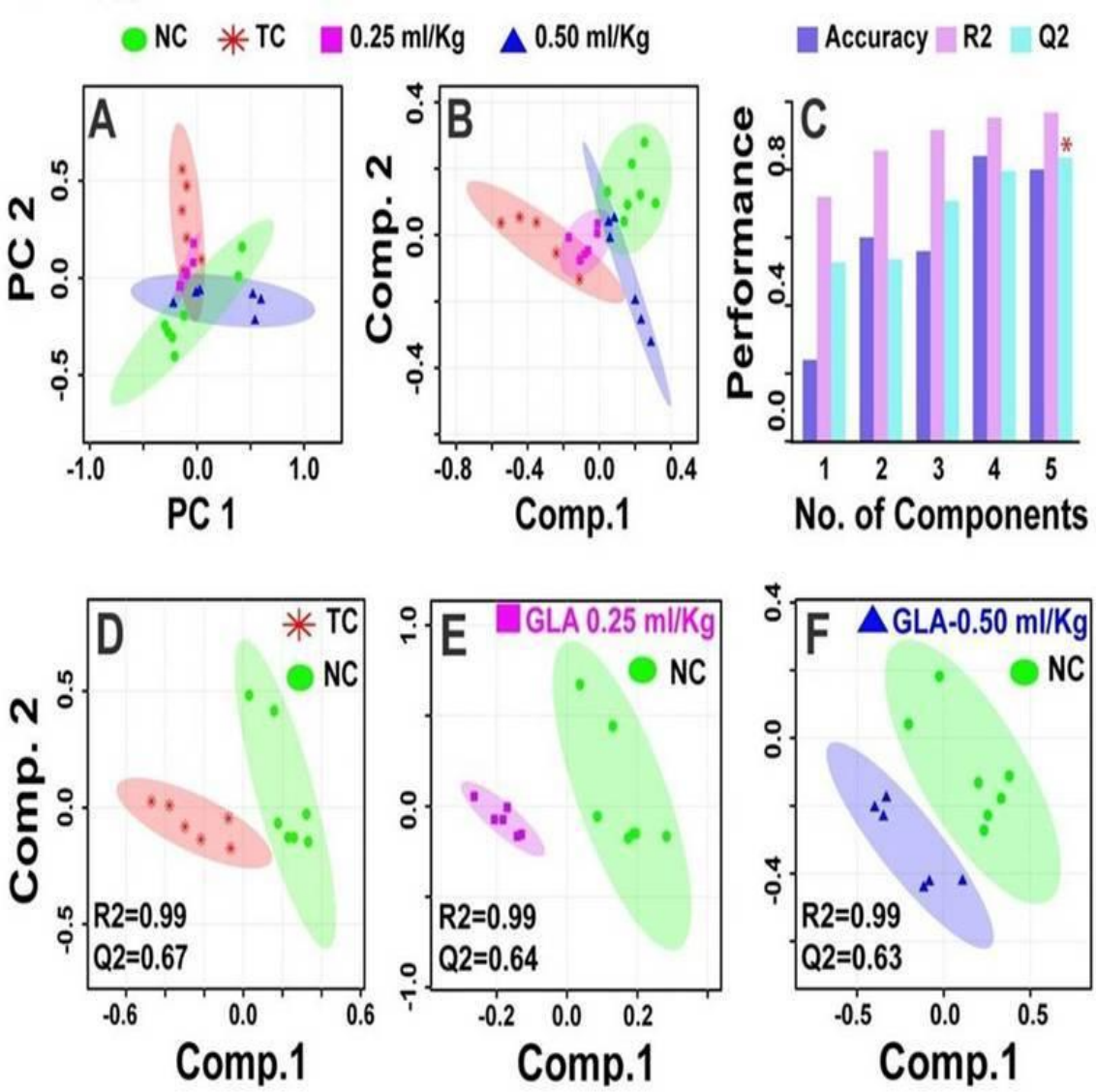

Normal control (NC), toxic control (TC), GLA (0.25 ml/kg) (D1) and GLA (0.5 ml/kg) (D2) were cumulatively analyzed through combined 2D PCA (A) and 2D PLS-DA (B) using 1D 1H NMR spectra. 95% confidence interval for each class is represented through color circles. Cross-validation of parameters for PLS-DA modeling (C), Pairwise PLS-DA score plots (D) between normal control (NC) and MNU treated toxic control (TC) group, (E) between NC and MNU+GLA (0.25ml/kg) and (F) between NC v/s MNU+GLA (0.5ml/kg).

4.2.6 Serum metabolic profiling using 1D ^{1}H NMR of GLA (DMBA)

The representative 1D ^{1}H CPMG NMR spectra of rat serum samples obtained from different groups with the assigned resonances of relevant metabolites is shown in figure 24. The NMR spectra showed signals mainly from lipids/lipoproteins [e.g. LDL, VLDL, PUFAs etc] and amino acids (e.g. alanine, valine, leucine, isoleucine, phenylalanine, histidine, tyrosine, glutamine, glutamate and proline etc.). Other identified metabolites were glucose, choline, creatine/creatinine, acetone, pyruvate, acetate, citrate, lactate, NAG, OAG.

Figure 24: Stack plot representation of 1D ^{1}H NMR spectra of rat sera treated with GLA and DMBA

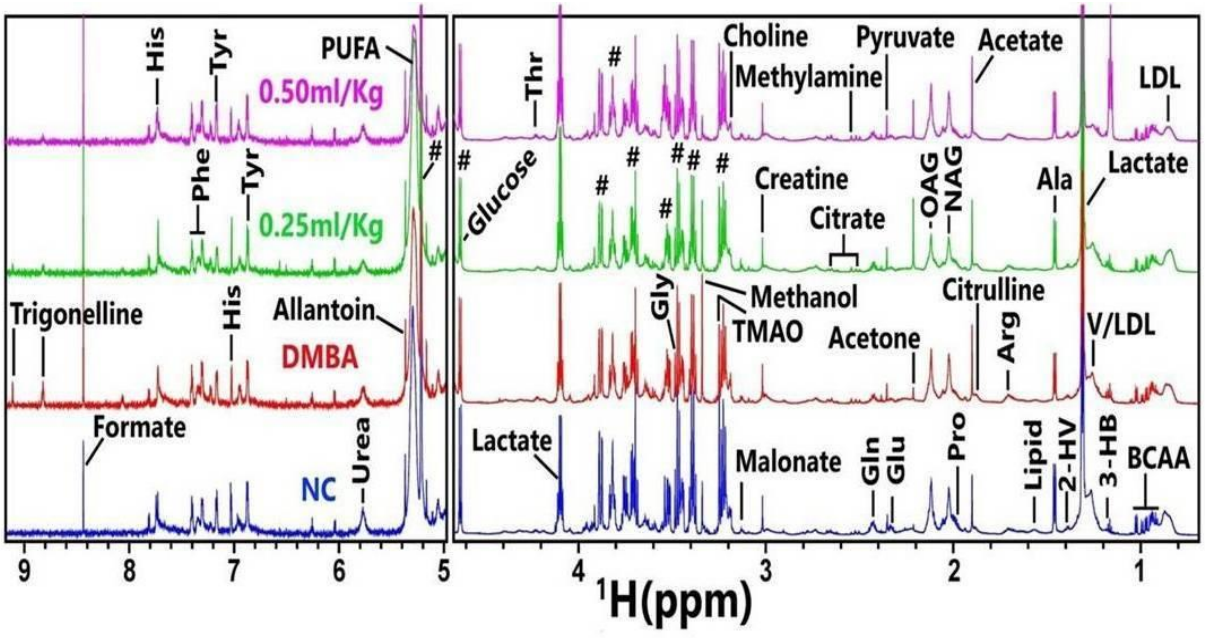

In figure, the peaks show the assignments of serum metabolites. The abbreviations used are: LDL/VLDL: low density lipoprotein/very-low density lipoproteins; PUFA: polyunsaturated fatty acids; BCAA: branched chain amino acid; 3-HB: 3-hydroxy-butyrate; 2-HV: 2-hydroxy-valerate; NAG: Nacetyl glycoproteins; OAG: O-acetyl glycoprotein; Pro: Proline; Glu: Glutamate; Gln: Glutamine; TMAO: Trimethylamine-N-oxide; Gly: Glycine; His: Histidine; Tyr: Tyrosine; Phe: Phenylalanine; Thr: Threonine; Ala: Alanine.

We implemented multivariate data analysis to find out the DMBA induced metabolic alterations and further to reveal the ameliorating effect of GLA treatment on DMBA induced metabolic changes. Unsupervised PCA score plots were constructed for an initial overview of the data set and identifying the outlier samples. Two outliers were detected, one from the toxic control and other from the normal control group. The outliers were excluded from both the data sets and the resulted data sets were then subjected to supervised OPLS-DA model to minimize the possible contribution of intergroup variability and to further improve the separation between the groups (Figure 25). The combined PCA score plot showed a clear trend of clustering in different groups and no further outlier samples were detected. The combined OPLS-DA score plot for all the groups (Figure 25A) showed that treated rat groups are well separated from normal control group with a significantly higher quality of fit and predictability (R2Y, Q2> 0.7). Moreover, the OPLS-DA model was further validated based on permutation statistics using 100 permutations. The careful inspection of combined OPLS-DA score plot also revealed that GLA 0.25ml/kg and GLA 0.5ml/kg treatments are mitigating the effect of DMBA induced toxicity as inferred by the shift of the GLA treatment group back towards the normal control group. Discriminatory metabolic marker, pairwise PCA and OPLS-DA (Figure 25) analysis was performed with all the three treated groups (DMBA, GLA 0.25ml/kg, and GLA 0.5ml/kg) in respect to normal control group to obtain the satisfactory classification and identification. The model parameters for the explained variation, R2Y, and the predictive capability, Q2, were significantly high (displayed in their respective OPLS-DA score-plots) in each case, indicating that the pairwise OPLS-

DA models constructed from CPMG spectra possessed satisfactory fit with good discriminatory power.

The visual inspection of the pairwise score plots showed a clear differentiation between normal control group and DMBA treated group indicating that significant metabolic changes were induced by DMBA treatment (Figure 25B). Next, to evaluate the biochemical effects of GLA treatment on DMBA induced toxicity, the altered metabolites were identified using OPLS-DA, S-plot and further tested for statistical significance at the level of $p<0.05$.

Figure 25: Combined and pairwise OPLS-DA analysis of rat sera treated with GLA and DMBA

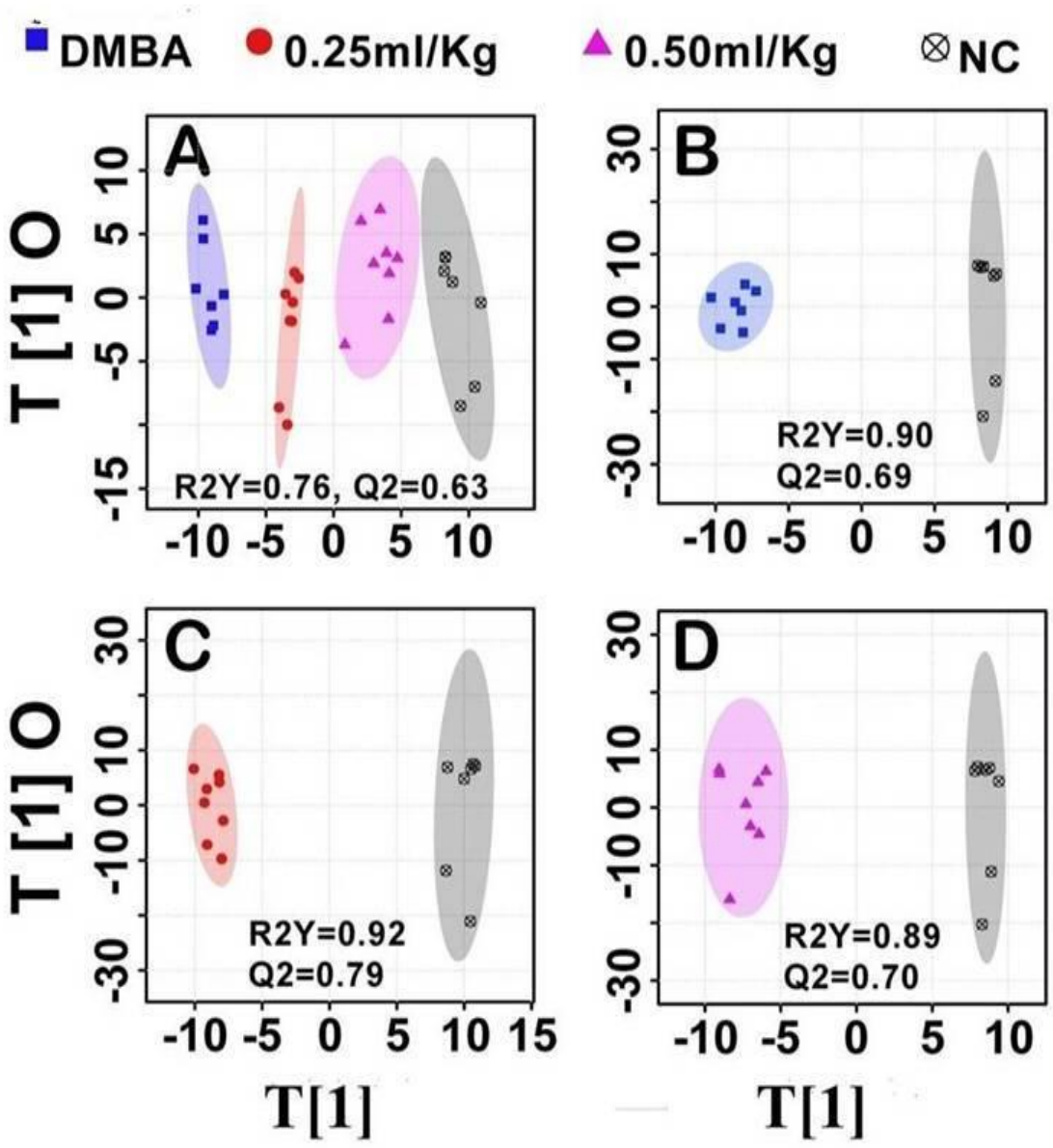

The 2D OPLS-D analysis of 1D ^{1}H CPMG NMR spectra (A) score plot derived from combined analysis comprising of all the groups: normal control (NC), toxic control (TC), GLA (0.25 ml/kg) and GLA (0.5 ml/kg). Pairwise analysis (B) between normal control (NC) and DMBA treated toxic control (TC) group, (C) between NC and DMBA+GLA (0.25 ml/kg), and (D) between NC and DMBA+GLA (0.5 ml/kg). Color circles indicate the 95%confidence interval for each class.

Overall, we identified fifteen metabolic markers significantly perturbed in the sera of DMBA treated rats compared to normal control rats. These marker metabolic entities along with their chemical shifts, their levels (increased or decreased) and p-value are listed in table 14. Compared with normal control group, DMBA treated rats had significantly elevated levels of lipids, VLDL/LDL lipoprotein, PUFA, OAG, creatine, and amino acids (arginine, citrulline, phenylalanine, histidine) in their sera, whereas, they were having decreased levels of glucose, pyruvate, trimethylamine (TMAO), and amino acids (glutamate, and glutamine) (Figure 26 and Table 14).Further, we found that the metabolic alterations which were observed in DMBA treated group get ameliorated after the GLA treatment. The metabolites which were increased or decreased in DMBA treated group such as lipids, LDL/VLDL, PUFAs, OAG, arginine, citrulline, phenylalanine returned to normal after GLA treatment (Figure 26).

Figure 26: Effect of GLA and DMBA treatment on biochemical parameters

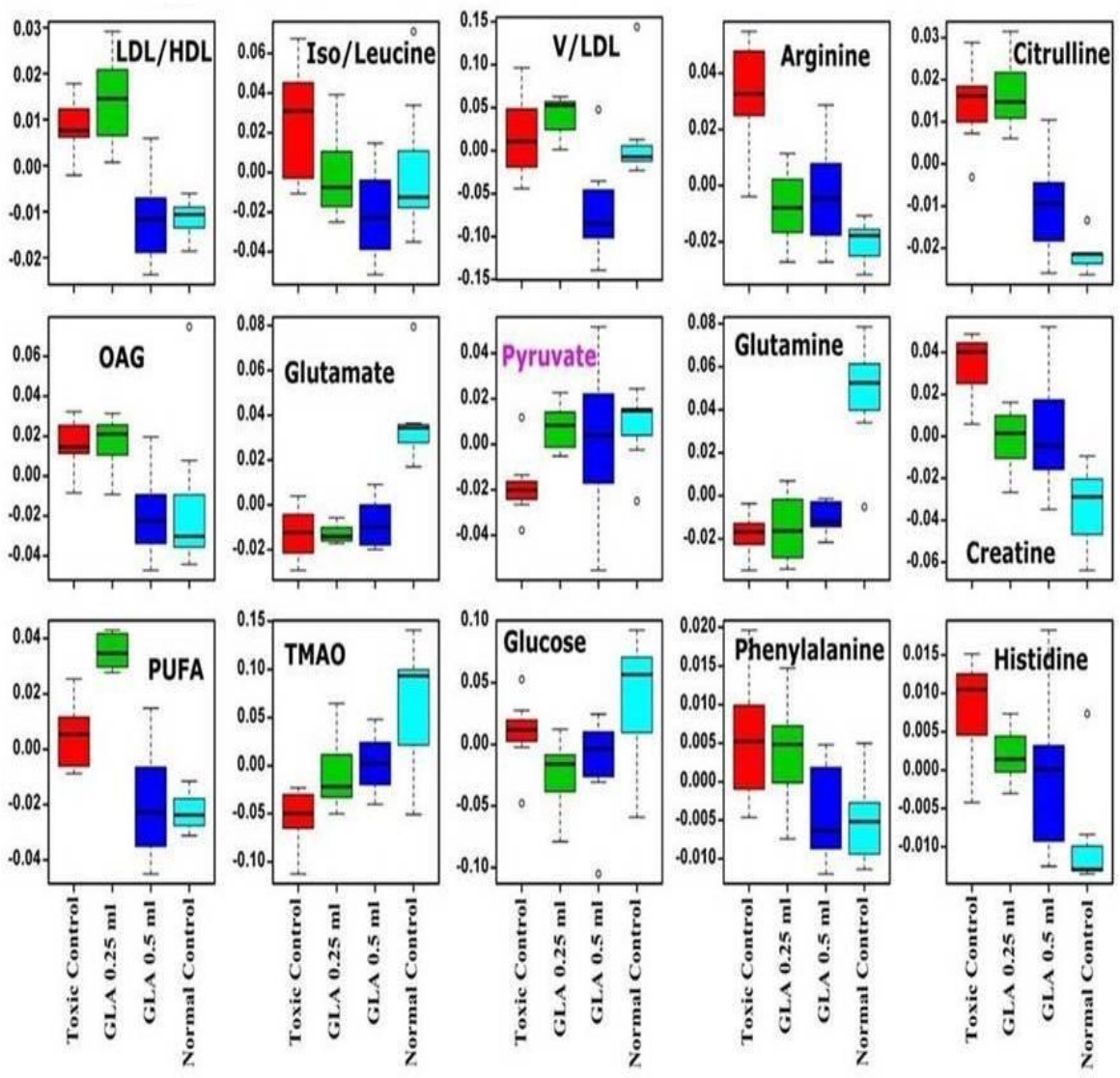

The box-cum-whisker plots are showing quantitative variations of relative signal integrals for serum metabolites relevant in the context of the pathophysiology of mammary gland cancer. The metabolite highlighted in pink are those which are non-significant ($p > 0.05$). In the box plots, the boxes denote interquartile ranges, horizontal line inside the box denote the median, bottom and top boundaries of boxes are 25^{th} and 75^{th} percentiles respectively. Lower and upper whiskers are 5^{th} and 95^{th} percentiles respectively.

Table 12: Metabolic variability's among the groups treated with DMBA and ALA when compared to normal control

#	^{1}H ppm	Metabolite (↓↑)	Control vs		
			DMBA	ALA-0.25	ALA-0.5
1	0.825-0.885	LDL	*(↑)	*(↑↑)	*(↑↑↑)
2	1.205-1.235	VLDL	*(↑)	*(↑↑)	*(↑↑↑)
3	5.245-5.355	PUFA	*(↑)	*(↑)	*(↑↑↑)
4	0.985	Isoleucine	(↓)#	*(↓↓)	(↓↓↓)#
5	7.025, 7.725	Histidine	*(↑)	*(↑↑)	*(↑↑↑)
6	7.405	Phenylalanine	*(↑)	(↓↓)#	*(↓↓)
7	1.455	Alanine	*(↓)	(↓↓)#	*(↓↓)
8	1.695-1.715	Arginine	*(↑)	(↓↓)#	(↓↓)#
9	2.435	Glutamine	*(↓)	*(↓↓↓)	*(↓↓)
10	1.995	Proline	*(↓)	(↑)	*(↓↓↓)
11	3.535	Glycine	*(↑)	*(↑)	*(↑)
12	6.885, 7.175	Tyrosine	(↑)#	*(↓↓↓)	*(↓↓)
13	1.865-1.885	Citrulline	*(↑)	(↑↑)#	(↑↑↑)#
14	3.015	Creatine	(↑)	*(↓↓)	*(↓↓)
15	1.895	Acetate	(↑)#	*(↓↓)	*(↓↓↓)
16	2.025	NAG	(↑)	*(↓↓↓)	*(↓↓)
17	2.115,2.125	OAG	(↑)#	*(↓↓)	*(↓↓)
18	2.325	Glutamate	*(↓)	*(↓↓↓)	*(↓↓)
19	3.885, 5.215	Glucose	*(↓)	*(↓)	*(↓)
20	3.605	Myo-Inositol	*(↑)	(↓↓)#	(↓↓↓)
21	1.315	Lactate	(↑)	*(↓↓)	*(↓↓)
22	3.185	Choline	*(↓)	(↓↓)#	*(↓↓)
23	5.365	Allantoin	*(↑)	(↑)#	*(↑)
24	8.435	Formate	*(↑)	*(↑↑)	(↑↑↑)#
25	8.825, 9.115	Trigonelline	*(↑)	(↑↑↑)#	(↑↑)#

The up and down arrows represent, respectively, increased and decreased metabolite levels. A ↑↑↑/↓↓↓ or ↑↑/↓↓ score was given to the metabolites of the treatment dose which showed ameliorating effects from DMBA towards control. Abbreviations used are as follows: LDL (low density lipoproteins); VLDL (very low density lipoproteins); NAG (N-acetyl glycoprotein); OAG (O-acetyl glycoprotein); PUFA (poly unsaturated fatty acids).

Note-: Symbols * = p-value < 0.05, # = VIP Score < 1.

Table 13: List of marker metabolites responsible for variation and class separation between normal control and toxic control (MNU) groups

#	Metabolite	^{1}H shift (ppm)	Toxic Control (↑↓)	GLA 0.25 ml	GLA 0.5 ml
1.	LDL	0.8275	↑ *	↑ *	↑ *
		0.8375	↑ *	↑ *	↑ *
2.	VLDL/LDL	0.8625	↑ *	↑ *	↑
		1.2725	↑ *	↑ *	↑ *
3.	Leucine	0.9325	↓ *	↓ *	↓*
4.	Valine	0.9525	↓ *	↓ *	↓ *
5.	Isoleucine	0.9875	↓ *	↓ *	↓ *
		0.9975	↓ *	↓ *	↓ *
6.	Alanine	1.4625	↓ *	↓	↑ *
7.	Lipid	1.5625	↑ *	↑ *	↑
8.	Arginine	1.8825	↑ *	↑ *	--
9.	Glutamate	2.3275	↓ *	↓ *	↓ *
10.	Glutamate/Pro	2.3375	↓ *	↓ *	↓ *
11.	Pyruvate	2.3525	↑ *	↑ *	↓
12.	Glutamine	2.4225	↓ *	↓ *	↓ *
13.	Lipid	2.7375	↑ *	↑ *	↑
14.	Nitroso-DMA	3.1325	↑ *	↑ *	↑ *
15.	Ch/GPC	3.1975	↑ *	↑ *	↓
		3.2025	↑ *	↑ *	↓
16.	Glycine	3.5375	↓	↓ *	↓
17.	Glucose	3.8875	↓ *	↓ *	↓ *
18.	Lactate	4.0975	↓	↑ *	↑
19.	PUFA	5.2925	↑ *	↑ *	↑
		5.2975	↑ *	↑ *	↑
20.	Tyrosine	7.3025	↓ *	↓ *	--
21.	Phenylalanine	7.4075	↓ *	↓ *	↓ *
22.	Histidine	7.7375	↓ *	↓ *	↓ *

* For statistical significance based on p-value ≤0.05. The metabolic biomarkers were identified from PLS-DA model analysis using VIP score >1.0 as the cut-off value for the discrimination significance and p-value ≤0.05 for statistical significance. The up and down arrows represent, increased (↑) and decreased (↓) levels in different groups with respect to the control.

Table 14: List of metabolites responsible for variation and class separation between the NC, DMBA and DMBA+GLA treatment at two doses 0.25 ml/kg and 0.5 ml/kg

The metabolic biomarkers were identified from OPLS-DA, S-plot for the discrimination significance and p-value δ0.05 for statistical significance. The up (↑) and down (↓) arrows represent, respectively, increased and decreased metabolite levels. A ↑↑↑/↓↓↓ or ↑↑/↓↓ score was given to the metabolites of the GLA treatment dose which showed ameliorating effects from DMBA towards control. "#" represents metabolites with mostprominent effect of GLA treatment.

S. No	Metabolite	ppm	NC vs.		
			DMBA	GLA-0.25 ml/kg	GLA-0.50 ml/kg
1	LDL/HDL	0.79	↑	↑↑	#
2	Iso/leucine	0.93	↑	#	↓↓
3	V/LDL	1.25	↑	↑↑	↓↓
4	Arginine	1.71	↑	↑↑↑	↑↑
5	Citrulline	1.85	↑	↑↑	↑↑↑
6	OAG	2.09	↑	↑↑	↑↑↑
7	Glutamate	2.33	↓	↓↓	↓↓↓
8	Pyruvate*	2.35	↓	↓↓↓	↓↓
9	Glutamine	2.43	↓	↓↓	↓↓↓
10	Creatine	3.01	↑	↑↑	↑↑↑
11	TMAO	3.25	↓	↓↓	↓↓↓
12	Glucose	3.87	↓	↓↓	↓↓↓
13	PUFA	5.25	↑	↑↑	#
14	Phenylalanine	7.29	↑	↑↑	#
15	Histidine	7.71	↑	↑↑	↑↑↑

Note: Metabolites which do not have p-value significant are represented by *****.

The DMBA and MNU induced changes indicated that subsets of metabolites were changed in similar way in all groups, which were ameliorated by ALA and GLA treatment. The decreased glucose and increased lactate and myo-inositol levels in DMBA& MNU are well correlated with Warburg effect and increased bioenergetics demand for cellular proliferated (increased glycolytic activity with increased lactate production). Further, significant increase in the levels of lipoproteins (LDL/VLDL) and PUFAs, in DMBA and MNU treated animals suggests increased requirement of the building blocks of the cell membranes in rapidly proliferating tumor cells. Exogenous ALA and GLA supplementation provided further increase in the levels of lipoproteins (LDL/VLDL) and PUFA's and the same could be attributed to the fact that ALA and GLA is a polyunsaturated fat. The lower levels for choline could be the consequence of excessive need for choline and its derivatives during rapid cell proliferation.

Inflammation is a most common clinical manifestation of various cancer types and triggers a hypercatabolic state, resulting in increased energy requirements [89]. Consistent with this phenomenon the increased concentrations of serum acetyl-glycoproteins (both NAG and OAG) (acute phase anti-inflammatory proteins expressed during inflammation and immune response) was recorded after the DMBA and MNU treatment and is in line with previous investigations in liver disease, inflammatory disease and cancer [90]. As expected, ALA and GLA (an anti-inflammatory PUFA) curtailed the expression of acute phase proteins expressed during inflammation.

The increased levels of amino acids like arginine, glycine, histidine, tyrosine, creatine and phenylalanine indicate abnormal/aberrant biosynthesis of amino acids in DMBA and MNU treated rats. The increased levels of arginine and citrulline suggest protein

catabolism, deriving overall picture of high metabolic activity, a hallmark for tumor progression [91]. The high metabolic activity as evident through increased levels of amino acids was also endorsed through increased levels of formate (a product of glycine metabolism through glycine succinate pathway). The decreased level of glucogenic amino acids (glutamate, glutamine, proline, isoleucine and alanine) in DMBA and MNU treated group suggests their increased utilization in energy production. Proline metabolism is especially important in nutrient stress, as it is interchangeably converted into glutamate and glutamine [92]. Concomitant ALA and GLA treatment further diminished the levels of glucogenic amines which could be accounted to the fact that exogenous ALA and GLA would have provided a faulty lipid to the fastly growing tumour cells. Whereas the requirement for the amino acids as a building block for cellular membranes was prevalent till such time.

The deregulated metabolites represent altered cancer cell energy metabolism including amino acid metabolism (glutamate, glutamine, alanine, etc.), glycolysis or gluconeogenesis (glucose, and lactate,) and lipid metabolism (LDL, VLDL, choline, and acetate) and are associated with high rate of glycolysis [93]. Most of the metabolic changes in DMBA and MNU treated animals were reset back to normal after ALA and GLA administration, suggesting that ALA and GLA has potential to balance the metabolic abnormalities in fastly growing cells.

4.2.8 Western blot analysis and qRT-PCR analysis

i) ALA (DMBA)

The expression of anti-apoptotic proteins (Bcl-2and Bcl-xl) was increased after DMBA administration with vice versa effect upon pro-apoptotic markers (BAD and BAX).

Treatment with ALA helped to restore the anti-apoptotic and pro-apoptotic markers favorably suggesting apoptosis. When perceived through the downstream markers of mitochondrial mediated apoptosis (VADC, cytochrome c, Apaf-1 and procaspase 9), DMBA afforded increased expression of VDAC, Apaf-1 and procaspase9 along with curtailment of cytochrome c expression (Figure 27). Treatment with ALA afforded marked regulation of apoptotic markers favoring apoptosis. Treatment with DMBA also afforded commendable hypoxia as perceived through increased expression of NFκBp65, UCHL-1, HIF-1α, FASN and SREBP-1c; and decreased expression of PHD-2.Concomitant ALA treatment afforded abatement of hypoxic markers significantly (Figure 28).

The genetic phenotypes for the protein markers for mitochondrial death pathway were validated through qRT-PCR assay (Figure 27). The findings from the immunoblotting assay were endorsed by the qRT-PCR studies, embarking that the effect of ALA is mediated through regulating the respective genetic phenotypes. The qRT-PCR studies for the hypoxic markers recorded similar pattern of fold changes as perceived through the immunoblotting assay (Figure 28).

Figure 27: Effect of ALA and DMBA upon mitochondrial associated protein signaling in mammary gland cells

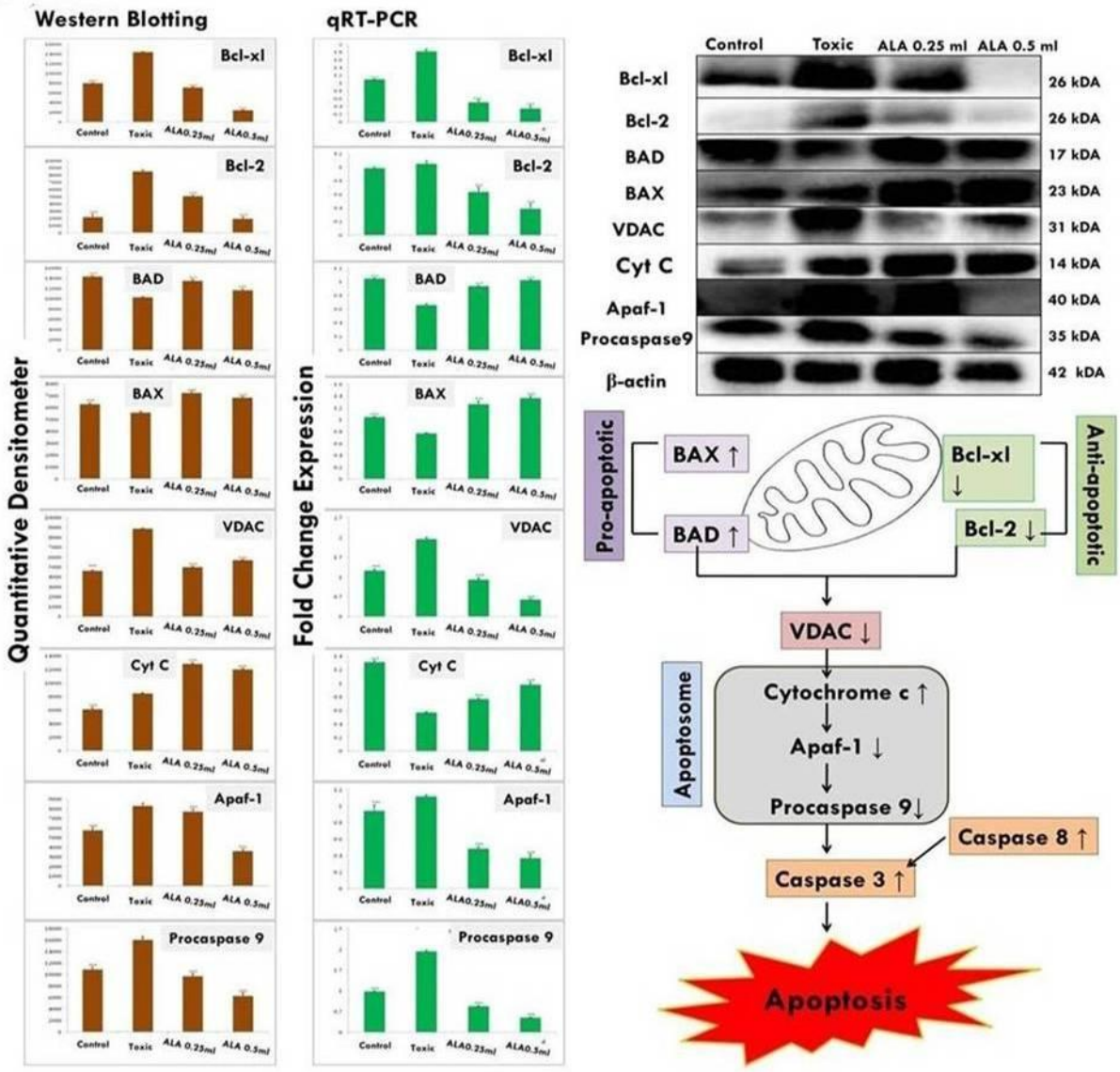

Protein extracted from individual groups [1-control, 2-DMBA treated, 3-ALA (0.25 ml/kg, p.o. + DMBA 8 mg/kg, i.v.) and 4- ALA (0.5 ml/kg, p.o. + DMBA 8 mg/kg, i.v.)] were subjected to immunoblotting of proapoptotic (BAX) and anti-apoptotic (Bcl-2 and Bcl-xl) protein with downstream apoptotic markers (VDAC, cytochrome-c, Apaf-1and procaspase 9) of respective pathway. mRNA expression of abovementioned protein were also in line with the findings of immunoblotting assay. β-actin was used as loading control. Each experiment was performed in triplicate. Values are presented as mean ± SD. Comparisons were made by the one-way ANOVA followed by Bonferroni multiple test. All groups were compared to the DMBA treated group (*p<0.05, **p<0.01, ***p<0.001).

Figure 28: Effect of ALA and DMBA on HIF-1α mediated hypoxic markers and fatty acid synthesis regulators

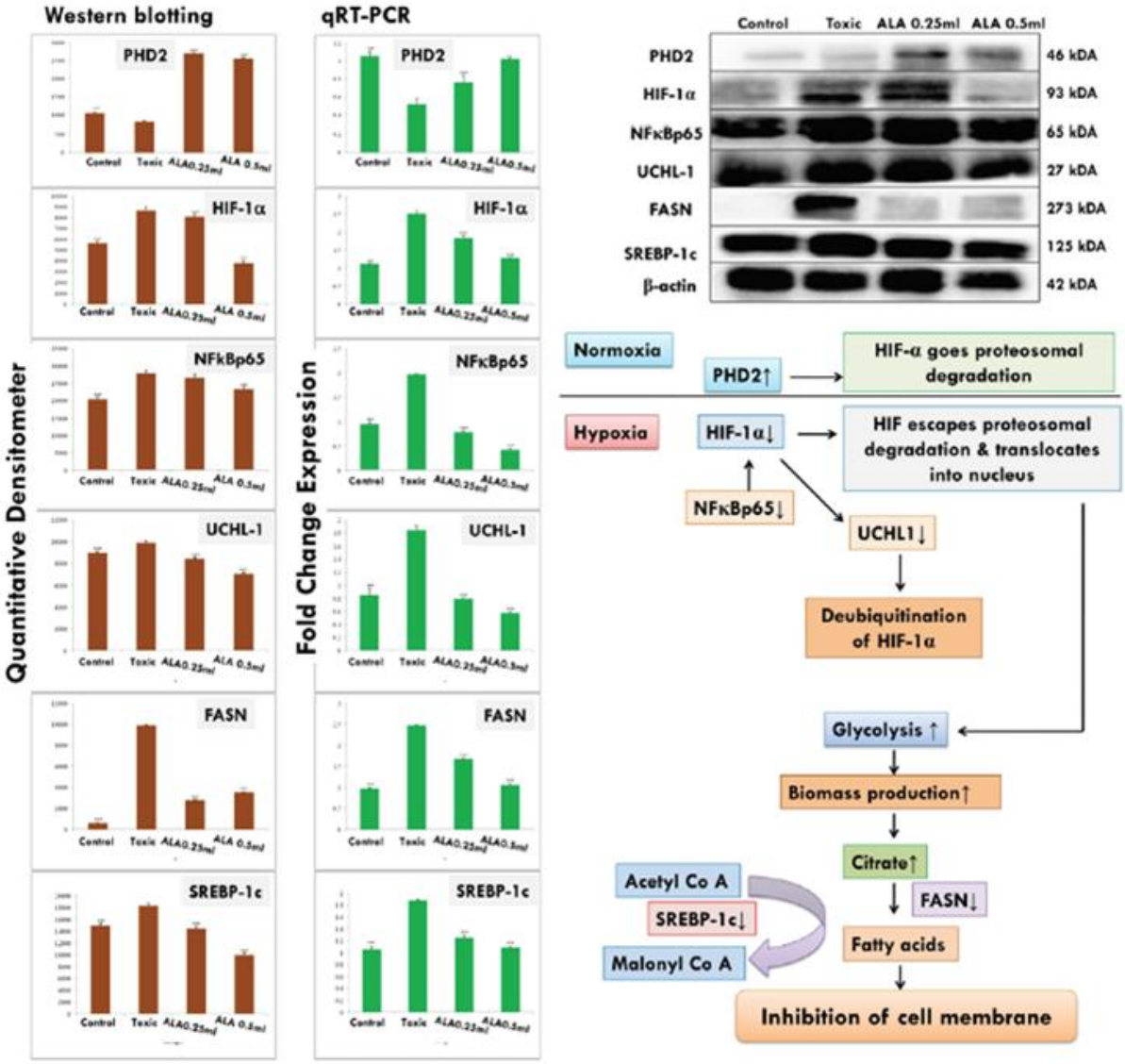

Immunoblotting of respective individual group [1-control, 2-DMBA treated, 3-ALA (0.25 ml/kg, p.o. + DMBA 8 mg/kg, i.v.) and 4- ALA (0.5 ml/kg, p.o.+ DMBA 8 mg/kg, i.v.)] for HIF-1α, PHD-2, and FASN conclude the hypoxic microenvironment after DMBA treatment. Perspective correlations of NFκBp65, UCHL-1 and SREBP-1c with the above mentioned protein are well defined through the experimental pathway. Excised mammary gland tissue sample lysed in trizol for RNA extraction and analyzed for the mRNA expression of HIF-1α, PHD-2, FASN, NFκBp65, UCHL-1 and SREBP-1c by qRT-PCR: fold induction is relative to cell under hypoxic conditions after normalization to the β-actin expression. Each experiment was performed in triplicate. Values are presented as mean ± SD. Comparisons were made on the basis of the one-way ANOVA followed by Bonferroni multiple test. All groups were compared to the DMBA treated group (*$p<0.05$, **$p<0.01$,***$p<0.001$).

ii) ALA (MNU)

The expression of the anti-apoptotic protein (Bcl-2 and Bcl-xl) of mitochondria-mediated death apoptosis pathway was increased after MNU treated group in comparison with control and the same was downregulated after ALA treatment. Pro-apoptotic protein (BAD) demonstrated downregulated expression in MNU treated group which was restored after ALA treatment. Treatment with ALA perceived downregulation of the downstream apoptotic marker (VDAC, Apaf-1, procaspase 9 and cytochrome c) (Figure 29). Immunoblotting assay also affirmed the increased expression of PHD-2 with ALA treatment, suggesting PHD2 activation. The same was further confirmed with decreased expression of HIF-1α, UCHL-1, FASN and SREBP-1c after ALA treatment (Figure 30). ALA also downregulate the expression of α-7nAchR, HMGB-1, TNF-α and NFκBp65 asserting its positive role in cholinergic anti-inflammatory pathway (Figure 31).

The immunoblotting assay ascertained mitochondrial-mediated apoptotic death induced by ALA and the same was subsequently affirmed through qRT-PCR studies. A significant decrease in the anti-apoptotic genes (Bcl-2 and Bcl-xl) were recorded after ALA treatment with vice-versa results for pro-apoptotic protein (BAD). The expression of downstream genes associated with mitochondrial-mediated apoptosis was favorably regulated after ALA treatment (Figure 29). Treatment with ALA favorably upregulated PHD-2 expression and subsequently diminished the expression of HIF-1 α, UCHL-1, FASN, and SREBP-1c (Figure 30). The mRNA expression of α-7nAchR, HMGB-1, TNF-α and NFκBp65 was also curtailed down after ALA treatment (Figure 31).

Figure 29: Effect of ALA and MNU upon mitochondrial mediated death apoptosis pathway

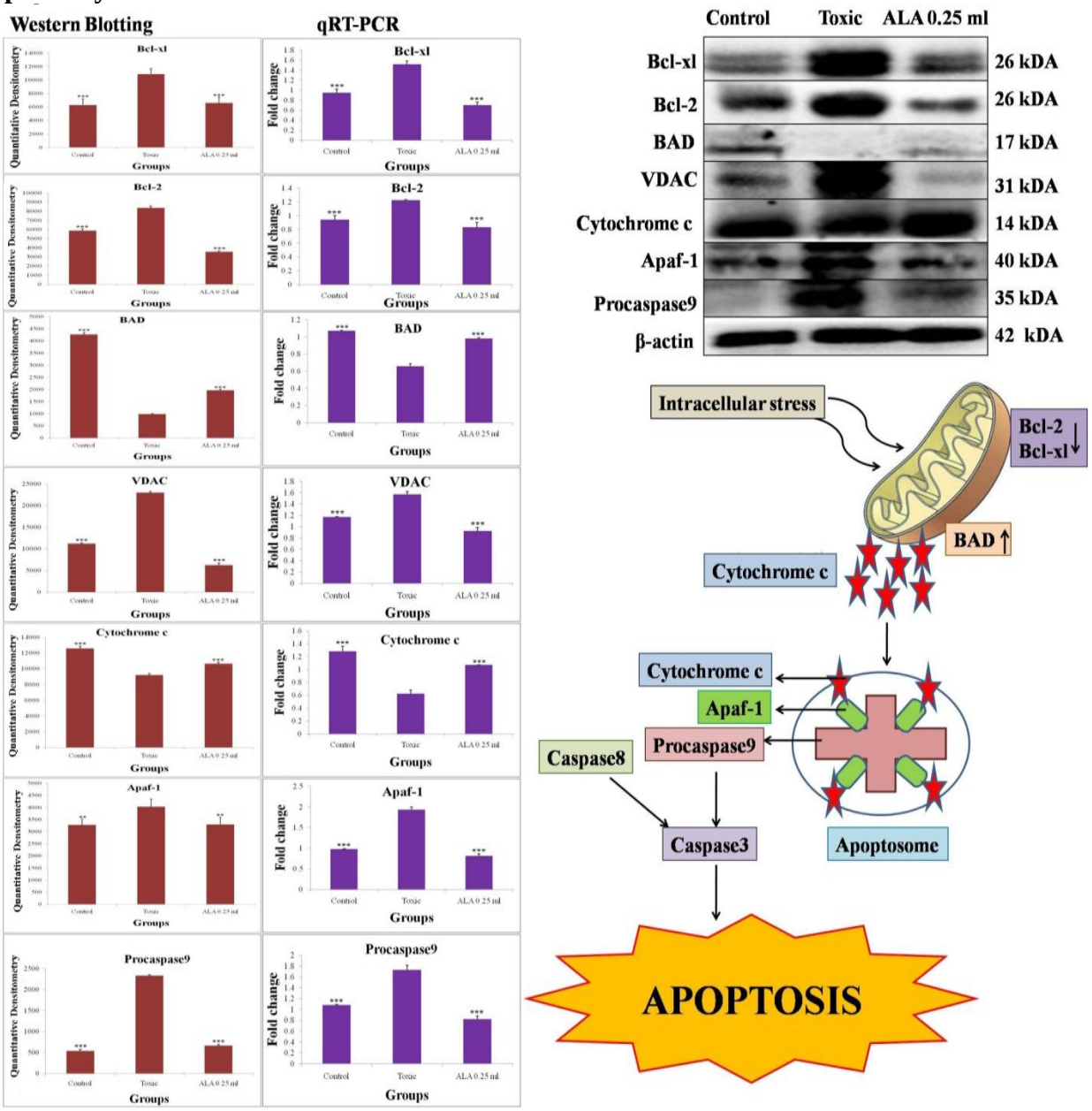

Protein was extracted from individual groups [1-control, 2-MNU treated and 3-ALA (0.25ml/kg, p.o.+MNU47mg/kg, i.v.)] and subjected to immunoblotting of proapoptotic (BAD) and anti-apoptotic (Bcl-2 and Bcl-xl) proteins with its downstream apoptotic markers (VDAC, cytochrome-c, Apaf-1and procaspase 9). mRNA expression of above mentioned proteins were also in line with the findings of immunoblotting assay. β-actin was used also loading control. Each experiment was performed in triplicate. Values are presented as mean ± SD. Comparisons are made by one-way ANOVA followed by Bonferroni multiple test. All groups are compared to the MNU treated group (*p<0.05, **p<0.01, ***p<0.001).

Figure 30: Effect of ALA and MNU on hypoxic pathway

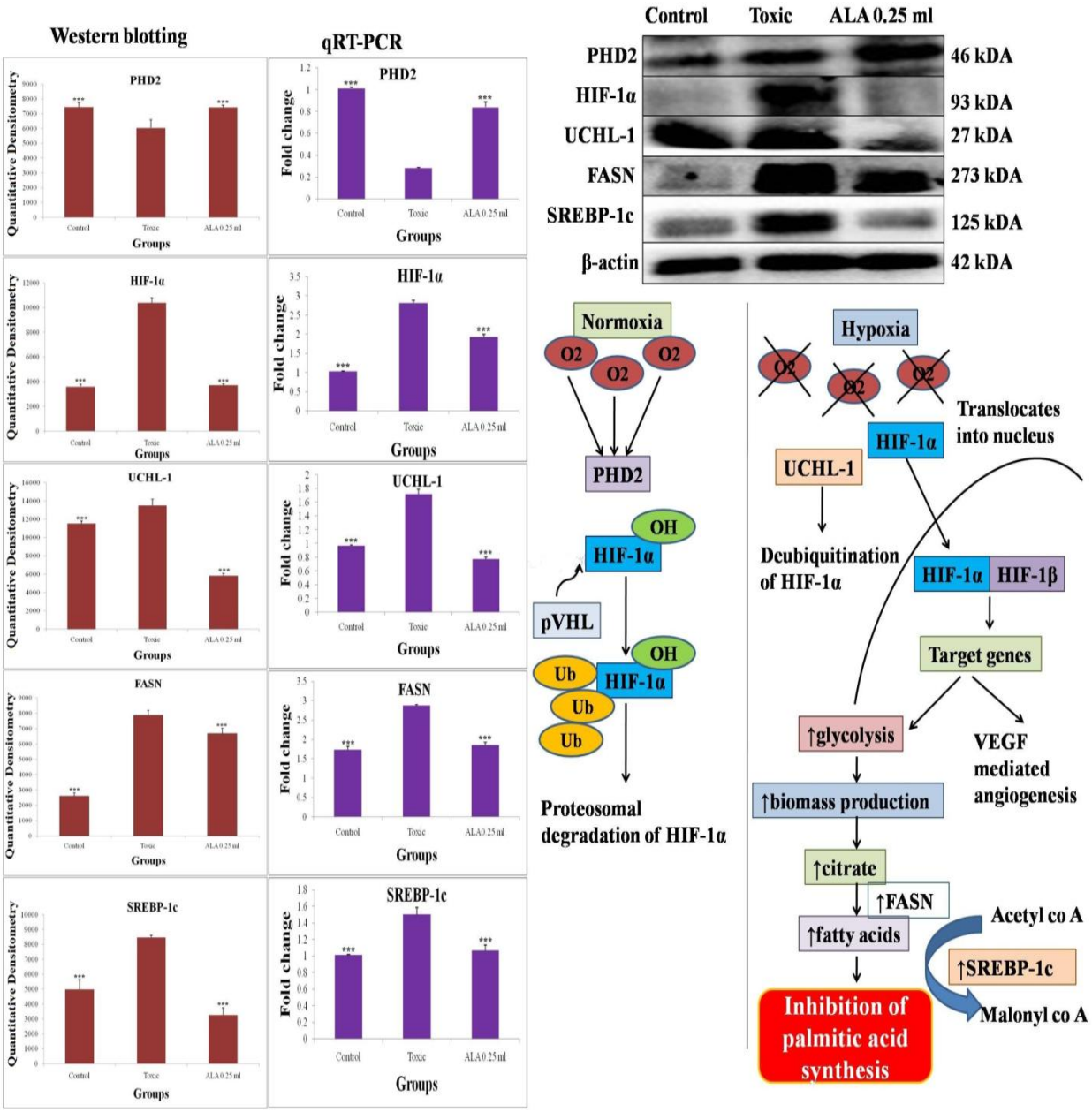

Immunoblotting of respective individual group [1-control, 2-MNU treated and 3-ALA (0.25ml/kg, p.o.+ MNU 47mg/kg, i.v.)] for the presence of PHD2, HIF-lα, UCHL-1, FASN and SREBP-1c was performed. Excised mammary gland tissue sample was lysed in trizol for RNA extraction and analyzed for the mRNA expression of PHD2, HIF-lα, UCHL-1, FASN and SREBP-lc by qRT-PCR: fold induction is relative to tissue under hypoxic conditions after normalization to the β-actin expression. Each experiment was performed in triplicate. Values are presented as mean ± SD. Comparisons are made on the basis of one- way ANOVA followed by Bonferroni multiple test. All groups are compared to the MNU treated group (*p<0.05, **p<0.01, ***p<0.001).

Figure 31: Effect of ALA and MNU on cholinergic anti-inflammatory pathway

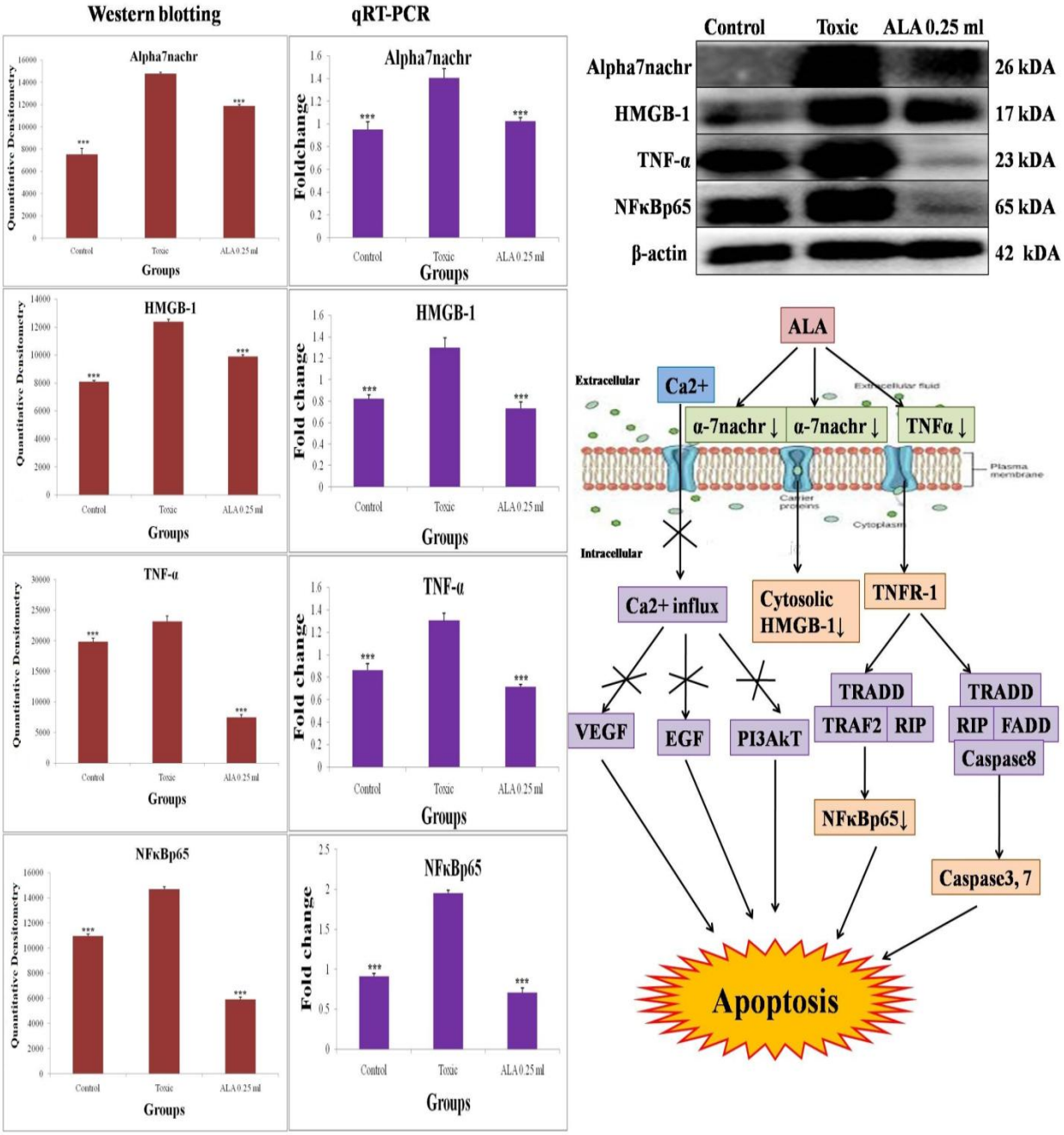

Immunoblotting of respective individual group [1-control, 2-MNU treated and 3-ALA (0.25ml/kg, p.o.+MNU47mg/kg,i.v.) for α-7nAchR, HMGB-1, TNF-α and NFκBp65 were conclude the cholinergic anti-inflammatory action of ALA and the same was verified through mRNA expression. Each experiment was performed in triplicate. Values were presented as mean ± SD. Comparisons are made on the basis of one-way ANOVA followed by Bonferroni multiple test. All groups are compared to the MNU treated group (*p<0.05, **p<0.01, ***p<0.001).

iii) GLA (DMBA)

After DMBA treatment, the expression of anti-apoptotic proteins (Bcl-2 and Bcl-xl) was increased with vice versa effect upon pro-apoptotic marker (BAX and BAD). GLA treatment helped to reinstate the anti-apoptotic and pro-apoptotic markers favorably advocating apoptosis. DMBA treatment upregulated the expression of downstream markers of mitochondria mediated apoptosis (VADC, cytochrome c, Apaf-1 and procaspase 9) along with curtailment of cytochrome c expression (Figure 32). GLA treatment afforded marked protection against the same and favoring apoptosis. DMBA treatment also afforded commendable hypoxia which was perceived through up-regulated expression of NFκBp65, UCHL-1, HIF-1α, FASN and SREBP-1c along withdown-regulated expression of PHD-2. GLA treatment upregulated the PHD-2 expression and diminished the hypoxic environment by downregulating the protein expressions of NFκBp65, UCHL-1, HIF-1α, FASN and SREBP-1c (Figure 33). The expression of α7nAchR and HMGB-1 was downregulated and TNF-α expression was increased after GLA treatment when scrutinized through immunoblotting analysis (Figure 34).

The fold change expressions of the genes were validated through qRT-PCR assay (Figure 32). The findings from the immunoblotting assay of the mitochondrial mediated apoptosis pathway were validated through fold change expression of genes and the same observations were found. The qRT-PCR studies for the hypoxic markers recorded similar pattern of fold changes as perceived through the immunoblotting assay (Figure 33).The mRNA expression of α7nAchR and HMGB-1 was downregulatedalong with increased expression of TNF-α after GLA treatment in qRT-PCR studies (Figure 34).

Figure 32: Effect of GLA and DMBA upon mitochondrial mediated pathway

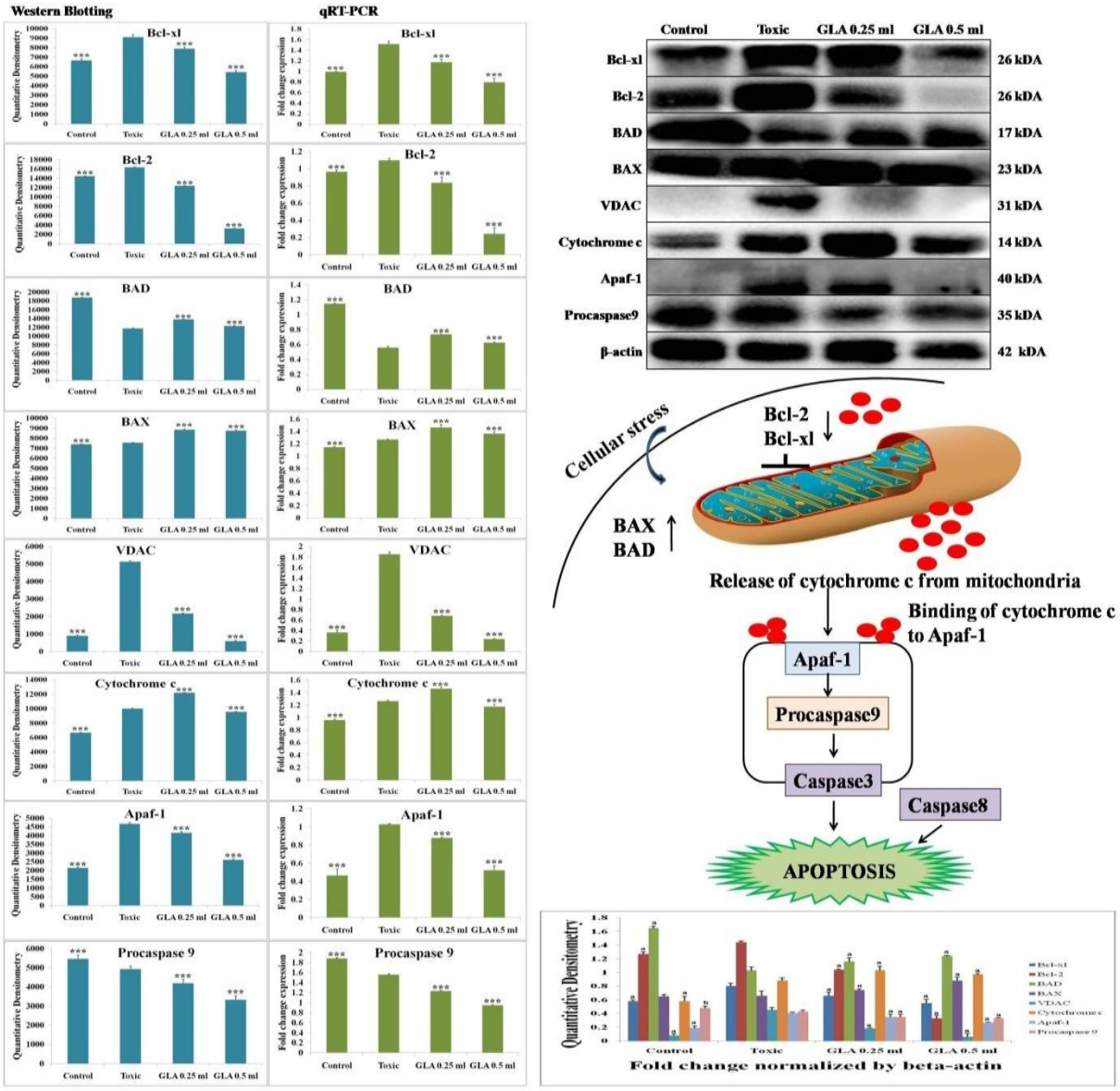

Proteins extracted from individual groups [1-control, 2-DMBA treated, 3-GLA (0.25 ml/kg, p.o.+DMBA 8 mg/kg,i.v.) and GLA (0.5 ml/kg, p.o.+DMBA 8 mg/kg, i.v.)] were subjected to immunoblotting of proapoptotic (BAD and BAX) and anti-apoptotic (Bcl-2 and Bcl-xl) protein with downstream apoptotic markers (VDAC, cytochrome-c, Apaf-1and procaspase9) ofrespective pathway. mRNA expression of above mentioned proteins were also in line with the findings of immunoblotting assay. β-actin was used as loading control. Each experiment was performed in triplicate. Values are presented as mean ± SD. Comparisons are made by the one way ANOVA followed by Bonferroni multiple test. All groups are compared to the DMBA treated group (*$p < 0.05$, **$p < 0.01$, ***$p < 0.001$ and a $p < 0.001$, b $p < 0.01$, c $p < 0.05$). The blots are normalized with respect to β-actin ratio.

Figure 33: Effect of GLA and DMBA on hypoxic cancer cells metabolic pathway

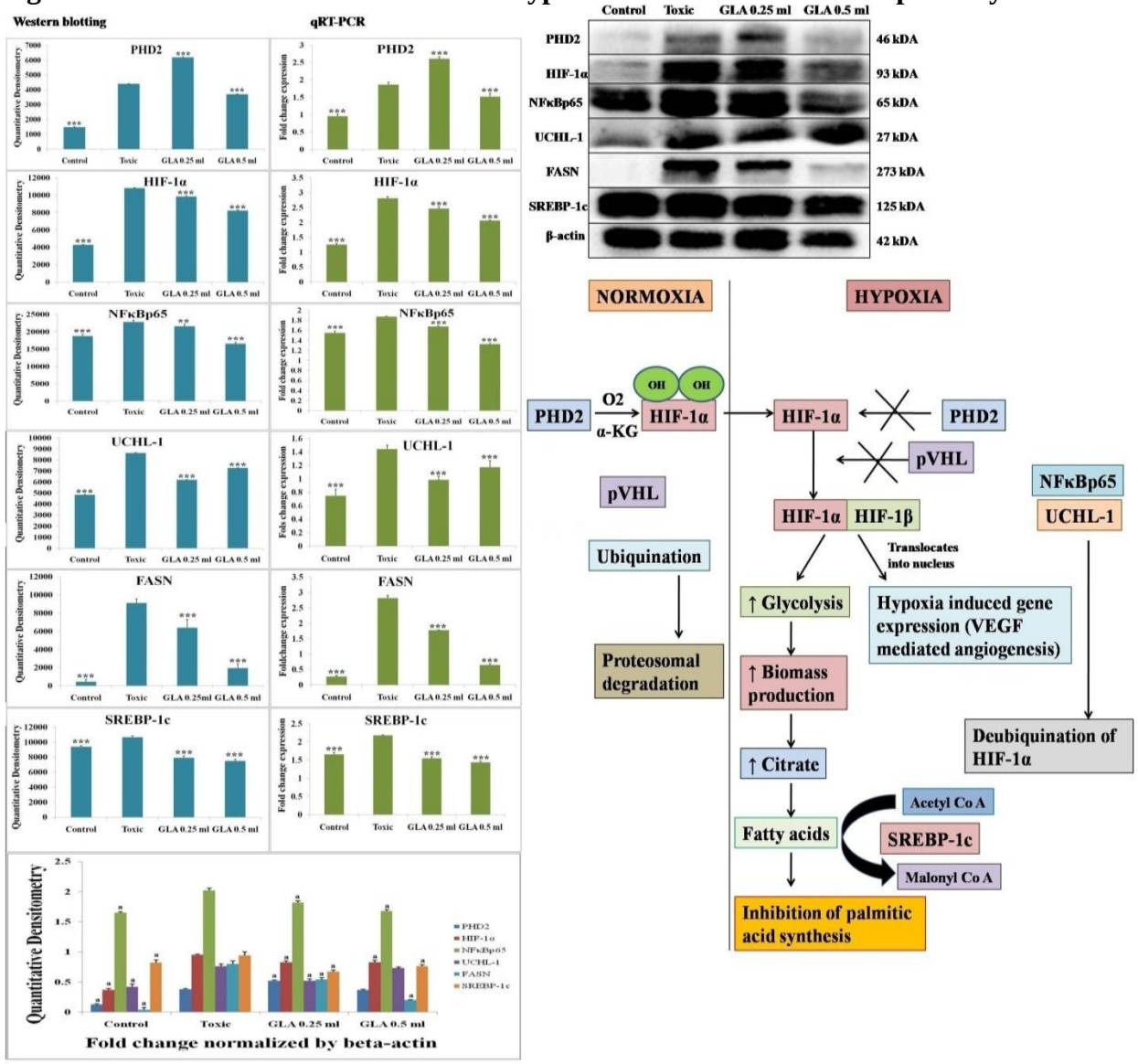

Immunoblotting of respective individual group [1-control, 2-DMBA treated, 3-GLA (0.25 ml/kg, p.o.+DMBA 8 mg/kg,i.v.) and GLA (0.5 ml/kg, p.o.+DMBA 8 mg/kg, i.v.)] was performed for PHD2, HIF-lα, UCHL-1, FASN and SREBP-1c. Excised mammary gland tissue sample was lysed in trizol for RNA extraction and analyzed for the mRNA expression of PHD-2, HIF-lα, UCHL-1, FASN and SREBP-lc by qRT-PCR: fold induction is relative to tissue under hypoxic conditions after normalization to the β- actin expression. Each experiment was performed in triplicate. Values are presented as mean ± SD. Comparisons are made on the basis of the one- way ANOVA followed by Bonferroni multiple test. All groups are compared tothe DMBA treated group (*$p < 0.05$, **$p < 0.01$, ***$p < 0.001$ and a $p < 0.001$, b $p < 0.01$, c $p < 0.05$). The blots are normalized with respect to β-actin ratio.

Figure 34: Effect of GLA and DMBA on Ca^{2+}influx and cholinergic anti-inflammatory pathway

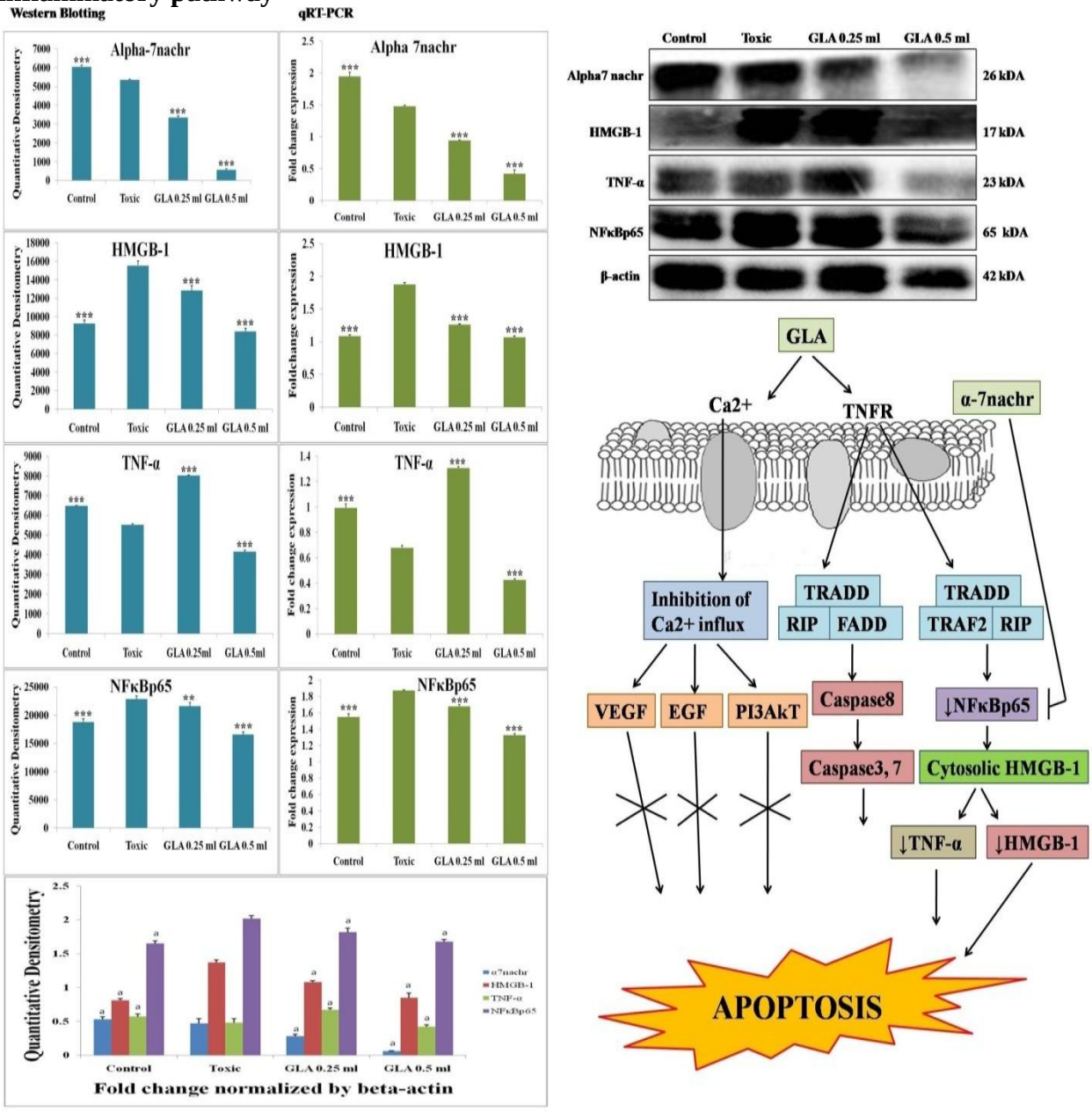

Immunoblotting of respective individual group [1-control, 2-DMBA treated, 3-GLA (0.25 ml/kg, p.o.+DMBA 8 mg/kg,i.v.) and GLA (0.5 ml/kg, p.o.+DMBA 8 mg/kg, i.v.)] for α-7nAchR, HMGB-1, TNF-α and NFκBp65 were conclude the cholinergic anti-inflammatory action of GLA after DMBA treatment and the same was verified through mRNA expression. Each experiment was performed in triplicate. Values were presented as mean ± SD. Comparisons are made on the basis of the one-way ANOVA followed by Bonferroni multiple test. All groups are compared to the DMBA treated group (*$p < 0.05$, **$p < 0.01$, ***$p < 0.001$ and a $p < 0.001$, b $p < 0.01$, c $p < 0.05$). The blots are normalized with respect to β-actin ratio.

iv) GLA (MNU)

MNU treatment increased the expression of anti-apoptotic proteins (Bcl-2, Bcl-xl) and decreased the expression of pro-apoptotic protein (BAD). GLA treatment causes apoptosis through restoration of anti and pro-apoptotic markers. The downstream markers of mitochondria mediated apoptosis pathway (VADC, Apaf-1 and procaspase 9) were upregulated along with downregulated expression of cytochrome c after MNU treatment (Figure 35). MNU treatment produces commendable hypoxia as perceived through up-regulated expression of NFκBp65, UCHL-1, HIF-1α, FASN and SREBP-1c; and down-regulated expression of PHD2. GLA treatment afforded abatement of hypoxic markers significantly (Figure 36).

The genetic phenotypes for the protein markers involved in mitochondrial death pathway were validated through qRT-PCR studies (Figure 35). The qRT-PCR assay validated the results obtained from immunoblotting analysis. The results revealed that GLA is also act through regulating the respective genetic phenotypes. The same pattern of results was perceived for hypoxic (Figure 36).

Figure 35: Effect of GLA and MNU on mitochondria mediated death apoptosis pathway

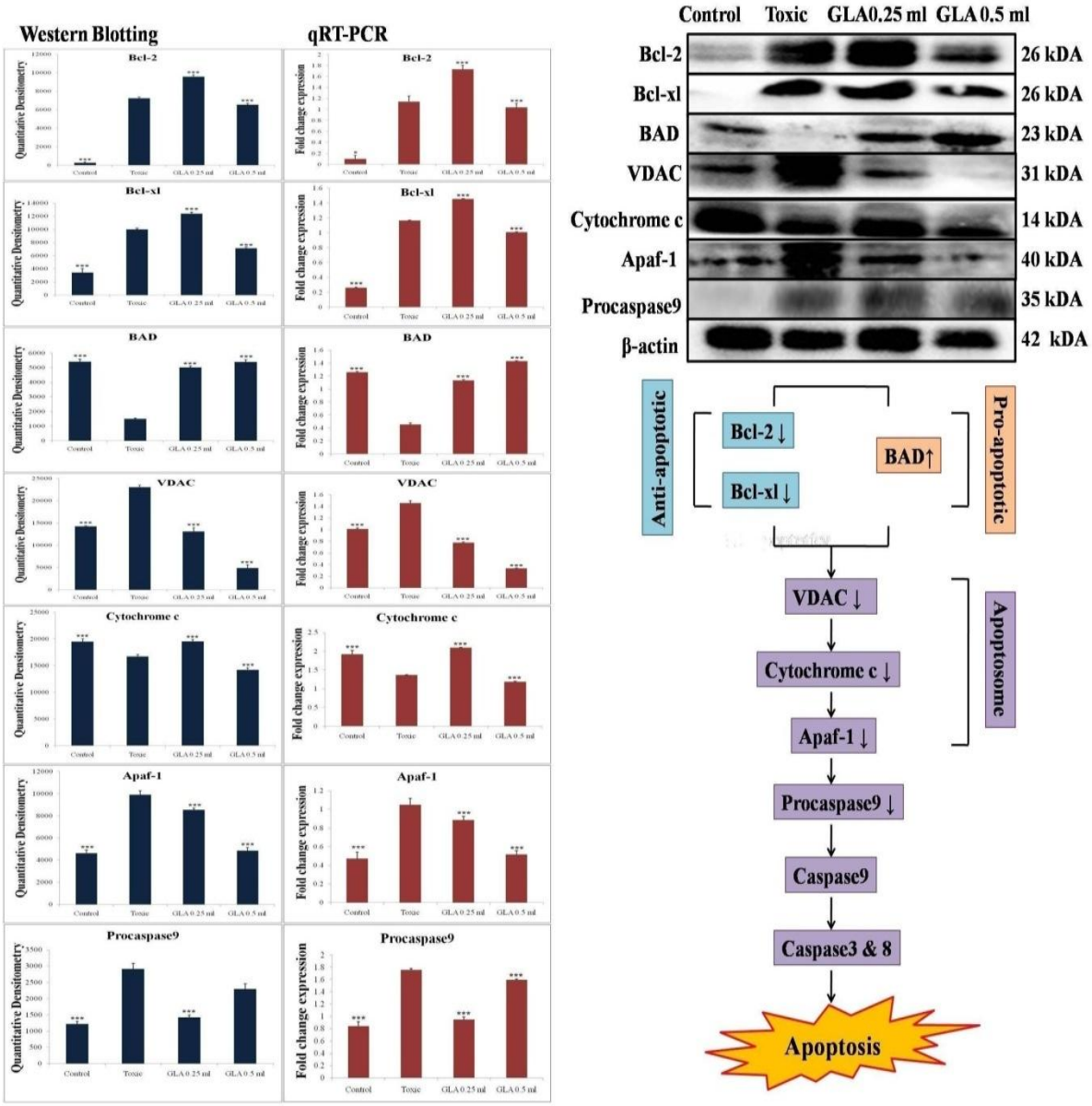

Protein was extracted from different groups [1-control, 2-toxic, 3-GLA (0.25 ml/kg+MNU 47 mg/kg, i.v.) and 4- GLA (0.5 ml/kg+MNU 47 mg/kg, i.v.)] and evalutaed for immunoblotting analysis of pro-apoptotic (BAX) and anti-apoptotic (Bcl-2 and Bcl-xl) protein along with downstream markers (VDAC, cytochrome-c, Apaf-1and procaspase 9) of respective pathway. The qRT-PCR studies have similar results as found in immunoblotting assay. The loading control is β-actin in this experiment. The experiment was performed in triplicate. Values are presented as mean ± SD. Comparisons are made on the basis of the one-way ANOVA followed by Bonferroni multiple test. All groups are compared to the MNU treated group (*p<0.05, **p<0.01, ***p<0.001).

Figure 36: Effect of GLA and MNU upon hypoxic pathway

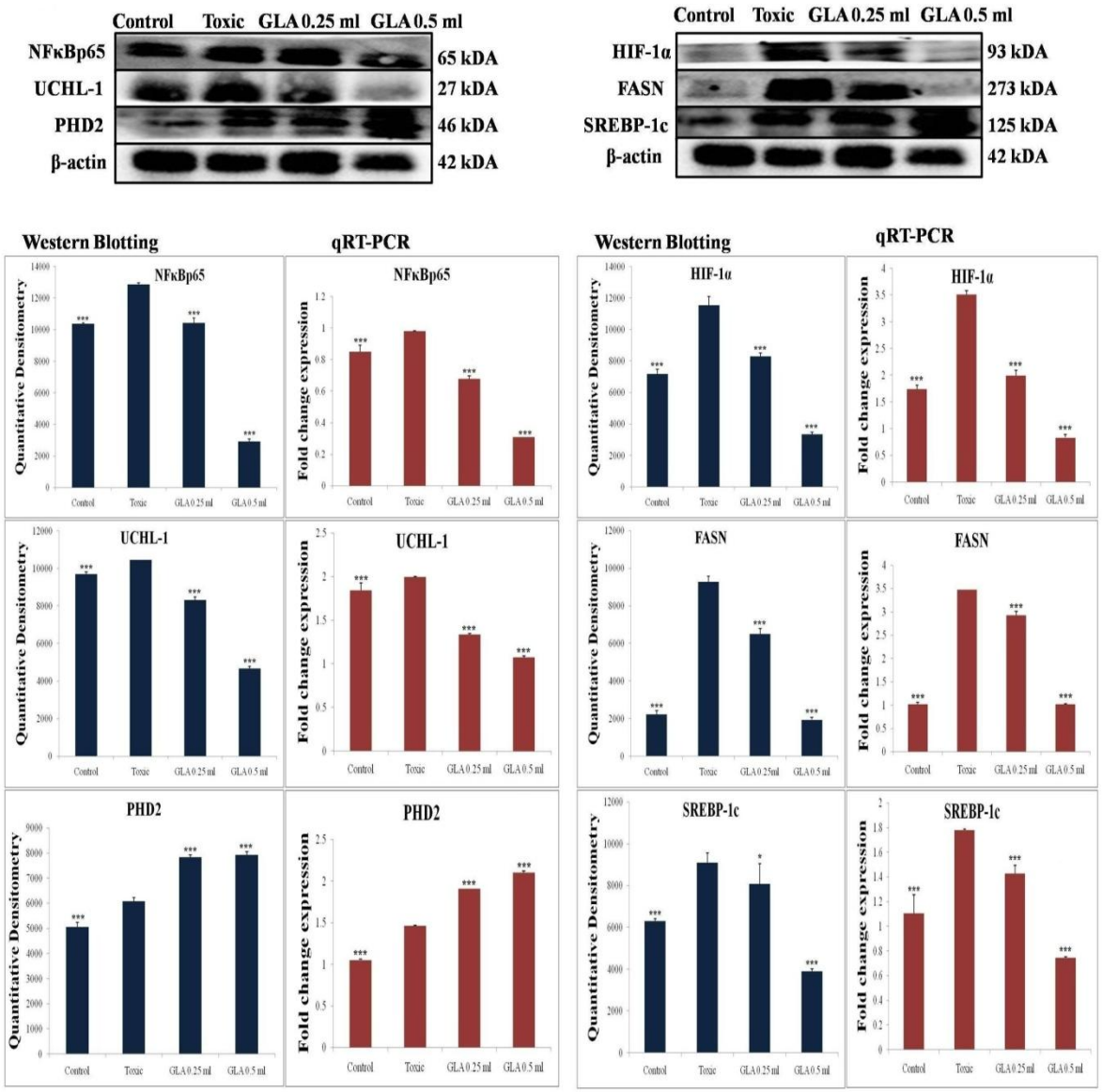

Protein was extracted from different groups [1-control, 2-toxic, 3-GLA (0.25 ml/kg +MNU 47 mg/kg, i.v.) and 4- GLA (0.5 ml/kg+MNU 47 mg/kg, i.v.)] for the evaluation of immunoblotting analysis of HIF-1α, PHD-2 and FASN. The correlation of NFκBp65, UCHL-1 and SREBP-1c with the above mentioned protein is well defined through the experimental pathway. For qRT-PCR analysis, excised mammary gland tissue sample was lysed in trizol for RNA extraction and analyzed for the mRNA expression of HIF-1α, PHD2, FASN, NFκBp65, UCHL-1 and SREBP-1c. The loading control is β-actinin. The experiment was performed in triplicate. Values are presented as mean ± SD. Comparisons are made on the basis of the one-way ANOVA followed by Bonferroni multiple test. All groups are compared to the MNU treated group (*p<0.05, **p<0.01, ***p<0.001).

The mitochondrial apoptosis is governed through series of pro-apoptotic and anti-apoptotic regulators [94]. The ALA and GLA decreased the expression of anti-apoptotic (Bcl-2 and Bcl-xl) along with increase in pro-apoptotic (BAX and BAD) markers. The mitochondrial apoptotic changes are further associated with decreased expression of VDAC, due to loss in the channel integrity with concomitant release of cytochrome c [95]. The immunoblotting and qRT-PCR studies affirmed the decreased expression of VDAC with concomitant increase in cytochrome c expression after the ALA and GLA treatment. Once released from mitochondria, cytochrome c binds with Apaf-1 and procaspase 9 to form adduct termed, apoptosome [96]. Apoptosome formation accounts for the decreased cytosolic levels of Apaf-1 and procaspase 9 and the same was evident after the ALA and GLA treatment. Apoptosome formation further cleaves the procaspase 9 to give active caspase 9 which is involved in the intrinsic apoptotic pathway and mediate the activation of effecter caspase 3 and 8 for execution of apoptosis [97].

It is well known that tumor cells require energy from glycolysis due to hypoxic condition of the cells (Warburg effect) [98]. HIF-1α regulates the hypoxia and is further regulated by 2-oxoglutarate and iron dependent hydroxylases enzyme PHD-2 [99]. It was previously reported that the increased glycolytic activity in tumor cells is combined with increased fatty acid synthase to meet the fatty acid requirements through *de novo* fatty acid synthesis [100]. GLA treatment increased the expression of PHD-2 and thereby curtailed the expression of HIF-1α when scrutinized through immunoblotting and qRT-PCR studies. The decreased expression of HIF-1α was cross validated through the decreased expression of NFκBp65 and UCHL-1. During deubiquination of HIF-1α, NFκBp65 imparts positive modulatory effect upon HIF-1α and UCHL-1 stabilizes HIF-1α [101]. GLA and ALA

treatment downregulated the protein and mRNA expression for NFκBp65 and UCHL-1, suggesting curtailment of cellular hypoxia. GLA and ALA treatment also decreased the expression of FASN and SREBP-1c, the markers for de novo fatty acid synthesis. Henceforth, it can be concluded that GLA and ALA has been demarcating effect upon DMBA and MNU induced hypoxia and downstream targets.

The Ca^{2+} influx regulating proteins play a pivot role in angiogenesis and trigger so many intercellular checkpoints to increase metastasis and invasiveness [102]. There is a positive correlation between Ca^{2+} channel influx with cellular migration and vascular invasiveness [103]. The decreased expression of VDAC after GLA and ALA treatment suggests stabilization of membrane potential transition pore (MPTP) and in Ca^{2+} influx. Subsequently the role of Ca^{2+} influx was validated trough α7nAchR proteins by which cholinergic anti-inflammatory pathway have been regulated [104]. In normal cell, Ca^{2+} trigger is requisite for maintaining cell physiology. The production of inflammatory cytokines is controlled by Ach and nicotine via α7nAchR [105]. α7nAchR have four transmembrane domains (TM1-4). A regulatory intracellular domain is located between TM3 and TM4 and forms a hetero or homo pentamers of α7nAchR which maintain integrity of central ion channel in transmembrane junction [106]. The entry of different cations (Na^{+}, K^{+} and Ca^{2+}) is regulated through nAchRs group of proteins and it is much more selective for Ca^{2+} influx [107]. The cations influx reduces the negative charge on intracellular side causing membrane depolarization. After initiation of membrane depolarization, the gates on the intracellular side of plasma membrane is open for the entry of voltage gated Ca^{2+} and leads to downstream activation of various intracellular angiogenic cascade [vascular endothelial growth factor (VEGF), endothelial growth factor

(EGF) and PI3AkT] [108]. Present study elucidates biphasic regulation of cancer cells by GLA and ALA through inhibition of Ca^{2+} influx and activation of cholinergic anti-inflammatory pathway. The α7nAchR mediated cholinergic signaling after GLA treatment was also pathway was also confirmed by increased expression of TNF-α. It was well established that TNF-α alone was ineffective in showing its anti-tumor activity without any internal or external stimuli [109]. It was hypothesized that increase TNF-α expression is mediated by TNFR-1 along with an extracellular domain (ECD), transmembrane domain (TMD) and an intracellular domain (ICD). The other subunit TNFR-2 is only expressed in immune cells whereas TNFR1 is ubiquitously expressed in all cell types [110]. α7nAchR pathway is initiated by TNFR-1 internal signaling consists of caspase 8. Caspase 8 is auto-activated by subtype TNFR-1which results in activation of caspase 3, caspase 7 and endonucleases [111]. Low dose of GLA and ALA (0.25 ml/kg) induced the expression of TNF-α as well as activated the downstream signaling cascade, which was evident through positive modulation of caspase-3, caspase-8 and downregulation in the HMGB-1 (promotes delocalization of homotrimer and causing systemic cleavage on receptor interacting protein). The tumor blood vessel permeability increased by the induction of TNF-α which deliberately augments the GLA and ALA concentration in mammary gland tissues was further confirmed by downstream expression of NFκBp65. Receptor interacting protein (RIP) is crucial for activation of NFκBp65 and plays an important role in acquisition of apoptosis. RIP consists of a death domain that can bind with other death domains in signaling molecules like fas associated death domain (FADD) and tumor necrosis factor associated death domain (TRADD) [112]. All in all, GLA and

ALA decreased the expression of α7nAchR, HMGB-1 and NFκBp65 along with increase expression of TNF-α to execute cholinergic anti-inflammatory pathway.

4.2 *C.elegans* study

4.2.1 Aldicarb assay

In comparison to the percentage of worms paralyzed in control (53.27 ± 1.27) we observed a significant increase in percentage of worms paralyzed upon treatment with 20% ALA (95.22 ± 0.22, p value = 0.001) and 40% ALA (95.44 ± 5.55, p value = 0.001). The effect of 5% and 10% ALA treatment on synaptic Ach levels although greater than control was statistically insignificant. The results implicate enhanced cholinergic neurotransmission as a result of ALA treatment (Figure 37A). Representative image of the paralyzed and un-paralyzed worms is shown in figure 37B.

Aldicarb assay relies on the AchE inhibitor mediated buildup of Ach orchestrating paralysis in worms. The percentage of worms paralyzed at a given time point is proportional to the levels of Ach in the synapse [113]. We observed significant enhancement in cholinergic transmission. The beneficial effects on cholinergic transmission could be related to inhibition of carcinogen induced mammary gland carcinoma through cholinergic anti-inflammatory pathway.

Figure 37: Effect of ALA on synaptic Ach levels

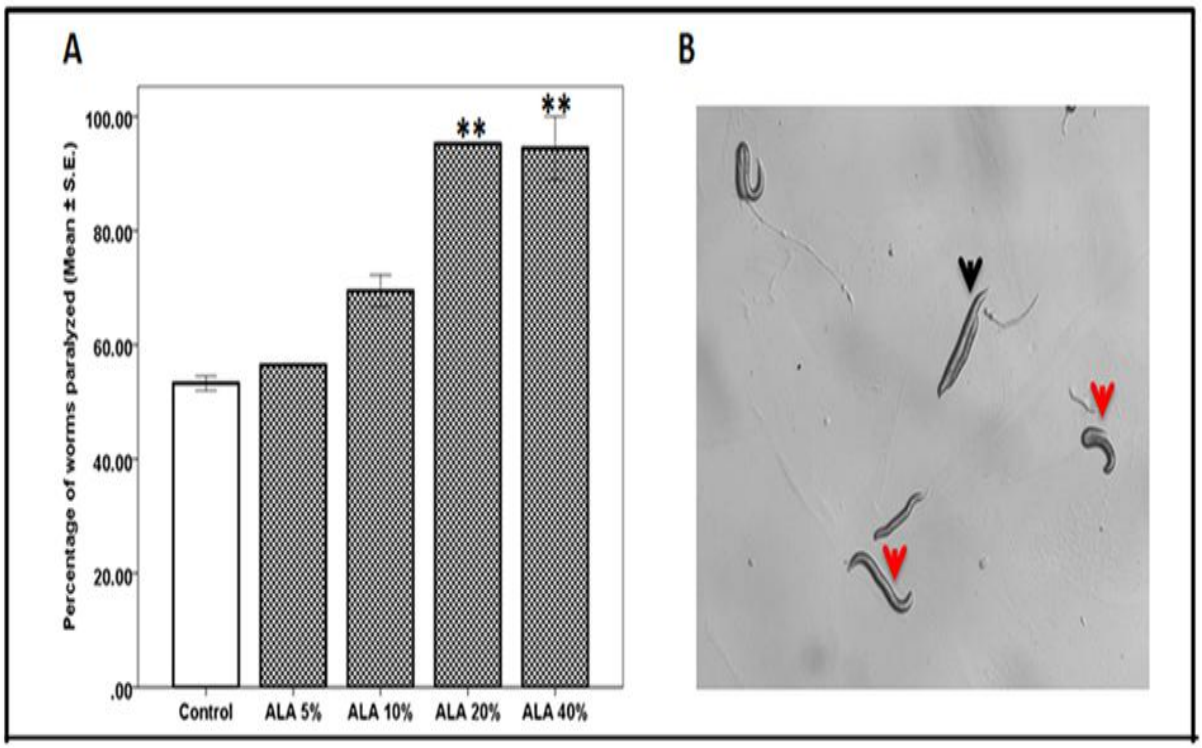

Aldicarb assay was performed by using different doses of ALA (5%, 10%, 20% and40%). In comparison to normal control (53.27±1.27), a significant increase in percentage of worms paralyzed upon treatment with 20% ALA (95.22±0.22, p value=0.001) and 40%ALA (95.44±5.55, p value=0.001) was observed. The results implicate enhanced cholinergic neurotransmission as a result of ALA treatment. The data is represented as mean ± S.E.M.

4.3.2 Effect of ALA on Ach and AchE activity

After studying the effect on synaptic and post synaptic neurotransmission, we studied the gross Ach levels and AchE activity in worms subjected to treatment with 20% and 40% ALA. We observed that in comparison to the normalized AchE activity in control (1.0 fold ± 0.00) there was a significant increase AchE activity in worms treated with 40% ALA (3.29 fold ± 0.12, p value = 0.001), however the alteration in AchE activity in animals treated with 20% ALA was statistically insignificant (Figure 38A). In connection with the AchE activity we also ascertained the effect of ALA (20% and 40%) on Ach

levels. Surprisingly in comparison to the normalized Ach levels in control (1.0 fold ± 0.02), we observed a significant increase in relative Ach levels in worms treated with 20% ALA (1.64 ± 0.01, p value = 0.001) and 40% ALA (4.54 ± 0.03, p value = 0.000) as shown in figure 38B. The results implied that although treatment led to increase in AchE activity yet Ach levels were considerably higher in worms treated with ALA.

Figure 38: Effect of ALA on Ach and AchE levels

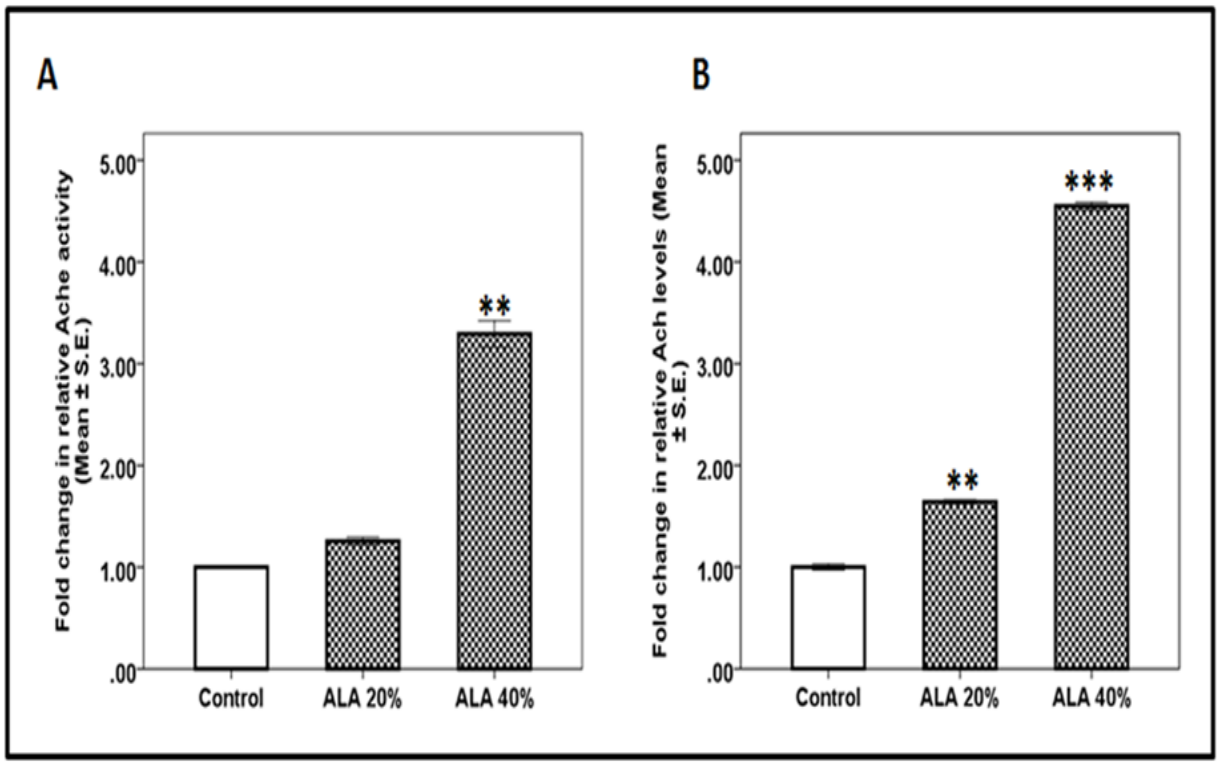

The Ach level and AchE activity was evaluated in worms' treatment with 20% and 40% ALA. ALA treatment lead to increase in AchE activity while Ach levels were considerably higher in worms treated with ALA. The data is represented as mean ± S.E.M.

After elucidating the effect of ALA on cholinergic function, we proceeded for qRT-PCR studies to gain further insights into the mechanisms involved. In comparison to the control we observed a significant downregulation in expression of genes ace-2 (0.14 ± 0.00). The mRNA expression was considerably augmented in genes ace-1 (6.58 ± 0.007),

cho-1 (8.37 ± 0.04), cha-1 (4.82 ± 0.1), unc-17 (4.79 ± 0.14) and unc-38 (1.06 ± 0.056). The fold change in relative expression of unc-50 was however close to unc-38 (Figure 39).

We observed a significant upregulation of ace-1 which could be attributed to the increased relative AchE activity. However paradoxically we also observed a significant downregulation of ace-2 and notably genes ace-1 and ace-2 code for AchE in *C.elegans.* The opposing effects observed in expression of these two genes could very well be attributed to the increased Ach and AchE activity. We also observed increased expression of genes cho-1, cha-1, unc-17. The decreased genomic expression of unc-38, which represents the α-7nachr subunit in *C.elegsns* validate the proteomic data of animal study. The gene cho-1 codes for choline transporter which is a rate limiting step in Ach synthesis [114]. Furthermore cha-1 encodes choline acetyl transferase which catalyses synthesis of Ach from choline. The synthesized Ach is transported to synapse through Ach transporter encoded by unc-17 [115]. The enhanced Aldicarb sensitivity could be linked with coherent upregulation of cho-1, cha-1 and unc-17. Henceforth, it was concluded that ALA has a marked effect on MNU induced mammary gland carcinoma.

Figure 39: Effect of ALA on genes related to Ach synthesis, transport, degradation and nicotinic Ach receptor

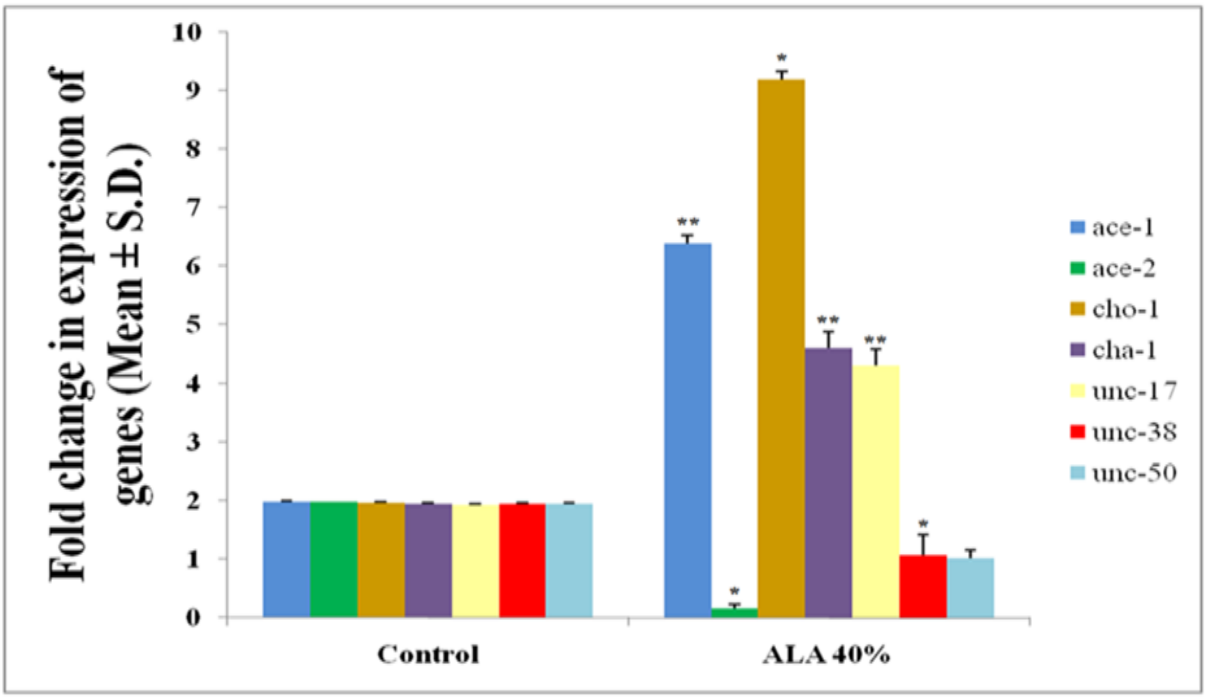

After elucidating the effect of ALA on cholinergic function, qRT-PCR studies were performed to gain further insights into the mechanisms involved. The data is represented as mean ± S.E.M.

4.2.3 Effect of ALA on lipid content

In comparison to the relative lipid content in control (112477.66 ± 18211.01) we observed a significant decrease in lipid content in worms treated with 40% ALA (9853.31 ± 5191.88, p = 0.000). The above results identified the lipid curtailing effects of ALA (Figure 40A, B).

4.2.4 Effect of ALA on mitochondrial content

Fluorescence microscopy followed by semi quantitative analysis revealed slight increase in mitochondrial content upon treatment with 40% ALA, which impart the safety of dose we have used in this study on normal cells. (Figure 40C, D).

The treated group shows an increase in mitochondrial membrane potential with greater red/orange fluorescence intensity, which replicates the safety of the dose used in the present study.

Figure 40: Effect of ALA upon lipid content and mitochondrial content

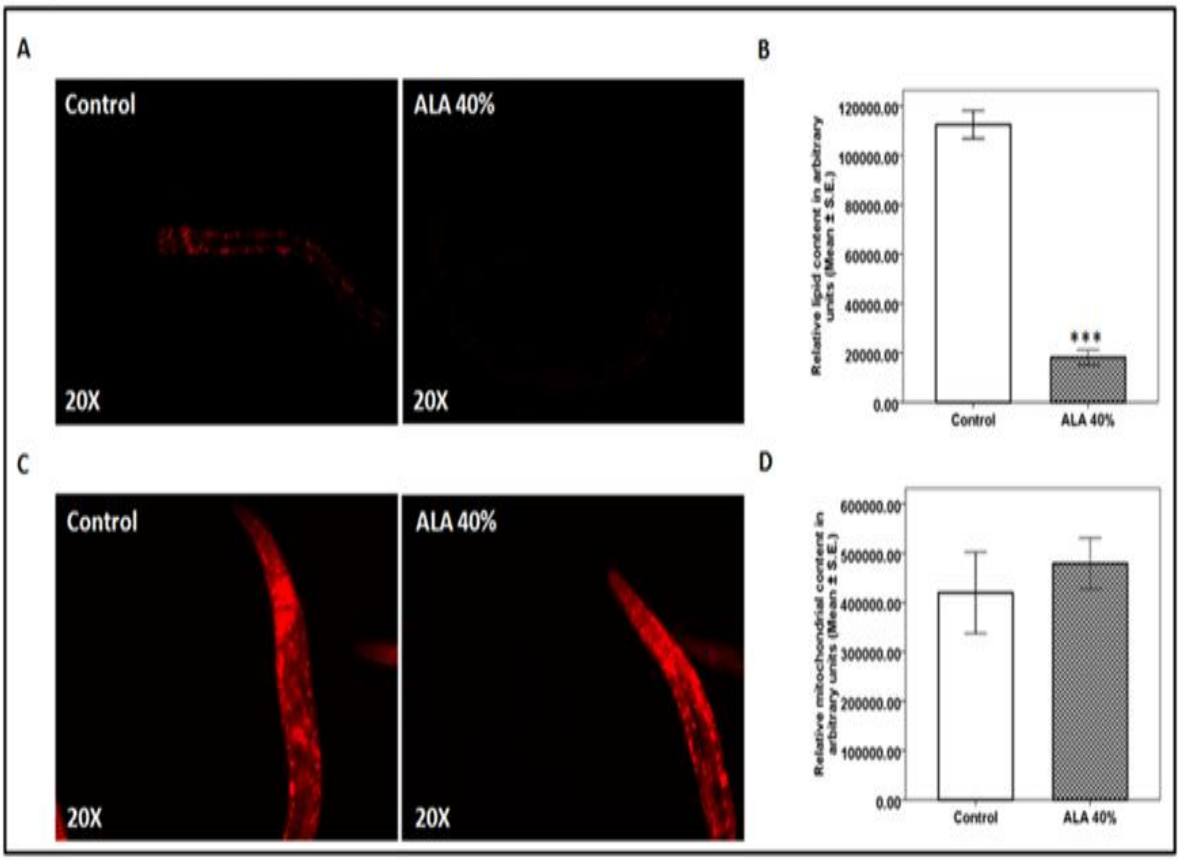

The effect of ALA on lipid content was studied using lipid specific dye Nile red through fluorescence microscopy followed by semiquantitative analysis. The results identified the lipid curtailing effects of ALA (A, B). In order to identify the possible effect of ALA on mitochondrial activity, mitotracker red dye was used which stains active mitochondria on the basis of membrane potential. Fluorescence microscopy followed by semiquantitative analysis revealed slight increase in mitochondrial content upon treatment with 40%ALA (C, D). The data is represented as mean ± S.E.M.

CHAPTER 5
SUMMARY AND CONCLUSION

Controversy exists regarding the role of dietary fat in breast cancer etiology. We have investigated the association of dietary PUFAs (ω-3 and ω-6 PUFAs) with *in vitro* and *in vivo* models of mammary gland carcinoma.

The *in vitro* studies on ER+ MCF-7 cells affirmed the significant cytotoxic and apoptotic potential of ALA and GLA when scrutinized through MTT assay, AO/EtBr and JC-1 staining. The ALA and GLA treated AO/EtBr stained cells were evident for the presence of apoptosis as visualized with nuclear shrinkage, chromatin condensation, fragmented nuclei and membrane blabbing. Considering the fact that mitochondria participates in apoptosis, the effect of ALA and GLA on mitochondrial membrane potential was validated through cationic dye JC-1.Therefore, JC-1 is considered to be an indicator of mitochondrial potential and decrease in mitochondrial membrane potential is an indicative of apoptosis as perceived after the ALA and GLA treatment. Treatment with GLA and ALA demonstrated cell cycle arrest in G0/G1 phase by presenting a lower % of G0/G1 cell population in comparison to control with a higher population of cell in G2/M phase. Subsequent studies affirmed the cell cycle arrest in G2/M phase by the ALA and GLA treatment. Translocation of PS to the outer leaflet of the cellular membrane is a key marker of apoptosis and was validated through Annexin-V labeled with FITC and PI in ALA and GLA treated group which indicate the initiation of programmed cell death in ER+ MCF-7 cells.

Subsequently, the effect of PUFAs was evaluated against chemical carcinogen induced mammary gland carcinoma models. In the present study, two carcinogens viz. DMBA and MNU were used. DMBA is a polycyclic aromatic hydrocarbon and the tumors produced from DMBA are morphologically and histopathologically very similar to

human tumors. DMBA is an indirect carcinogen, and requires metabolic activation by cytochrome P450 enzymes to reactive metabolites, i.e. dihydrodiolepoxides and forms mutagenic DNA adduct. Mainly two enzymes viz. cytochrome P4501B1 (CYP1B1) and microsomal epoxide hydrolase (EPHX1) are responsible for DMBA bio activation. Whereas, MNU is a direct carcinogen and it doesn't require any intermediate. Electrophilic diazonium cation formation of an intermediate of alkylnitrosourea is a well establish mechanism in mammalians, which further needs cytochrome P450 activation to exhibit its mutagenic potential. The possible site of alkylation in guanine base pair is either in nitrogen or oxygen because of high abundance of electron. This alkylation leads to generation of a fast (N (7)-methyl guanine) as well as a slow (O (6)-methyl guanine) intermediate. The hydrogen bonding properties of guanine was changed due to methylation at the O (6)-position and thereby inducing guanine to adenosine transition followed by DNA damage. The MNU and DMBA induced rat models are very much similar with human ER+ breast cancers in terms of histopathology and other hormonal manipulations.

Afterwards, the effect of ALA and GLA was evaluated upon autonomic dysfunction. It was a well known fact that autonomic dysfunction, cardiovascular complications, poor quality of life and premature mortality is very common to several types of cancer chemotherapeutic regimen and it may be shepherded to increased sympathetic activity and decreased vagal tone. In fact, autonomic dysfunction is now a day is considered as a non-invasive prognostic marker for chemotherapeutic regime The HR, R wave amplitude and RR interval are the crucial markers of autonomic dysfunction, which were positively modulated after ALA and GLA treatment. Treatment group embarked a marked positive

regulation of the HRV factors, which is indicative of the positive regulation of autonomic dysfunction by both PUFA and also ensure its long term safety in chemotherapeutic regimen.

The biochemical markers could be majorly categorized as the ones associated with antioxidant defense or to the physiological mechanisms, and authors validated both. ROS are constantly produced in all aerobic cells and are counter balanced by the antioxidant enzymatic defense. However, during anaerobic/hypoxic conditions like cancer (due to increased cellular proliferation), the counter balance effects of antioxidant enzymes are subsided. The damage to the cellular lipids and proteins can be validated through increased production of TBARs and PC respectively; which was very well evident after the DMBA and MNU treatment. The increased ROS production also inhibits the enzymatic antioxidant defense of GSH, SOD and catalase, as they all work in tandem to curtail ROS through series of peroxidation, dismutation and oxidation reactions. The decrease in the enzymatic defense of SOD, catalase and GSH suggest their increased utilization which was profoundly evident after the DMBA and MNU treatment. It would be appropriate to remark that ALA and GLA administration curtailed the levels of TBARs and PC with restoration of enzymatic antioxidant defense of SOD, catalase and GSH.

The mammary gland tissues were further evaluated in terms of morphological analysis using carmine staining, H&E staining and SEM. Cancer progression is defined by two hallmarks named as cellular proliferation and angiogenesis. The results of carmine staining were event with increased in number of ABs and lobules and the same was subsided after ALA and GLA treatment. In case of H&E staining, there was a scattered

pattern of CEC whereas LCT and DCT were hard to identify along with loss of duct and MEC. ALA and GLA treatment restored all the cellular architecture to the normal. Marked proliferation after the toxicant administration was observed with increase in micro vessel formation, loss of intra-arterial cushion and vascular conglomeration, when perceived through SEM analysis. ALA and GLA treatment demarcated a marked impression on cellular architecture and morphology of the mammary gland tissue and decreased the growth of enlarged capillaries (the sign of rapidly growing tumors). Henceforth, ALA and GLA imparted dose-dependent curtailment of cellular proliferation and therefore warrants further validation through more stringent markers.

Afterwards, the metabolic analysis of the serum was evaluated using ^{1}H NMR studies. The results shows that the increased concentrations of serum acetyl-glycoproteins (both NAG and OAG) (acute phase anti-inflammatory proteins expressed during inflammation and immune response) was recorded after the toxic treatment and is in line with previous investigations in liver disease, inflammatory disease and cancer. As expected, ALA and GLA (an anti-inflammatory PUFA) curtailed the expression of acute phase proteins expressed during inflammation. The increased levels of amino acids like arginine, glycine, histidine, tyrosine, creatine and phenylalanine indicates abnormal/aberrant biosynthesis of amino acids in toxicant treated rats. The increased levels of arginine and citrulline suggest protein catabolism, deriving overall picture of high metabolic activity, a hallmark for tumor progression. The high metabolic activity as evident through increased levels of amino acids was also endorsed through increased levels of formate (a product of glycine metabolism through glycine succinate pathway). The decreased level of glucogenic amino acids (glutamate, glutamine, proline, isoleucine and alanine) in

toxicant treated group expressed their increased utilization in energy production. Proline metabolism is especially important in nutrient stress, as it is interchangeably converted into glutamate and glutamine. Concomitant drug treatment further diminished the levels of glucogenic amines which could be accounted to the fact that exogenous PUFA would have provided a faulty lipid to the fastly growing tumour cells. Whereas the requirement for the amino acids as a building block for cellular membranes was prevalent till such time. The deregulated metabolites represent altered cancer cell energy metabolism including amino acid metabolism (glutamate, glutamine, alanine, etc.), glycolysis or gluconeogenesis (glucose, and lactate,) and lipid metabolism (LDL, VLDL, choline, and acetate) and are associated with high rate of glycolysis. Most of the metabolic changes in toxicant treated animals were reset back to normal after PUFA administration, suggesting that the ALA and GLA have potential to balance the metabolic abnormalities in fastly growing cells.

To evaluate the proteomic signal from different identified protein associated with mitochondrial mediated death apoptosis pathway, hypoxic microenvironment, calcium influx and involvement of anti-cholinergic pathway, immunoblotting and qRT-PCR assay were performed. In terms of apoptosis, both drugs have produced marked protection against toxicant induced carcinogenesis. Treatment groups indicate decreased expression of anti-apoptotic proteins (Bcl-2 and Bcl-xl) along with positive modulation of BAD and BAX, a pro-apoptotic member to the Bcl-2 family. Similar findings were found with mRNA expression when scrutinized with qRT-PCR. Cytochrome c is released due to loss of channel integrity and the decreased expression of VDAC validates the same. After ALA and GLA treatment, the protein and mRNA expression of VDAC and cytochrome c

confirm the same. Cytochrome crelease then triggers the congregation of cytoplasmic apoptosome. The apoptosome is a complex formed of Apaf-1, cytochrome c and procaspase 9. Apoptosome formation decreased the cytosolic levels of Apaf-1 and procaspase 9 and the same findings were observed after ALA and GLA treatment. Procaspase 9 was cleaved with the formation of apoptosome and leads to the formation of active caspase 9which results in the activation of caspase 3 and 8. The caspase activation leads to activation of downstream caspase cascade and leading to apoptosis. ALA and GLA treatment increased cytosolic caspase 3 and 8 and thereby accredits apoptosis.

It is well known that tumor cells require energy from glycolysis due to hypoxic condition of the cells (Warburg effect). HIF-1α regulates the hypoxia and is further regulated by 2-oxoglutarate (2-OG) and iron dependent hydroxylases enzyme PHD-2. It was previously reported that the increased glycolytic activity in tumor cells is combined with increased FASN to meet the fatty acid requirements through de novo fatty acid synthesis. ALA and GLA treatment increased the expression of PHD-2 and thereby curtailed the expression of HIF-1α when scrutinized through immunoblotting and qRT-PCR studies. The decreased expression of HIF-1α was cross validated through the decreased expression of NFκBp65and UCHL-1. During deubiquination of HIF-1α, NFκBp65 imparts positive modulatory effect upon HIF-1α and UCHL-1 stabilizes HIF-1α. ALA and GLA treatment downregulated the protein and mRNA expression forNFκBp65 and UCHL-1; suggesting curtailment of cellular hypoxia. ALA and GLA treatment also decreased the expression of FASN and SREBP-1c, the markers for de novo fatty acid synthesis.

The Ca^{2+} influx regulating proteins play a pivot role in angiogenesis and trigger so many intercellular checkpoints to increase metastasis and invasiveness. There is a positive

correlation between Ca^{2+} channel influx with cellular migration and vascular invasiveness. The decreased expression of VDAC after drug treatment suggests stabilization of membrane potential transition pore (MPTP) and in Ca^{2+} influx. Subsequently, the role of Ca^{2+} influx was validated trough α7nAchR proteins by which cholinergic anti-inflammatory pathway have been regulated. In normal cell, Ca^{2+} trigger is requisite for maintaining cell physiology. The production of inflammatory cytokines is controlled by Ach and nicotine via α7nAchR. α7nAchR have four transmembrane domains (TM1-4). A regulatory intracellular domain is located between TM3 and TM4 and forms a hetero or homo pentamers of α7nAchR which maintain integrity of central ion channel in transmembrane junction. The entry of different cations (Na^+, K^+ and Ca^{2+}) is regulated through nAchRs group of proteins and it is much more selective for Ca^{2+} influx. The cations influx reduces the negative charge on intracellular side causing membrane depolarization. After initiation of membrane depolarization, the gates on the intracellular side of plasma membrane is open for the entry of voltage gated Ca^{2+} and leads to downstream activation of various intracellular angiogenic cascade [vascular endothelial growth factor (VEGF), endothelial growth factor (EGF) and PI3AkT]. Present study elucidates biphasic regulation of cancer cells by GLA and ALA through inhibition of Ca^{2+} influx and activation of cholinergic anti-inflammatory pathway. The α7nAchR mediated cholinergic signaling after drug treatment was also pathway was also confirmed by increased expression of TNF-α.

From the above findings, it was concluded that ALA and GLA ameliorate the morphological, biochemical and associated biological effects of MNU and DMBA. In summary, the present study has assessed the anticancer effects of ω-3 and ω-

6PUFAswhen consumed or treated individually. ALA and GLA can differentially inhibit mammary tumor development by changing the cell membrane fatty acid composition, suppressing eicosanoid biosynthesis and influencing signaling transcriptional pathways to inhibit cell proliferation and induce apoptosis. This study also provided evidence for using ω-3 and ω-6PUFAsas a nutritional intervention in the treatment of ER+ breast cancer to enhance conventional therapeutics, or potentially lowering effective doses. Our results suggest the possible therapeutic potential of PUFAs against mammary gland carcinoma without any untoward effect. It last, it was also conclude that the mechanism of action of ALA and GLA is mitochondrial mediated death apoptosis pathway, inhibition of hypoxic pathway along with inhibition of anti-inflammatory cholinergic pathway.

REFERENCES

1. Remusat L, Derenne S and Robert F. New insight on aliphatic linkages in the macromolecular organic fraction of Orgueil and Murchison meteorites through ruthenium tetroxide oxidation. Geochimica et Cosmochimica Acta. 2005, 69(17), 4377-4386.

2. Grimsgaard S, Bønaa KH and Bjerve KS. Fatty acid chain length and degree of unsaturation are inversely associated with serum triglycerides. Lipids. 2000, 35(11), 1185-93.

3. Ander B et al. Polyunsaturated fatty acids and their effects on cardiovascular disease. Exp Clin Cardiol. 2003, 8(4), 164–172.

4. Abedi and Sahari. Long-chain polyunsaturated fatty acid sources and evaluation of their nutritional and functional properties. Food Sci Nutr. 2014, 2(5), 443–463.

5. Simon C. Dyall. Interplay Between n-3 and n-6 Long-Chain Polyunsaturated Fatty Acids and the Endocannabinoid System in Brain Protection and Repair. Lipids. 2017, 52(11), 885–900.

6. Lone AM and Taskén K. Proinflammatory and Immunoregulatory Roles of Eicosanoids in T Cells. Front Immunol. 2013, 4, 130.

7. Rafael Zárate et al. Significance of long chain polyunsaturated fatty acids in human health. Clin Transl Med. 2017, 6: 25.

8. Kaur N, Chug V, and Gupta AK. Essential fatty acids as functional components of foods-a review. J Food Sci Technol. 2014, 51(10), 2289–2303.

9. M. de Lorgeril et al. Alpha-linolenic acid in the prevention and treatment of coronary heart disease. European Heart Journal Supplements (2001) 3 (Supplement D), D26–D32.

10. Khan et al. Bioengineered Plants Can Be a Useful Source of Omega-3 Fatty Acids. Biomed Res Int. 2017, 2017, 7348919.

11. Harnack K, Andersen G, and Somoza V. Quantitation of alpha-linolenic acid elongation to eicosapentaenoic and docosahexaenoic acid as affected by the ratio of n6/n3 fatty acids. Nutr Metab (Lond). 2009, 6, 8.

12. Liu J and David W. L. Ma. The Role of n-3 Polyunsaturated Fatty Acids in the Prevention and Treatment of Breast Cancer. Nutrients. 2014, 6(11), 5184–5223.

13. Swanson D, Block R, and MousaSA. Omega-3 Fatty Acids EPA and DHA: Health Benefits Throughout Life. Adv Nutr. 2012, 3(1), 1–7.

14. Yadav et al. Comparative efficacy of alpha-linolenic acid and gamma-linolenic acid to attenuate valproic acid-induced autism-like features. Journal of Physiology and Biochemistry. 2017, 73(2), 187–198.

15. Kelavkar et al. Prostate Tumor Growth Can Be Modulated by Dietarily Targeting the 15-Lipoxygenase-1 and Cyclooxygenase-2 Enzymes. Neoplasia. 2009, 11(7), 692–699.

16. Nowsheen et al. HER2 overexpression renders human breast cancers sensitive to PARP inhibition independently of any defect in homologous recombination DNA repair. Cancer Res. 2012, 15, 72(18), 4796–4806.

17. MacLennan M and David WL Ma. Role of dietary fatty acids in mammary gland development and breast cancer. Breast Cancer Res. 2010, 12(5), 211.

18. Ayala A, Muñoz MF and ArgüellesS. Lipid Peroxidation: Production, Metabolism, and Signaling Mechanisms of Malondialdehyde and 4-Hydroxy-2-Nonenal. Oxidative Medicine and Cellular Longevity, 2014 (2014), Article ID 360438, 31 pages.

19. Jones and Ashrafi. Caenorhabditis elegans as an emerging model for studying the basic biology of obesity. Dis Model Mech. 2009, 2(5-6), 224–229.

20. Leung et al. Caenorhabditis elegans: An Emerging Model in Biomedical and Environmental Toxicology. Toxicological Sciences, 2008, 106 (1), 5–28.

21. Watts and Browse. Genetic dissection of polyunsaturated fatty acid synthesis in Caenorhabditis elegans. Proc Natl Acad Sci U S A. 2002 99(9), 5854–5859.

22. Patterson et al. Health Implications of High Dietary Omega-6 Polyunsaturated Fatty Acids. J Nutr Metab. 2012, 2012, 539426.

23. Artemis P. Simopoulos. An Increase in the Omega-6/Omega-3 Fatty Acid Ratio Increases the Risk for Obesity. Nutrients. 2016, 8(3), 128.

24. Xu Y and Qian SY. Anti-cancer activities of ω-6 polyunsaturated fatty acids. Biomed J. 2014, 37(3), 112-9.

25. Tuncer and Banerjee. Eicosanoid pathway in colorectal cancer: Recent updates. World J Gastroenterol. 2015, 21(41), 11748–11766.

26. Orsavova et al. Fatty Acids Composition of Vegetable Oils and Its Contribution to Dietary Energy Intake and Dependence of Cardiovascular Mortality on Dietary Intake of Fatty Acids. Int J Mol Sci. 2015, 16(6), 12871–12890.

27. Jeromson et al. Omega-3 Fatty Acids and Skeletal Muscle Health. Mar Drugs. 2015, 13(11), 6977–7004.

28. Azrad M, Turgeon C and Wahnefried WD. Current Evidence Linking Polyunsaturated Fatty Acids with Cancer Risk and Progression. Front Oncol. 2013, 3, 224.

29. Cao et al. Gamma-Linolenic Acid Suppresses NF-κB Signaling via CD36 in the Lipopolysaccharide-Induced Inflammatory Response in Primary Goat Mammary Gland Epithelial Cells. Inflammation. 2016, 39(3), 1225-37.

30. Lakshmi et al. Down-regulated peroxisome proliferator-activated receptor γ (PPARγ) in lung epithelial cells promotes a PPARγ agonist-reversible proinflammatory phenotype in chronic obstructive pulmonary disease (COPD). J Biol Chem. 2014, 289(10), 6383-93.

31. Undurti N Das and N Madhavi. Effect of polyunsaturated fatty acids on drug-sensitive and resistant tumor cells in vitro. Lipids Health Dis. 2011, 10, 159.

32. Nguyen NM et al. Maternal intake of high n-6 polyunsaturated fatty acid diet during pregnancy causes transgenerational increase in mammary cancer risk in mice. Breast Cancer Res. 2017, 19, 77.

33. Ouldamer L et al. N-3 Polyunsaturated Fatty Acids of Marine Origin and Multifocality in Human Breast Cancer. PLoS One. 2016, 11(1), e0147148.

34. Wiggins AK, Mason JK and Thompson LU. Growth and gene expression differ over time in alpha-linolenic acid treated breast cancer cells. Exp Cell Res. 2015, 333(1), 147-54.

35. Zou Z et al. n-3 polyunsaturated fatty acids and HER2-positive breast cancer: interest of the fat-1 transgenic mouse model over conventional dietary supplementation. Biochimie. 2014, 96:22-7.

36. Wiggins AKA et al. α-linolenic acid reduces growth in four breast cancer cell lines with varying receptor expression in high and low estrogen environments. The FASEB Journal. 2013, 27 (1).

37. Zheng JS et al. Intake of fish and marine n-3 polyunsaturated fatty acids and risk of breast cancer: meta-analysis of data from 21 independent prospective cohort studies. BMJ. 2013, 346, f3706.

38. Murff HJ et al. Dietary Polyunsaturated Fatty Acids and Breast Cancer Risk in Chinese Women: A Prospective Cohort Study. Int J Cancer. 2011, 128(6), 1434–1441.

39. Kim JY et al. Growth-inhibitory and proapoptotic effects of alpha-linolenic acid on estrogen-positive breast cancer cells. Ann N Y Acad Sci. 2009, 1171, 190-5.

40. Kapoor R and Huang YS. Gamma linolenic acid: an antiinflammatory omega-6 fatty acid. Curr Pharm Biotechnol. 2006, 7(6), 531-4.

41. Menendez JA et al. HER2 (erbB-2)-targeted effects of the □-3 polyunsaturated. Fatty acid α-linolenic acid (ALA; 18:3n-3) in breast cancer cells: the «fat features» of the «Mediterranean diet» as an «anti-HER2 cocktail». Clinical and Translational Oncology. 2006, 8(11), 812–820.

42. Watkins G et al. Gamma-Linolenic acid regulates the expression and secretion of SPARC in human cancer cells. Prostaglandins Leukot Essent Fatty Acids. 2005, 72(4), 273-8.

43. Larsson SC et al. Dietary long-chain n−3 fatty acids for the prevention of cancer: a review of potential mechanisms. The American Journal of Clinical Nutrition, 2004, 79 (6), 935–945.

44. Kenny FS et al. Gamma linolenic acid with tamoxifen as primary therapy in breast cancer. Int J Cancer. 2000, 85(5), 643-8.

45. Pender-Cudlip MC et al. Delta-6-desaturase activity and arachidonic acid synthesis are increased in human breast cancer tissue. Cancer Science. 2013, 104 (6), 60-764.

46. Levin G et al. Differential metabolism of dihomo-gamma-linolenic acid and arachidonic acid by cyclo-oxygenase-1 and cyclo-oxygenase-2: implications for cellular synthesis of prostaglandin E1 and prostaglandin E2. Biochem J. 2002, 365(Pt 2), 489–496.

47. Kapoor R and Yung-Sheng H. Gamma Linolenic Acid: An Antiinflammatory Omega-6 Fatty Acid. Current Pharmaceutical Biotechnology, 2006, 7 (6), 531-534(4).

48. Horrobin DF. Nutritional and medical importance of gamma-linolenic acid. Progress in Lipid Research, 1992, 31 (2), 163-194.

49. Kaur N, Chugh V, and Gupta AK. Essential fatty acids as functional components of foods- a review. J Food Sci Technol. 2014, 51(10), 2289–2303.

50. Simopoulos AP. An Increase in the Omega-6/Omega-3 Fatty Acid Ratio Increases the Risk for Obesity. Nutrients. 2016, 8(3), 128.

51. Coblijn BG and Murphy EJ. Alpha-linolenic acid and its conversion to longer chain n−3 fatty acids: Benefits for human health and a role in maintaining tissue n−3 fatty acid levels. Progress in Lipid Research, 2009, 48 (6), 355-374.

52. Shaikh SR and Edidin M. Polyunsaturated fatty acids and membrane organization: The balance between immunotherapy and susceptibility to infection. Chem Phys Lipids. 2008, 153(1), 24–33.

53. Calder PC. Omega-3 Fatty Acids and Inflammatory Processes. Nutrients. 2010, 2(3), 355–374.

54. Keiler AM et al. Evaluation of estrogenic potency of a standardized hops extract on mammary gland biology and on MNU-induced mammary tumor growth in rats. J Steroid Biochem Mol Biol. 2017, 174, 234-241.

55. Johnson KM et al. Toward Hypoxia-Selective DNA-Alkylating Agents Built by Grafting Nitrogen Mustards onto the Bioreductively Activated, Hypoxia-Selective DNA-Oxidizing Agent 3-Amino-1,2,4-benzotriazine 1,4-Dioxide (Tirapazamine). J. Org. Chem., 2014, 79 (16), 7520–7531.

56. Christmann M et al. O(6)-Methylguanine-DNA methyltransferase (MGMT) in normal tissues and tumors: enzyme activity, promoter methylation and immunohistochemistry. Biochim Biophys Acta. 2011, 1816(2), 179-90.

57. Kerdelhuéa B, Forest C and Coumoul X. Dimethyl-Benz (a)anthracene: A mammary carcinogen and a neuroendocrine disruptor. Biochimie Open, 2016, 3, 49-55.

58. Ciolino HP et al. Effect of Curcumin on the Aryl Hydrocarbon Receptor and Cytochrome P450 1A1 in MCF-7 Human Breast Carcinoma Cells. Biochemical Pharmacology, 1998, 56 (2), 197-206.

59. Buxant F et al. Preexposure of MCF-7 breast cancer cell line to dexamethasone alters the cytotoxic effect of paclitaxel but not 5-fluorouracil or epirubicin chemotherapy. Breast Cancer (Dove Med Press). 2017, 9, 171–175.

60. Gomez Perez M et al. Neutral Red versus MTT assay of cell viability in the presence of copper compounds. Anal Biochem. 2017, 535, 43-46.

61. Riyasdeen A et al. Antiproliferative and apoptosis-induction studies of a metallosurfactant in human breast cancer cell MCF-7. RSC Adv, 2014,4, 49953-49959.

62. Wafai RA et al. Chemosensitivity of MCF-7 cells to eugenol: release of cytochrome-c and lactate dehydrogenase. Scientific Reports, 2017, 7, Article number: 43730.

63. Jin S et al. Daidzein induces MCF-7 breast cancer cell apoptosis via the mitochondrial pathway. Annals of Oncology, 2010, 21 (2), 263–268.

64. Han X et al. Inhibitory effects and molecular mechanisms of tetrahydrocurcumin against human breast cancer MCF-7 cells. Food & Nutrition Research, 2016, 60(1).

65. Mishra RK et al. Palonosetron attenuates 1,2-dimethyl hydrazine induced preneoplastic colon damage through downregulating acetylcholinesterase expression and up-regulating synaptic acetylcholine concentration. RSC Adv., 2016, 6, 40527-40538.

66. Manral C et al. Effect of β-sitosterol against methyl nitrosourea-induced mammary gland carcinoma in albino rats. BMC Complementary and Alternative Medicine, 2016, 16, 260.

67. De Assis S et al. Changes in Mammary Gland Morphology and Breast Cancer Risk in Rats. J. Vis. Exp, 2010, (44), e2260, doi, 10.3791/2260.

68. Patricia A et al. A Developmental Atlas of Rat Mammary Gland Histology. Journal of Mammary Gland Biology and Neoplasia, 2000, 5 (2), 165–185.

69. Yoshida H et al. Scanning electron microscopy of 7, 12-dimethylbenz (a)-anthracene-induced mammary carcinoma in the female Sprague-Dawley rat. Virchows Archiv B, 1980, 32, 105.

70. Kaithwas G and Majumdar D. In vitro antioxidant and in vivo antidiabetic, antihyperlipidemic activity of linseed oil against streptozotocin-induced toxicity in albino rats. European J of Life Science and Technology. 2012, 114 (11), 1237-1245.

71. Lauridsen M et al. Human Urine as Test Material in 1H NMR-Based Metabonomics: Recommendations for Sample Preparation and Storage. Anal. Chem., 2007, 79 (3), 1181–1186.

72. Smolinska A et al. NMR and pattern recognition methods in metabolomics: From data acquisition to biomarker discovery: A review. Analytica Chimica Acta, 2012, 750, 82-97.

73. Cloarec O et al. Statistical Total Correlation Spectroscopy: An Exploratory Approach for Latent Biomarker Identification from Metabolic 1H NMR Data Sets. Anal. Chem., 2005, 77 (5), 1282–1289.

74. Ward JL et al. Assessment of 1H NMR spectroscopy and multivariate analysis as a technique for metabolite fingerprinting of Arabidopsis thaliana. Phytochemistry, 2003, 62 (6), 949-957.

75. Lorente L et al. Serum caspase-3 levels and mortality are associated in patients with severe traumatic brain injury. BMC Neurol. 2015, 15, 228.

76. Kruger N.J. The Bradford Method for Protein Quantitation. In: Walker J.M. (eds) The Protein Protocols Handbook. Humana Press, 2002, 15-21.

77. Saji S et al. Estrogen receptors α and β in the rodent mammary gland. PNAS, 2000, 97 (1), 337–342.

78. Papaconstantinou AD et al. Gene expression profiling in the mammary gland of rats treated with 7, 12-dimethylbenz[a]anthracene, Int. J. Cancer, 2006, 118, 17–24.

79. Oh KH and Kim H. Aldicarb-induced Paralysis Assay to Determine Defects in Synaptic Transmission in Caenorhabditis elegans. Bio Protoc. 2017, 7(14), e2400.

80. Lee J, Kim KY and Paik YK. Alteration in cellular acetylcholine influences dauer formation in Caenorhabditis elegans. BMB Rep. 2014, 47(2), 80–85.

81. Zhou Q, Li H and Xue D. Elimination of paternal mitochondria through the lysosomal degradation pathway in C. elegans. Cell Res. 2011, 21(12), 1662–1669.

82. Judith Rumin et al. The use of fluorescent Nile red and BODIPY for lipid measurement in microalgae. Biotechnol Biofuels. 2015, 8, 42.

83. Ly K, Reid SJ, and Snell RG. Rapid RNA analysis of individual Caenorhabditis elegans. MethodsX. 2015, 2, 59–63.

84. Martin G et al. Phosphatidylserine externalization in human sperm induced by calcium ionophore A23187: relationship with apoptosis, membrane scrambling and the acrosome reaction. Human Reproduction. 2005, 20(12), 3459–3468.

85. Lakoski SG et al. Autonomic Dysfunction in Early Breast Cancer: Incidence, Clinical Importance, and Underlying Mechanisms. Am Heart J. 2015, 170(2), 231–241.

86. Rani A et al. α-Chymotrypsin regulates free fatty acids and UCHL-1 to ameliorate N-methyl nitrosourea induced mammary gland carcinoma in albino wistar rats. Inflammopharmacology. 2016, 24, 277-286.

87. Birben E et al. Oxidative Stress and Antioxidant Defense. World Allergy Organ J. 2012, 5(1), 9–19.

88. Serini S et al. Dietary n-3 Polyunsaturated Fatty Acids and the Paradox of Their Health Benefits and Potential Harmful Effects. Chem. Res. Toxicol., 2011, 24 (12), 2093–2105.

89. Schcolnik-Cabrera A et al. Understanding tumor anabolism and patient catabolism in cancer-associated cachexia. Am J Cancer Res. 2017, 7(5), 1107–1135.

90. Cray C, Zaias J and Altman NH. Acute Phase Response in Animals: A Review. Comp Med. 2009, 59(6), 517–526.

91. Wu G et al. Arginine metabolism and nutrition in growth, health and disease. Amino Acids. 2009, 37(1), 153–168.

92. Mahipant G et al. The significance of proline and glutamate on butanol chaotropic stress in Bacillus subtilis 168. Biotechnol Biofuels. 2017, 10, 122.

93. Singh A et al. 1H NMR Metabolomics Reveals Association of High Expression of Inositol 1, 4, 5 Trisphosphate Receptor and Metabolites in Breast Cancer Patients. PLoS One. 2017; 12(1): e0169330.

94. Wang C and Youle RJ. The Role of Mitochondria in Apoptosis. Annu Rev Genet. 2009, 43, 95–118.

95. Camara AKS et al. Mitochondrial VDAC1: A Key Gatekeeper as Potential Therapeutic Target. Front Physiol. 2017, 8, 460.

96. Zhou M et al. Atomic structure of the apoptosome: mechanism of cytochrome c- and dATP-mediated activation of Apaf-1. Genes Dev. 2015, 29(22), 2349–2361.

97. Bratton SB and Salvesen GS. Regulation of the Apaf-1–caspase-9 apoptosome. J Cell Sci. 2010, 123(19), 3209–3214.

98. Jiang B. Aerobic glycolysis and high level of lactate in cancer metabolism and microenvironment. Genes & Diseases. 2017, 4 (1), 25-27.

99. Yang M et al. Prolyl hydroxylase domain enzymes: important regulators of cancer metabolism. Hypoxia (Auckl). 2014, 2, 127–142.

100. Singh M et al. Prolyl hydroxylase mediated inhibition of fatty acid synthase to combat tumor growth in mammary gland carcinoma.Breast Cancer. 2016, 23 (6), 820–829.

101. Goto Y et al. UCHL1 provides diagnostic and antimetastatic strategies due to its deubiquitinating effect on HIF-1α. Nat Commun. 2015, 23, 6, 6153.

102. Pedriali G et al. Regulation of Endoplasmic Reticulum–Mitochondria Ca2+ Transfer and Its Importance for Anti-Cancer Therapies. Front Oncol. 2017, 7, 180.

103. Azimi I, Roberts-Thomson SJ, and Monteith GR. Calcium influx pathways in breast cancer: opportunities for pharmacological intervention. Br J Pharmacol. 2014, 171(4), 945–960.

104. Millet T et al. Role of the α7 Nicotinic Acetylcholine Receptor and RIC-3 in the Cholinergic Anti-inflammatory Pathway. Cent Nerv Syst Agents Med Chem. 2017, 17(2), 90-99.

105. Zdanowski R et al. Role of α7 nicotinic receptor in the immune system and intracellular signaling pathways. Cent Eur J Immunol. 2015, 40(3), 373–379.

106. de Jonge WJ and Ulloa L. The alpha7 nicotinic acetylcholine receptor as a pharmacological target for inflammation. Br J Pharmacol. 2007, 151(7), 915–929.

107. Wu ZS et al. Ion channels gated by acetylcholine and serotonin: structures, biology, and drug discovery. Acta Pharmacol Sin. 2015, 36(8), 895–907.

108. Moccia F, Berra-Romani R, and Tanzi F. Update on vascular endothelial Ca2+ signalling: A tale of ion channels, pumps and transporters. World J Biol Chem. 2012, 26, 3(7), 127–158.

109. Lo ZYS, Steer JH and Joyce DA. Tumor necrosis factor-alpha promotes survival in methotrexate-exposed macrophages by an NF-kappaB-dependent pathway. Arthritis Res Ther. 2011, 13(1), R24.

110. Turner MD et al. Cytokines and chemokines: At the crossroads of cell signalling and inflammatory disease. Biochimica et Biophysica Acta (BBA) - Molecular Cell Research, 2014, 1843 (11), 2563-2582.

111. Richter C et al. The Tumor Necrosis Factor Receptor Stalk Regions Define Responsiveness to Soluble versus Membrane-Bound Ligand. Molecular and Cellular Biology, 2012, 32(13), 2515-29.

112. Pobezinskaya YL and Liu Z. The role of TRADD in death receptor signaling. Cell Cycle. 2012, 11(5), 871–876.

113. Gaffney CJ et al. Methods to Assess Subcellular Compartments of Muscle in C. elegans. J Vis Exp. 2014, (93), 52043.

114. Mullen GP et al. Choline Transport and de novo Choline Synthesis Support Acetylcholine Biosynthesis in Caenorhabditis elegans Cholinergic Neurons. Genetics. 2007, 177(1), 195–204.

115. Matthies DS et al. The Caenorhabditis elegans Choline Transporter CHO-1 Sustains Acetylcholine Synthesis and Motor Function in an Activity-Dependent Manner. Journal of Neuroscience. 2006, 26 (23), 6200-6212.

APPENDIX-I

ANIMAL APPROVAL CERTIFICATE

INSTITUTIONAL ANIMAL ETHICAL COMMITTEE (IAEC)
BABU BANARASI DAS NORTHERN INDIA INSTITUTE OF TECHNOLOGY, LUCKNOW

(Reg. No. 809/03/c/CPCSEA dt: 15-10-2003 under the rules 5(a) of the "Breeding of and Experiments on Animals (Control & Supervision Rules 1998")

Ref : **BBDNIIT/IAEC/021/2014**

Date : *May 19, 2014*

CERTIFICATE

This is to certify that Mr./Ms. **Shubhadeep Roy** is permitted to carry out experiments on animals for the research work entitled ***Effect of Alpha Linolenic acid and Gamma Linolenic acid on Breast Cancer Risk: Evaluation of Synergistic efficacy with an Anticancer Drug*** as per the details mentioned and after observing the usual formalities laid down by IAEC as per the provisions made by CPCSEA.

B.B.D.N.I.I.T. Director (Pharmacy) LUCKNOW

Chairperson
Institutional Animal Ethics Committee
Babu Banarasi Das Northern India Institute of Technology,
Lucknow-227105

APPENDIX-II

PLAGIARISM REPORT

Sources | Highlights

Document	Subhadeep Roy.pdf (D37272493)
Submitted	2018-04-06 13:14 (+05:0-30)
Submitted by	shodhganga.bbau@gmail.com
Receiver	gbl.bbau.bbau@analysis.urkund.com
Message	Subhadeep Roy, Department of Pharmaceutical Sciences, subhadeep.roygood@gmail.com Show full message

0% of this approx. 49 pages long document consists of text present in 0 sources.

Rar

Reset | Export | Share

96% # 1 Active

1 Warnings

[5]. The large body of evidences suggests the role of PUFAs metabolites in carcinogenesis and tumour progression as well. PUFA are the precursors for various essential signalling molecules like eicosanoids including the prostanoids, leukotrienes (LTs), and lipoxins (LXs). Prostanoids include prostaglandins (PGs), prostacyclins (PGIs), and thromboxanes (TXs) along with LTs and LXs are key mediators of inflammatory cascade [6]. The majority of physiological disorder considering the inflammatory background of above mentioned diseases and formation of essential signalling molecules (eicosanoids), leads to the assumption that ω- 3 and ω-6 PUFAs plays a significant role in their pathophysiology and might be acting through down-regulation/up-regulation of the inflammatory cascade respectively [7]. The ω-3 family of PUFAs mainly comprises of alpha linolenic acid (ALA), eicosapentaenoic acid (EPA) and

ALA (18: 3, ω-3) cannot be synthesized by the human body and needs to be obtained from dietary sources [1]. ALA is the major plant-based PUFA and is found in walnuts, flaxseeds, hemp seeds and their oils. ALA is also found in rapeseed (canola) oil; and to smaller amounts in soya oil and green-leafy vegetables [2]. ALA is metabolized by series of desaturation and elongation reactions of long chain fatty acids, among which eicosapentanoic acid (EPA, 20:5, ω-3) and docosahexaenoic acid (DHA, 22:6 ω-3) are of prime biological importance [3]. EPA and DHA are vital in regulating membrane fluidity, protein and cellular functions, eicosanoid metabolism, gene expression and cell signaling [4]. EPA and DHA are obtained from fish oil or derived from plant lipids rich in ALA. EPA and DHA integrate a cascade that runs alongside and emulates with the inflammatory cascade governed by the arachidonic acid (AA) (20: 4, ω-6) metabolism [5]. A previous report has taken account that the EPA cascade softens

APPENDIX-III

PUBLICATIONS

Alpha-linolenic acid stabilizes HIF-1 α and downregulates FASN to promote mitochondrial apoptosis for mammary gland chemoprevention

Subhadeep Roy[1], Atul Kumar Rawat[2], Shreesh Raj Sammi[3], Uma Devi[4], Manjari Singh[1], Swetlana Gautam[1], Rajnish Kumar Yadav[1], Jitendra Kumar Rawat[1], Lakhveer Singh[1], Mohd. Nazam Ansari[5], Abdulaziz S. Saeedan[5], Rakesh Pandey[3], Dinesh Kumar[2] and Gaurav Kaithwas[1]

[1]Department of Pharmaceutical Sciences, Babasaheb Bhimrao Ambedkar University, Lucknow (UP), India

[2]Central for Biomedical Research, Sanjay Gandhi Post Graduate Institute of Medical Sciences Campus, Lucknow (UP), India

[3]Department of Microbial Technology and Nematology, CSIR-Central Institute of Medicinal and Aromatic Plants, Lucknow (UP), India

[4]Department of Pharmaceutical Sciences, Faculty of Health and Medical Sciences, Sam Higginbottom Institute of Agricultural Sciences and Technology, Allahabad (UP), India

[5]Department of Pharmacology, College of Pharmacy, Prince Sattam Bin Abdulaziz University, Al-Kharj, KSA

Correspondence to: *Gaurav Kaithwas,* ***email:*** *gauravpharm@hotmail.com*

Keywords: *alpha linolenic acid, apoptosis, polyunsaturated fatty acid, hypoxia, fatty acid synthase*

Received: *February 06, 2017* ***Accepted:*** *June 12, 2017* ***Published:*** *July 25, 2017*

ABSTRACT

Alpha linolenic acid is an essential polyunsaturated fatty acid and is reported to have the anti-cancer potential with no defined hypothesis or mechanism/s. Henceforth present study was in-quested to validate the effect of alpha linolenic acid on mitochondrial apoptosis, hypoxic microenvironment and de novo fatty acid synthesis using *in-vitro* and *in-vivo* studies. The IC_{50} value of alpha linolenic acid was recorded to be 17.55μM against ER+MCF-7 cells. Treatment with alpha linolenic acid was evident for the presence of early and late apoptotic signals along with mitochondrial depolarization, when studied through acridine orange/ethidium bromide and JC-1 staining. Alpha linolenic acid arrested the cell cycle in G2/M phase. Subsequently, the *in-vivo* efficacy was examined against 7, 12-dimethylbenz anthracene induced carcinogenesis. Treatment with alpha linolenic acid demarcated significant effect upon the cellular proliferation as evidenced through decreased in alveolar bud count, restoration of the histopathological architecture and loss of tumor micro vessels. Alpha linolenic acid restored the metabolic changes to normal when scrutinized through ^{1}H NMR studies. The immunoblotting and qRT-PCR studies revealed participation of mitochondrial mediated death apoptosis pathway and curtailment of hypoxic microenvironment after treatment with alpha linolenic acid. With all above, it was concluded that alpha linolenic acid mediates mitochondrial apoptosis, curtails hypoxic microenvironment along with inhibition of de novo fatty acid synthesis to impart anticancer effects.

INTRODUCTION

α-Linolenic acid (ALA) (18: 3, ω-3) is an essential polyunsaturated fatty acid (PUFA). ALA (18: 3, ω-3) cannot be synthesized by the human body and needs to be obtained from dietary sources [1]. ALA is the major plant-based PUFA and is found in walnuts, flaxseeds, hemp seeds and their oils. ALA is also found in rapeseed (canola) oil; and

International Journal of Biochemistry and Cell Biology 96 (2018) 51–62

Contents lists available at ScienceDirect

International Journal of Biochemistry and Cell Biology

journal homepage: www.elsevier.com/locate/biocel

GLA supplementation regulates PHD2 mediated hypoxia and mitochondrial apoptosis in DMBA induced mammary gland carcinoma

Subhadeep Roy[a], Manjari Singh[a], Atul Rawat[b], Uma Devi[c], Swetlana Gautam[a], Rajnish Kumar Yadav[a], Jitendra Kumar Rawat[a], Md. Nazam Ansari[d], Abdulaziz S. Saeedan[d], Dinesh Kumar[b], Gaurav Kaithwas[a,*]

[a] Department of Pharmaceutical Sciences, Babasaheb Bhimrao Ambedkar University (A Central University), Vidya Vihar, Raebareli Road, Lucknow, 226025 UP, India
[b] Centre for Biomedical Research, Sanjay Gandhi Post Graduate Institute of Medical Sciences Campus Raibareli Road, Lucknow, 226014 UP, India
[c] Department of Pharmaceutical Sciences, Faculty of Health and Medical Sciences, Sam Higginbottom Institute of Agricultural Sciences and Technology, Naini, Allahabad, UP, India
[d] Department of Pharmacology, College of Pharmacy, Prince Sattam Bin Abdulaziz University, Al-Kharj, Saudi Arabia

ARTICLE INFO

Keywords:
Gamma linolenic acid
7, 12-Dimethylbenz (a) anthracene
Hypoxia
Mitochondria mediated death apoptosis
Breast cancer
alpha-7-nachr

ABSTRACT

The aim of the present study is to evaluate the effect of gamma linolenic acid (GLA) on mitochondrial mediated death apoptosis, hypoxic microenvironment and cholinergic anti-inflammatory pathway against 7, 12-dimethylbenz (a) anthracene (DMBA) induced mammary gland carcinoma. The effects of GLA were evaluated morphologically and biochemically against DMBA induced mammary gland carcinoma. The metabolic study was done for evaluation of biomarkers using ^{1}H NMR. The present study was also verified through immunoblotting and qRT-PCR studies for the evaluation of various pathways. GLA treatment has a delineate implementation upon morphology of the tissues when evaluated through carmine staining, hematoxyline and eosin staining and scanning electron microscopy. GLA also demarked a commendatory proclamation of the fifteen key serum metabolites analogous with amino acid metabolism and fatty acid metabolism when recognized through ^{1}H NMR studies. The immunoblotting and qRT-PCR studies accomplished that GLA mediated mitochondrial death apoptosis, curtail hypoxic microenvironment along with hindrance of *de novo* fatty acid synthesis and also mediate the cholinergic anti-inflammatory pathway to proclaim its anticancer effects.

1. Introduction

Polyunsaturated fatty acids (PUFAs) play a predominant role in the cell membrane formation and are also important for the functioning of membrane proteins and membrane fluidity. PUFAs synchronize several cellular processes, functions and gene expression (Kaur et al., 2014). GLA is a member of the ω-6 family of PUFAs and is transfigured into arachidonic acid (AA) by series of desaturation and elongation reactions. AA is further metabolized by cyclooxygenase enzyme into 2-series prostaglandins or through the 5-lipoxygenase enzymes into leukotrienes and 5-hydroxy-eicosatetranoic acid, which are the major determinants for cellular inflammation (Ricciotti and FitzGerald, 2011). GLA is found in animals and plants, oils like sunflower, soy bean and grape seed and is very much found in daily diet (Bederska-Łojewska et al., 2013). Considering the fact that GLA is metabolized to AA and majority of the product of AA metabolism are pro-inflammatory, the GLA has been also considered to be pro-inflammatory in nature. Consistent intake of GLA is expected to promulgate inflammatory cascade

Abbreviations: AA, arachidonic acid; AB, alveolar bud; AAA, aromatic amino acid; BCAA, branched chain amino acid; BSA, bovine serum albumin; BMRB, biological magnetic resonance databank; CEC, cuboidal epithelial cell; CPMG, carr–purcell–meiboom–gill; DMBA, 7, 12-dimethylbenz (a) anthracene; DCT, dense connective tissue; DTT, dithiothreitol; ECG, electrocardiograph; ECD, extracellular domain; EBSS, eagle's balanced salt solution; FASN, fatty acid synthase; FADD, fas associated death domain; GLA, gamma linolenic acid; GSH, glutathione; HR, heart rate; HRV, heart rate variability; HF, high frequency; HIF-1α, hypoxia inducible factor-1α; HBSS, hank's balanced salt solution; HMDB, human metabolome database; ICD, intracellular domain; LF, low frequency; LCT, loose connective tissue; LDL, low density lipoprotein; MEC, myoepithelial cell; MPTP, membrane potential transition pore; NAG, *n*-acetyl-glycoprotein; NO, nitric oxide; OAG, *o*-acetyl-glycoprotein; OPLS-DA, orthogonal projection to latent structure with discriminant analysis; PUFA, polyunsaturated fatty acid; PC, protein carbonyl; PCA, partial component analysis; PHD2, prolyl hydroxylase-2; RIP, receptor interacting protein; SEM, scanning electron microscopy; SOD, superoxide dismutase; TBARs, thiobarbituric acid reactive substances; TM, transmembrane; TMD, transmembrane domain; TRADD, tumor necrosis factor associated death domain; TMAO, trimethylamine; VLF, very low frequency; VLDL, very low density lipoprotein; VEGF, vascular endothelial growth factor; VLF, very low frequency; VLDL, very low density lipoprotein

* Corresponding author at: Department of Pharmaceutical Sciences, School of Bioscience and Biotechnology, Babasaheb Bhimrao Ambedkar University (A Central University), Vidya Vihar, Raebareli Road, Lucknow, 226 025 UP, India.
E-mail address: gauravk@bbau.ac.in (G. Kaithwas).

https://doi.org/10.1016/j.biocel.2018.01.011
Received 18 November 2017; Received in revised form 30 December 2017; Accepted 13 January 2018

Publications from the present research work

- ✓ **Subhadeep Roy**, Manjari Singh…Gaurav Kaithwas. "GLA supplementation regulates PHD2 mediated hypoxia and mitochondrial apoptosis in DMBA induced mammary gland carcinoma". Int J Biochem Cell Biol. 2018 Jan 17. pii: S1357-2725(18)30017-7. doi: 10.1016/j.biocel.2018.01.011 (IF-3.5).
- ✓ **Subhadeep Roy**…Manjari Singh**…**Gaurav Kaithwas. "Alpha-linolenic acid arbitrates mitochondrial apoptosis, curbs the hypoxic microenvironment and de novo fatty acid synthesis to impart anticancer effects". Oncotarget (IF-5.168).

Publications under communication from the present work

- ✓ **Subhadeep Roy**…Gaurav Kaithwas. Mechanistic evaluation of GLA mediated mitochondrial apoptosis and curtailment of HIF-1α along with fatty acid synthesis in mammary gland cancer. **BMC Cancer (IF-3.2)** (Under Review).
- ✓ **Subhadeep Roy**…Gaurav Kaithwas. ALA mediated biphasic downregulation of α-7nAchR/HIF-1α along with mitochondrial apoptosis pathway in mammary gland cancer. **Journal of Cellular Physiology (4.1)** (Under Review).
- ✓

Publications related to research work

- ✓ Swetlana Gautam…, **Subhadeep Roy**…Gaurav Kaithwas. "DuCLOX-2/5 Inhibition Attenuates Inflammatory Response and Induces Mitochondrial Apoptosis for Mammary Gland Chemoprevention" Front. Pharmacol., 06 April 2018, https://doi.org/10.3389/fphar.2018.00314 (IF-4.4).
- ✓ Manjari Singh…**Subhadeep Roy**…Gaurav Kaithwas. "Chemical activation of prolyl hydroxylase-2 by BBAP1 down regulates hypoxia inducible factor-1α and fatty acid synthase for mammary gland chemoprevention". RSC Advances (Accepted for publication). (IF-3.1).
- ✓ Rajnish Kumar Yadav, **Subhadeep Roy…**Gaurav Kaithwas. "Modulation of oxidative stress response by flaxseed oil: Role of lipid peroxidation and underlying mechanisms" Prostaglandins and Other Lipid Mediators 135 (2018) 21–26. (IF-2.6)
- ✓ Swetlana Gautam…**Subhadeep Roy…**Gaurav Kaithwas. "Rifaximin, a pregnane X receptor (PXR) activator regulates apoptosis in a murine model of breast cancer". RSC Adv., 2018, 8, 3512–3521 (IF-3.1).
- ✓ Vidhata Rani…**Subhadeep Roy…**Gaurav Kaithwas. "Effects of minocycline and doxycycline against terbutaline induced early postnatal autistic changes in albino rats". Physiology & Behavior 183 (2018) 49–56 **(IF-2.341).**
- ✓ Rani A, **Subhadeep Roy…**Kaithwas G. "α-Chymotrypsin regulates free fatty acids and UCHL-1 to ameliorate N-methyl nitrosourea induced mammary gland carcinoma in

albino wistar rats". Inflammopharmacology. 2016 Oct; 24(5):277-286. Epub 2016 Sep 26. (IF- 2.590).

- ✓ Shreesh Raj Sammi…**Subhadeep Roy…**Gaurav Kaithwas. "Galantamine attenuates N,N-dimethyl hydrazine induced neoplastic colon damage by inhibiting acetylcholinesterase and bimodal regulation of nicotinic cholinergic neurotransmission". European Journal of Pharmacology 818 (2018) 174–183 (2.896).
- ✓ Manjari Singh…**Subhadeep Roy**…Gaurav Kaithwas. "Prolyl hydroxylase mediated inhibition of fatty acid synthase to combat tumor growth in mammary gland carcinoma", Breast Cancer. 2016 Nov; 23(6):820-829 (IF 1.572).
- ✓ Rakesh K. Mishra…**Subhadeep Roy…**Gaurav Kaithwas. "Palonosetron attenuates 1, 2-dimethyl hydrazine induced preneoplastic colon damage through downregulating acetylcholinesterase expression and up-regulating synaptic acetylcholine concentration", RSC Adv., 2016,6,40527 (IF-3.108).
- ✓ Chetan Manral, **Subhadeep Roy…**Gaurav Kaithwas, "Effect of β-sitosterol against methyl nitrosourea-induced mammary gland carcinoma in albino rats." BMC Complementary and Alternative Medicine, 2016; 16: 260 (IF- 2.28).
- ✓ Virendra Tiwari, **Subhadeep Roy…**Gaurav Kaithwas. "Redefining the role of peripheral LPS as a neuroinflammatory agent and evaluating the role of hydrogen sulphide through metformin intervention". Inflammopharmacology. 2016 Oct; 24(5):253-264 (IF 2.590).
- ✓ Uma Devi…**Subhadeep Roy…**Gaurav Kaithwas. "Experimental Models for Autistic Spectrum Disorder-Follow Up For the Validity", Review Journal of Autism and Developmental Disorders, 2016, 3(4), 358–376.
- ✓ Yadav S…**Roy S…**Kaithwas G. "Comparative efficacy of alpha linolenic acid and gamma-linolenic acid to attenuate valproic acid-induced autism-like features". J Physiol 2017 May; 73(2):187-198 (IF- 2.444).

Presentations/conferences attended

- ✓ Certificate of participation in 15th Indo-US Flow Cytometry workshop **in Application of Flow Cytometry in Biomedical Research** from 29th-31st October, 2014. BBAU, Lucknow.

- ✓ Certificate of participation in Workshop on **NMR/MRI (From molecules to human behavior)** from June 21-27, 2015, BBAU, Lucknow.

- ✓ Certificate of presentation from 2016 **AAPS Annual Meetings and Exposition** for presentation of paper in poster session on November 13-17, 2016, Denver, USA.

- ✓ Best presentation award in International seminar on **"Nanoformulations and Translational Research. Small getting bigger"** in oral presentation section, February 02-03, 2015, BBAU, Lucknow.